Tailoring structure and properties of polyelectrolyte-based material via materials selection and post-assembly treatment

By

Xuejian Lyu

A Dissertation

Submitted to the Faculty of

WORCESTER POLYTECHNIC INSTITUTE

in partial fulfillment of the requirements for the

Degree of Doctor of Philosophy in

Mechanical Engineering

APPROVED:

_____

Dr. Amy M. Peterson, Advisor

Associate Professor of Plastic Engineering

University of Massachusetts Lowell

_____

Dr. Richard D. Sisson, Jr.

Director of Manufacturing and Materials Engineering

Worcester Polytechnic Institute

Table of Contents

Abstract

Although polyelectrolyte-base materials have demonstrated uses in a wide range of applications, controlling properties of polyelectrolyte-based materials is challenging because of their sensitivity to material and processing parameters. This dissertation focused on fundamental science of polyelectrolyte-based materials. Although polyelectrolyte-based materials like PEMs and PECs have a wide range of potential applications, the relationship between structure and properties of those materials is still not fully understood. In this work, factors that can affect the structure and properties of PEMs and PECs were studied. Based on those results, potential approaches to tailor structure and properties of polyelectrolyte-based materials can be developed.

The role of the chemistry and molecular weight of first layer of a PEM was studied. By changing first layer materials, PEMs showed different internal structure, mass accumulation, and surface morphology. Quartz crystal microbalance with dissipation monitoring (QCM-D) was used to monitor the PEM assembly process. First layer choice affects the total mass accumulation of the PEM as well as the stoichiometry and thickness of the PEM. PEM topography is also affected by first layer choice. Combined with the stoichiometry results, these findings indicate that the structure of a PEM is fundamentally different depending on first layer chemistry and molecular weight. Selection of appropriate first layer material is therefore an important consideration in the design of a PEM and changing first layer material may be a facile way to tailor the structure and properties of PEMs.

Another category of polyelectrolyte-based materials, PECs, which are formed through electrostatic interactions between oppositely charged polyelectrolytes, have garnered sustained interest for their range of potential applications. Since water plays an important role in the structure and properties of polyelectrolyte-based materials, humidity controlled dynamic mechanical

analysis (DMA) was used to characterize the thermomechanical properties of dried polyelectrolytes and PECs with different thermal and humidity histories. After exposure to higher humidities (humidity tempering), both room temperature storage modulus and flexural modulus of the resulting PEC increased. Water from the humid air plasticized the PEC, increasing mobility and facilitating chain reorganization during humidity tempering, which resulted in a structure with more intrinsic electrostatic bonds (cross-links) and higher moduli. Storage conditions and relative humidity were demonstrated to influence thermal transitions and mechanical properties of PEC, which highlighted the potential of polyelectrolyte-based materials for new applications where tailoring of mechanical properties is desired.

Acknowledgment

As I'm finishing this dissertation, I cannot help to notice the guide, accompany, encouragements, and advises from those who helped me to get this point of my life and research career. There is no word that can express my appreciation, and there is no way I can finish this dissertation without the support and guidance I have received from them.

First of all, I would like to express my deeply appreciation to my academic advisor, Dr. Amy M. Peterson. I would like to tell you that I feel very lucky to get in to your lab after I choose WPI to do my graduate studies. Thanks for your mentoring, which not only helped me with my research, but also helped me fitting into a whole new culture, after I left my own country for the first time in my life. Thanks for the advise on my research projects, which gave me not only research abilities, but also the ability of critical thinking. Thanks for the help in manuscript writing, which makes me more confident on expressing my thoughts.

Thanks for my lab mates and colleagues (Tone, Ivan, Masi, Jake, Aaron, Claire…). Thanks for being such great company. I'm so glad to have this excellent experience, with the thoughtful ideas from you and good research environment created by all lab members.

Thanks for my friends at WPI (Haixuan, Lite, Yuan, Mingchao, Chengrui…) that makes the life far from home become so enjoyable. You made this experience one of my best in my life. Special thanks to Haixuan, my first and best roommate since I came to this country, for the supporting and struggling we experienced together when facing a completely new environment.

I will never be able to conduct any research or experiments without equipment and training. Thank you, Professor Burnham, Sarkar and Dr. Li (WPI), for allowing me to use the equipment and giving me the training. To Andy Butler and Daryl Johnson (WPI), thank you for the help and expertise on equipment operation.

Last, but certainly not least, I would like to acknowledge my family members. Thanks to my parents, Hongzhi Lyu and Yuanmin Duna, for your selflessly love and support. The gift I get from you is not only the love and care since my childhood, but also the way you taught me how to think and make decisions in my life. Thanks to my wife, Xiaoye Qi, for you accompany and support, since the first time we met. You helped me overcome so many difficulties and struggles. Thanks for being such a great partner, I am grateful to have you by my side.

Abbreviations

A	Surface area of the crystal
AFM	Atomic force microscope
BMP2	Bone morphogenetic protein 2
c	Crosslink density
DMA	Dynamic mechanical analysis
DSC	Differential Scanning Calorimetry
σ_{max}	Flexural stress
E	Actual modulus
E_0	Modulus without plasticizer
E_{bend}	Flexural modulus
ε_{max}	Flexural strain
f_0	The resonant frequency of the quartz crystal
Δf	Frequency change of the deposited film
G	Shear modulus
LbL	Layer-by-layer
Δm	Mass change of the deposited film
MW	Molecular weight
M_t (Chapter 4)	The mass of the PEC after storage under a specified RH for time t
M_t (Chapter 5)	Water absorbed at time t
M_∞	Water absorbed at saturation
M_0	The initial PEC mass
n	Exponent to describe the diffusion mechanism

$\bar{n}$	Geometric mean number of bonds in the network chain
ρ_q	The density of the quartz crystal
μ_q	The shear modulus of the quartz crystal
PAA	Poly(allylamine hydrochloride)
PAH	Poly(allylamine hydrochloride)
PDADMAC	Poly(diallyldimethylammonium chloride)
PEC	Polyelectrolyte complexes
PEM	Polyelectrolyte multilayers
PEI	Polyethylenimine
PLH	Poly-L-histidine hydrochloride
PSS	Poly(sodium 4-styrenesulfonate)
PMAA	Poly(methacrylic acid)
QCM-D	Quartz crystal microbalance with dissipation monitoring
q	Dimensional factor for backbone with carbon−carbon single bonds
RH	Relative humidity
RMS	Root mean square
R_q	Roughness
r_p	Molar ratio of the plasticizer
TGA	Thermogravimetric analysis
T_g	Glass transition temperatures
ν	Number of moles of sub chains per unit volume
wt.%	Weight percent of water in PEC

Chapter 1: Research Summary

1.1 Specific Aims

Polyelectrolyte-based materials, such as PEMs and PECs, has experienced sustained interests for decades. PEMs and PECs have been applied as biomedical coatings, tissue scaffold and drug delivery materials.[1–8] The structure and properties of polyelectrolyte-based materials can be drastically influenced by many factors, such as assembly conditions and post-assembly treatment, which makes the processing of those materials challenging.[9–12]

The overall goal of this dissertation was to develop fundamental science-based approaches to precisely tailor the structure and properties of polyelectrolyte-based materials. To achieve this goal, three specific aims were pursued: **Aim I**, Tuning PEMs structure and surface property by first layer material selection. The structure of a PEM is fundamentally different depending on the first layer chemistry and molecular weight. By exploring the influence of first layer material on PEM structure and properties, approaches to manipulate PEM properties without changing surface chemistry can be developed. **Aim II,** Study the effect of storage condition and thermal treatment on PECs. Storage conditions change water content in PEC, while thermal treatment will affect the interactions between water and the PEC. Thermal transition and mechanical properties of PECs will be further influenced. **Aim III,** Tailoring mechanical properties of the PEC using humidity tempering. The effect of water was further studied quantitively. Tempering PECs under certain relative humidity conditions causes molecular rearrangement and results in changing of mechanical properties. Room-temperature and humidity-assisted approaches for mechanical property manipulation can be developed based on this study.

1.2 Dissertation Outline

In Chapter 3, PDADMAC/PSS PEMs were assembled with different polycations as the first layer material. The assembly process was tracked using QCM-D, with mass accumulation of each individual layer recorded. Surface morphology and chemistry was characterized by AFM and water contact angle measurements. Dry thickness of PEM was measured by ellipsometry. Those properties were compared between PEMs with different first layer material and the influence of the first layer materials was discussed.

In Chapter 4, mechanical properties of polyelectrolytes stored under different conditions (ambient and desiccator) were characterized using DMA. Polyelectrolytes undergoes a heat-cool-heat cycle and the thermal transitions under first and second heating step were compared. PECs assembled with PDADMAC/PSS were also characterized by DMA. It was shown in this chapter that water content of polyelectrolytes and PECs will affect the mechanical properties dramatically. PECs of PDADMAC and PSS revealed a humidity history-dependent thermal transition

In Chapter 5, effect of humidity history on the structure and property of PECs was further characterized. Humidity controlled DMA was used to track the mechanical response of PEC during humidity change. Humidity tempering was done by keeping PEC under 50% relative humidity for 25 hours. Water content of PECs under different humidity conditions was also tracked to quantitively study the relationships between water and PEC mechanical properties. A description of the relationship between modulus and crosslink density was applied to describe the crosslink density change during humidity tempering and the effect of water on crosslink density was discussed based on this relationship.[13,14] Flexural testing of PECs demonstrated a stiffness increase after room temperature humidity tempering.

In Chapter 6, drug delivery materials based on bioderived polyelectrolytes were assembled and characterized. Starch was used to fabricate oral drug delivery patches. Degradation behavior of starch films were studied. Starch films were further functionalized with the goal of improving adhesion property in all oral environment. Humidity controlled DMA was further applied to study the mechanical response of gelatin films under humidity variation. Gelatins from different sources were fabricated into thin films and characterized using humidity controlled DMA.

References

(1) Etienne, O.; Picart, C.; Taddei, C.; Haikel, Y.; Dimarcq, J. L.; Schaaf, P.; Voegel, J. C.; Ogier, J. A.; Egles, C. Multilayer Polyelectrolyte Films Functionalized by Insertion of Defensin: A New Approach to Protection of Implants from Bacterial Colonization. *Antimicrob. Agents Chemother.* **2004**.

(2) Macdonald, M. L.; Samuel, R. E.; Shah, N. J.; Padera, R. F.; Beben, Y. M.; Hammond, P. T. Tissue Integration of Growth Factor-Eluting Layer-by-Layer Polyelectrolyte Multilayer Coated Implants. *Biomaterials* **2011**.

(3) Lee, I. C.; Wu, Y. C. Assembly of Polyelectrolyte Multilayer Films on Supported Lipid Bilayers to Induce Neural Stem/Progenitor Cell Differentiation into Functional Neurons. *ACS Appl. Mater. Interfaces* **2014**.

(4) Arntz, Y.; Ball, V.; Benkirane-Jessel, N.; Boulmedais, F.; Debry, C.; Dimitrova, M.; Elkaim, R.; Haikel, Y.; Hemmerl, J.; Lavalle, P.; et al. Polymers in Biomaterials Science: From

Surface Functionalisation to Tissue Engineering. *Actual. Chim.* **2007**.

(5) Zhang, C.; Hirt, D. E. Layer-by-Layer Self-Assembly of Polyelectrolyte Multilayers on Cross-Section Surfaces of Multilayer Polymer Films: A Step toward Nano-Patterning Flexible Substrates. *Polymer*. **2007**.

(6) Huang, X.; Zacharia, N. S. Surfactant Co-Assembly and Ion Exchange to Modulate Polyelectrolyte Multilayer Wettability. *Soft Matter* **2013**.

(7) Fakhrullin, R. F.; Zamaleeva, A. I.; Minullina, R. T.; Konnova, S. A.; Paunov, V. N. Cyborg Cells: Functionalisation of Living Cells with Polymers and Nanomaterials. *Chemical Society Reviews*. 2012.

(8) Thompson, M. T.; Berg, M. C.; Tobias, I. S.; Rubner, M. F.; Van Vliet, K. J. Tuning Compliance of Nanoscale Polyelectrolyte Multilayers to Modulate Cell Adhesion. *Biomaterials* **2005**.

(9) Dautzenberg, H. Polyelectrolyte Complex Formation in Highly Aggregating Systems. 1. Effect of Salt: Polyelectrolyte Complex Formation in the Presence of NaCl. *Macromolecules* **1997**.

(10) Gucht, J. van der; Spruijt, E.; Lemmers, M.; Cohen Stuart, M. A. Polyelectrolyte Complexes: Bulk Phases and Colloidal Systems. *J. Colloid Interface Sci.* **2011**, *361* (2), 407–422.

(11) Porcel, C.; Lavalle, P.; Ball, V.; Decher, G.; Senger, B.; Voegel, J. C.; Schaaf, P. From Exponential to Linear Growth in Polyelectrolyte Multilayers. *Langmuir* **2006**, *22* (9), 4376–4383.

(12) Holmberg, K. Organic Reactionsin Microemulsions Krister. *Curr. Opin. Colloid Interface Sci.* **2003**, *8*, 145–155.

(13) Jaber, J. A.; Schlenoff, J. B. Mechanical Properties of Reversibly Cross-Linked Ultrathin

Polyelectrolyte Complexes. *J. Am. Chem. Soc.* **2006**, *128* (9), 2940–2947.

(14) Smith, T. L. Modulus of Tightly Crosslinked Polymers Related to Concentration and Length of Chains. *J. Polym. Sci. Polym. Symp.* **1974**, *46* (1), 97–114.

Chapter 2: Introduction

2.1 Polyelectrolytes

Polyelectrolytes are polymers with ionically dissociable repeating units. Based on the type of charges carried on the molecular chain after ionic dissociation, polyelectrolytes can be classified into three groups: polycations, which carry positive charges; polyanions, which carry negative charges; and polyampholytes, which bear both cationic and anionic repeating units. Polyelectrolytes are described as either being "strong" or "weak" based on the degree of ionic dissociation in solution. The counterions of strong polyelectrolytes fully dissociate in solution. On the other hand, counterion dissociation is only partial for weak polyelectrolytes, with the degree of dissociation dictated by polyelectrolyte isoelectric point and solution pH. Many biomacromolecules are polyelectrolytes, such as proteins, polypeptides, glycosaminoglycans, and DNA. Many synthetic polyelectrolytes are also commercially available. Two strong polyelectrolytes are the primary materials used in this dissertation. Figure 1 gives the repeat unit structures of these two common synthetic polyelectrolytes: poly(diallyldimethylammonium chloride) (PDADMAC), which is a strong polycation, and poly(4-styrenesulfonate) (PSS), which is a strong polyanion. These polyelectrolytes were chosen for investigation because they are the canonical polycation and polyanion. Therefore, there is a wealth of literature to compare our findings to, and our results will be broadly beneficial to the field.[1–4]

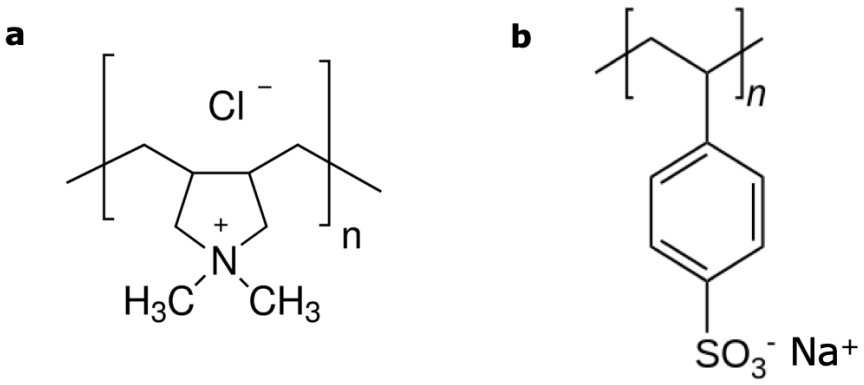

Figure 1. Molecular structure of a) PDADMAC and b) PSS

In aqueous solutions, polyelectrolyte counterions dissociate. This, along with the greater mobility achieved through solvation, allows for interactions between charges on a single chain, interactions between different chains and between counterions. All of these interactions will affect the molecular conformation of polyelectrolytes.[5] Under low ionic strength, the counterions released from a polyelectrolyte chain tend to remain dissociated in solution while the charges along the polyelectrolyte chain will repulse between each other because they all have the same charge. As a result, the chain adopts a stiff expanded conformation. Under high ionic strength, the charge repulsion along the chain is screened by counterions, which decreases the chain stiffness and lead to a soft coil-like chain conformation.[5] Molecular conformation affects interactions between polyelectrolytes which leads to differences in structure and performance of polyelectrolyte-based materials.

2.2 Polyelectrolyte Multilayers (PEMs)

2.2.1 PEM assembly methods

PEMs are assembled through layer-by-layer deposition of oppositely charged polyelectrolytes. Since they were first described in the early 1990's, multi-functional polymer structures have been prepared based on this layer-by-layer polyelectrolyte deposition techinique.[6] PEM coatings have been applied as superhydrophobic[7] and nano-patterned surfaces,[8,9] as well as corrosion inhibition[10] and self-healing coatings.[11] One important application of PEMs is controlled release of biologically relevant molecules from PEM coatings or capsules.[12–17]

Layer-by-layer dip coating is a common method for PEMs fabrication. Solutions of polycations and polyanions are prepared separately. The first layer is deposited by immersing the substrate into one polyelectrolyte solution. After the first layer deposition, the substrate is rinsed by water to remove the loosely attached molecules. The dipping and rinsing process is repeated with an oppositely charged polyelectrolyte solution. Figure 2 shows a typical layer-by-layer dip coating method. Other PEMs assembly methods have also been studied, including spin coating and spray coating.[18–20]

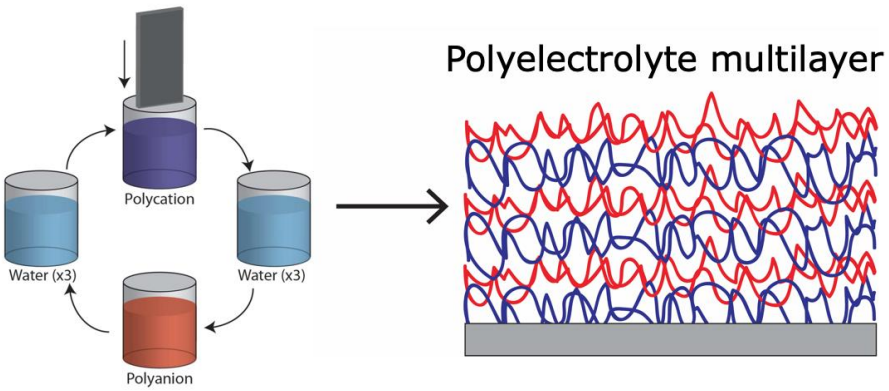

Figure 2. Layer-by-layer dip coating of PEMs

Two typical growth behaviors are observed in PEMs. One is linear growth, which means the thickness and mass of the PEM increases linearly with deposited layer number.[21] The other growth behavior is exponential growth, which means that the thickness and mass of the PEM increase exponentially with layer number.[22,23] During linear growth of PEMs, the polyelectrolyte in solution is adsorbed onto the previous polyelectrolyte layer via electrostatic force, which results in a charge overcompensation and inversion on the PEM surface. The polyelectrolyte layers in linear growth PEMs tend to interpenetrate only with neighboring layers.[24] However, in exponential growth PEMs, at least one polyelectrolyte is able to diffuse across layers during the deposition process.[25] The growth behavior of PEMs can be altered between those two categories by changing the assembly parameters. For example, PEMs assembled from poly(allylamine hydrochloride) (PAH) and PSS, or PDADMAC and PSS, which have typical linear growth behavior under room temperature and low salt concentration, will have exponential growth behavior under high salt concentration.[26,27] PEMs with different growth behavior (linear or exponential) are expected to have different internal structures and mechanical properties, which can affect their performance and appropriateness for potential applications. Ionic strength in the solution and the charge density of polyelectrolytes are key factors that can affect polyelectrolyte adsorption, which is important in layer-by-layer deposition of polyelectrolytes.[28,29] A critical charge density is necessary to obtain steady film growth during polyelectrolyte deposition.[30]

2.2.2 Mechanism of polyelectrolytes adsorption

Polyelectrolytes are adsorbed onto oppositely charged surfaces during the deposition process. The surface charge is typically inversed after the adsorption of an additional layer, which is

important for the following layer deposition. The adsorption of a polyelectrolyte layer will lead to a charge overcompensation. For polyelectrolytes adsorbed directly on the substrate surface, i.e. the first layer of a PEM, the layer conformation is affected by charge density and flexibility of the polyelectrolyte chain.[31] For flexible chains, large charge overcompensation is provided by the loops and tails of the chain. On the other hand, the adsorption of rigid chains will lead to a more flat layer conformation, which results in a small charge overcompensation.[31,32] As discussed in the previous section, the flexibility of polyelectrolyte chains can be affected by the ionic strength of polyelectrolyte solutions. Thus, large charge overcompensation will be achieved under higher ionic strength with more flexible chains, while small charge overcompensation will occur under lower ionic strength with stiffer chains.

After the first layer adsorption, each additional polyelectrolyte layer will be deposited onto a previous polyelectrolyte layer. Therefore, interlayer diffusion plays an important role in multilayer deposition process. A model developed by Donath *et al.* described that, during the adsorption of an addition polyelectrolyte layer, one third of the charges in the additional layer will diffuse in and form ion pairs with the previous layer. The other two thirds of the additional layer will be compensated by small counterions in solution, which can form ion pairs after adsorption of following layer.[33] However, this model can only be used to describe linear growth behavior, which means thickness and mass of PEMs increase linearly with layer number. Other models that can be used to describe exponential growth behavior of PEMs were developed as well.[26,34] Those models described a molecular diffusion behavior during polyelectrolyte adsorption process. In the exponential growth behavior, at least one kind of polyelectrolytes is able to diffuse across layers. During the adsorption process, the excess polyelectrolytes in the entire PEM will diffuse across the layers and reach the interface between the PEM and polyelectrolyte solution to compensate

with newly adsorbed polyelectrolyte. With increasing layer numbers, the amount of excess polyelectrolyte in PEM increases, so the PEM will be able to compensate more income polyelectrolytes. This results in an increase of adsorption amount of polyelectrolyte with layer number increase, which makes the growth behavior exponential.

2.2.3 Factors Controlling Growth Behavior of PEMs

PEMs exhibit two typical growth behavior: linear and exponential. Materials selection can influence the growth behavior of PEMs. Under low salt concentration, PEMs assembled from PAH/PSS, or PDADMAC/PSS, have typical linear growth behavior. However, PEMs assembled from hyaluronic acid (HA)/poly-L-lysine (PLL) or poly-L-glutamic acid (PGA)/PLL grow exponentially under the salt concentration. The exponential growth behavior of the PEM is related with the diffusion of polyelectrolytes across the multilayers during deposition process.[21,34,35] For PEMs with exponential growth behavior, at least one polyelectrolyte is able to diffuse across layers, while for linear growth PEMs, polyelectrolytes are not able to diffuse into the multilayers. During the adsorption process, the excess polyelectrolytes within the multilayers will move to the PEM surface and compensate with the newly adsorbed oppositely charged polyelectrolytes. With the thickness increases, polyelectrolyte uptake capacity of the PEM increases as well, which results in an exponential growth behavior.

Molecular weight can influence the diffusivity of polyelectrolytes through the PEM. For example, low molecular weight PLL can diffuse through the entire multilayer construct during the deposition of (HA/PLL) PEMs, while the diffusion of high molecular weight PLL is restricted.[26] The stronger coiling of high molecular weight polyelectrolytes also makes the charges along the

chain harder to access compared to low molecular weight polyelectrolytes, which results in a nonstoichiometry with excess amount of high molecular weight polyelectrolytes in the PEM.[36]

Charge density of polyelectrolytes can affect the growth behavior of the PEM. A minimum charge density is necessary to achieve continuous growth of the PEM. Below a certain charge density, there are insufficient ion pairs to form stable PEMs.[36] Beside charge density, charge distribution along the polyelectrolyte chain also plays an important role. PEMs can be assembled from a block-copolymer with a short strongly charged block, while the number of charged units along the polyelectrolyte chains is only 10% of the total monomer number. The charge density of this block-copolymer is lower than the critical charge density required for PEM formations when using polyelectrolytes with evenly distributed charged units.[37]

The formation of PEMs can be strongly influenced by the salt concentration in solution. The counterions can screen the charge repulsion along the polyelectrolyte chains and results in a more coiled structure. This will lead to a thicker PEM. Adding salt also reduces the number of ion pairs, which decreases the stability of the PEM. However, this will increase the diffusivity of polyelectrolytes within the PEM, as the interaction between polyelectrolytes are weakened.[37] Increase of diffusivity can result in an exponential growth behavior, as discussed in the previous section. For example, the growth behavior of PEMs assembled from PAH/PSS and PDADMAC/PSS can be changed from linear to exponential when the salt concentration is increased.[26,27]

2.2.4 Applications of PEMs

Since Decher's pioneering research in the early 1990's,[6,38] PEMs have been extensively studied and different applications of PEMs have been developed. PEMs are widely used for controlling

and modifying the surface properties of bulk materials, especially in the field of implantable biomedical materials.[39,40] Examples of PEMs applications in the biomedical field include controlling cell transfection or differentiation,[41,42] obtaining nanopatterned surfaces, design of a superhydrophobic surface, and functionalization of living cells.[43–45] PEMs can be used to manipulate cell adhesion and growth behavior by changing the stiffness of the coating. For example, the mechanical property of PEM coating assembled from poly(acrylic acid) (PAA) and PAH can be tuned by varying the assembly pH. PAA/PAH PEMs have higher elastic modulus with higher crosslink density, which results in better cell adhesion and growth.[46] Stiffness of PEMs can also be tailored by having different polyelectrolyte combinations in one PEM. PEMs assembled from poly-l-lysine (PLL) and PAH can be stiffened by adding stiffer PSS/PAH bilayers onto the film surface.[47]

PEMs have also been applied as drug-eluting coatings for biomedical implants, due to the ability to coat substrate with complex geometry and the capacity of loading and releasing drugs. PEMs have previously been used for the controlled release of BMP-2 from orthopedic implant surfaces. Macdonald *et al*. first demonstrated that PEMs are capable of control the release of BMP-2, while the released BMP-2 maintained its ability to induce bone differentiation.[40] Peterson *et al* showed that growth factors adsorbed on PEMs coated anodized titanium surface can achieve a sustained release over 25 days.[48] Salvi *et al.* demonstrated that the release behavior of BMP-2 covered by poly-L-histidine (PLH) and poly(methacrylic acid) (PMAA) multilayers can be changed by varying the assembly pH of the PEM.[14]

2.3 Polyelectrolyte Complexes (PECs)

2.3.1 Thermodynamics of PEC formation

PECs can be assembled by mixing aqueous solutions of oppositely charged polyelectrolyte, which result in phases stabilized by electrostatic interactions between oppositely charged polyelectrolyte chains.[49,50] Polyelectrolyte chains in solution are surrounded by a layer of small counterions. This counter ion layer has a lower entropy than the free counterions in solution. During complexation, the small counterions surrounding the polyelectrolyte chain are released into solution, which increases system entropy.[51] Enthalpy change also plays a role in driving complexation. While entropy change always contribute to the complexation by being positive, complexation enthalpy can vary between positive and negative, as polyelectrolyte complexation can be either exothermic or endothermic depending on salt concentration (Figure 3).[52] Under low salt concentration, the electrostatic energy difference between separate polyelectrolyte and polyelectrolyte complexes is large enough to make the complexation exothermic. Under high salt concentration, the energy released by forming new ion pairs between polyelectrolyte chains cannot compensate for the energy gap created by the release of small counterions, which makes the complexation endothermic.

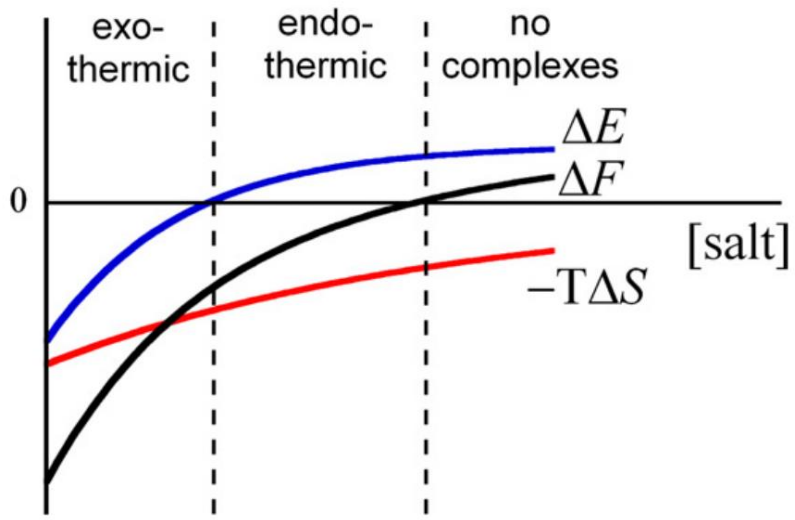

Figure 3. Qualitative picture of the effect of salt concentration of total complexation free energy (ΔF), Coulombic energy (ΔE) and entropic contribution (-TΔS). Adapted from ref [52].

2.3.2 Factors controlling PEC assembly and properties

2.3.2.1 Effect of salt concentration

As discussed in previous sections, the counterions concentration in polyelectrolyte solutions can affect the molecular conformation by screening charge interactions along polyelectrolyte chains.[5] Upon increasing the ionic strength of polyelectrolyte solutions, polyelectrolyte chain conformation can change from a stiff rod-like conformation to a soft coil-like conformation. This change in molecular conformation will further affect the structure and properties of assembled PECs. Wang *et al.* previously reported that by doping a PDADMAC/PSS PEC using KBr salt solutions of different concentrations, PECs can be changed from solid complexes to liquid complex coacervates.[2] Salt doping breaks the ion pairs between polyelectrolyte chains and decreases the crosslink density of PEC network.

$$Pol^{+}Pol^{-} + A^{+} + B^{-} = Pol^{+}B^{-} + Pol^{-}A^{+} \quad (1)$$

The doping process is illustrated in Equation 1, where salt ions are represented by A^+ and B^-, polyelectrolyte ion pairs are represented by Pol^+Pol^-. Salt doping was also used to improve the processability of PECs. The Schlenoff group used salt water to plasticize as-assembled PECs and then processed the PECs via extrusion.[3] Extrusion was possible under room temperature and in aqueous environment. The extruded PECs exhibited tough and dense structures.

2.3.2.2 Effect of assembly pH

Strong polyelectrolytes will fully disassociate under most conditions, so varying pH value of the solution will not dramatically affect the linear charge density on the molecular chain. However, for weak polyelectrolytes, linear charge density can be varied a lot by changing the solution pH, as their degrees of disassociation are pH dependent. For example, PAA, which is a weak polyelectrolyte and has a pK_a around 4.5, will depronated under low pH condition.[53] This property can be used to block the electrostatic interaction between oppositely charged polyelectrolytes and prevent complexation under certain pH condition.[54] Okeyo *et al*. developed a photo-directed complexation method by using a photoacid generator that can change the local pH of the precursor polyelectrolytes solution.[55] PSS and PAH were previously dissolved in basic solution together with the acid generator, in which the protonation (disassociation) of PAH was prohibited. Under UV initiation, pH value of the precursor solution was decreased, which caused protonation of PAH, and resulted in complexation with PSS. This approach can be applied to photo-trigged 3D printing of PEC micro-structure.

2.3.2.3 Other factors influencing PEC properties

Materials selection, including using polyelectrolytes with different molecular weights or chain lengths, will affect the properties of PECs. For example, PECs assemble from chitosan and poly (methacrylic acid) (PMAA), the molecular weight of PMAA will influence the stability of PEC.[56]

By increasing the molecular length of PMAA, the PEC stability decreased, with increased solubility in solution. This is due to the different chain conformation of polyelectrolyte with different molecular weight, which affects the percentage of charge on molecular chain that participated the complexation.

The mixing ratio of oppositely charged polyelectrolyte solutions can affect the stoichiometry of PEC. Stoichiometric PECs are charge neutralized, as the polyelectrolyte are complexed in 1:1 charge ratio. For complexation between PSS and PDADMAC in pure water, mixing ratio does not substantially affect the stoichiometry of assembled PECs.[50] However, for PECs formed between PSS and a PDADMAC-PAA copolymer, quasi-soluble PEC were formed under a non-stoichiometric mixing ratio. PEC particles formed under this condition have a charge neutral core, while the excess charges form an outer layer that stabilize the PEC particle through electrostatic repulsion.[57]

2.3.3 Thermal transitions in PECs

Similar to charge neutral polymers, glass transitions or glass-transition-like thermal transitions exist in PECs as well. The relaxation of PEC networks under the influence of water was observed decades ago by Michaels *et al*.[58] However, the measurement of thermal transitions of PECs has been complicated by their affinity to water. Shamoun *et al*. reported that no thermal transition was observed for dried PECs assembled from PDADMAC and PSS.[59] Under the plasticization of water, the glass transition temperature (T_g) of PECs can be lowered and observed.[60,61]

Zhang *et al*. quantitively demonstrated the relationship between water molecules and the glass-transition-like thermal transition temperature in recent studies.[62,63] The inverse of transition temperature 1/T has a linear relationship with ln ($n_{water}/n_{intrinsic\ ion\ pair}$), where ($n_{water}/n_{intrinsic\ ion\ pair}$)

represents the number of water molecules surrounding each intrinsic ion pair of PEC. This relationship was demonstrated to be applicable to PECs assembled from weak polyelectrolytes combination of PAA/PAH under different pH conditions and strong polyelectrolytes combinations of PDADMAC/PSS under different salt concentrations. This means the relationship can be considered as a general rule for PEC systems. These studies indicate that the underlying mechanism of thermal transitions in PECs is dominated by the weakening of intrinsic ion pairs via water-ion pair interaction.

2.3.4 Biomedical Applications of PECs

As PECs have many similarities in structure and properties to natural biological tissues, they are studied as tissue scaffold and drug delivery materials.[64–66] The properties of PECs are highly responsive to environment change and assembly conditions, as discussed in previous sections. The charged unit provided by polyelectrolytes can affect cell attachment and early stage proliferation.[67] The physical and chemical properties of PECs allow them to closely mimic the property of the extracellular matrix (ECM). Because of the good biocompatibility under hydration state, hydrated PECs can work as tissue scaffold.[68]

PECs have also been studied as drug encapsulation delivery materials in past decades. The drugs or active substance can be incorporated within PECs by entrapping the solution-dissolved drug during PEC precipitation, or by adsorbing the substance into as-synthesized PEC particles.[69–71] Shiraishi *et al*. demonstrated that drug release rate can be manipulated by changing the molecular weight of polyelectrolytes, and *in vivo/in vitro* drug release behavior was studied.[72] Wen-Ching *et al*. developed PEC micro-spheres that have drug delivery ability while having high resistivity

under acidic conditions. These materials are designed for use as oral drug delivery systems when intestinal absorption is preferred.[73]

Conclusions

In this chapter, the mechanisms of PEMs and PECs formation were discussed. Applications of polyelectrolyte-based materials were introduced as well. The structure and properties of polyelectrolyte-based materials can be affected by different factors including materials selection, assembly conditions and post-assembly treatments. The functionality and performance of PEMs and PECs in those applications are determined by their structure and properties. Those properties include surface chemistry, topography, stiffness, glass transition temperature, etc. However, the relationship between internal structures and properties are still not fully understood. The overall goal of this research is to develop approaches to achieve fully tailorable properties of polyelectrolyte-based materials. To achieve this goal, materials selection and post-assembly treatment were applied to tailor the structure and properties of polyelectrolyte-based materials, which will be discussed in following chapters.

References

(1) Dautzenberg, H. Polyelectrolyte Complex Formation in Highly Aggregating Systems. 1. Effect of Salt: Polyelectrolyte Complex Formation in the Presence of NaCl. *Macromolecules* **1997**, *30* (25), 7810–7815.

(2) Wang, Q. F.; Schlenoff, J. B. The Polyelectrolyte Complex/Coacervate Continuum. *Macromolecules* **2014**, *47* (9), 3108–3116.

(3) Shamoun, R. F.; Reisch, A.; Schlenoff, J. B. Extruded Saloplastic Polyelectrolyte Complexes. *Adv. Funct. Mater.* **2012**, *22* (9), 1923–1931.

(4) Karibyants, N.; Dautzenberg, H. Characterization of PSS/PDADMAC-Co-AA Polyelectrolyte Complexes and Their Stoichiometry Using Analytical Ultracentrifugation. *Macromolecules* **1997**, *9297* (97), 7803–7809.

(5) Dobrynin, A. V; Rubinstein, M. Theory of Polyelectrolytes in Solutions and at Surfaces. **2005**, *30*, 1049–1118.

(6) Decher, G.; Hong, J. D.; Schmitt, J. Buildup of Ultrathin Multilayer Films by a Self-Assembly Process: III. Consecutively Alternating Adsorption of Anionic and Cationic Polyelectrolytes on Charged Surfaces. *Thin Solid Films* **1992**, *210–211* (PART 2), 831–835.

(7) Zhai, L.; Cebeci, F. C.; Cohen, R. E.; Rubner, M. F. Stable Superhydrophobic Coatings from Polyelectrolyte Multilayers. *Nano Lett.* **2004**, *4* (7), 1349–1353.

(8) Hiller, J.; Mendelsohn, J. D.; Rubner, M. F. Reversibly Erasable Nanoporous Anti-Reflection Coatings from Polyelectrolyte Multilayers. *Nat. Mater.* **2002**, *1* (1), 59–63.

(9) Kim, Y. S.; Lee, H. H.; Hammond, P. T. High Density Nanostructure Transfer in Soft Molding Using Polyurethane Acrylate Molds and Polyelectrolyte Multilayers. *Nanotechnology* **2003**, *14* (10), 1140–1144.

(10) Andreeva, D. V.; Skorb, E. V.; Shchukin, D. G. Layer-by-Layer Polyelectrolyte/Inhibitor Nanostructures for Metal Corrosion Protection. *ACS Appl. Mater. Interfaces* **2010**, *2* (7), 1954–1962.

(11) Wang, X.; Liu, F.; Zheng, X.; Sun, J. Water-Enabled Self-Healing of Polyelectrolyte

Multilayer Coatings. *Angew. Chemie - Int. Ed.* **2011**, *50* (48), 11378–11381.

(12) Zhu, Y.; Shi, J.; Shen, W.; Dong, X.; Feng, J.; Ruan, M.; Li, Y. Stimuli-Responsive Controlled Drug Release from a Hollow Mesoporous Silica Sphere/Polyelectrolyte Multilayer Core-Shell Structure. *Angew. Chemie - Int. Ed.* **2005**, *44* (32), 5083–5087.

(13) Berg, M. C.; Zhai, L.; Cohen, R. E.; Rubner, M. F. Controlled Drug Release from Porous Polyelectrolyte Multilayers. *Biomacromolecules* **2006**, *7* (1), 357–364.

(14) Salvi, C.; Lyu, X.; Peterson, A. M. Effect of Assembly pH on Polyelectrolyte Multilayer Surface Properties and BMP-2 Release. *Biomacromolecules* **2016**, *17* (6), 1949–1958.

(15) Peterson, A. M.; Pilz-Allen, C.; Möhwald, H.; Shchukin, D. G. Evaluation of the Role of Polyelectrolyte Deposition Conditions in Growth Factor Release. *J. Mater. Chem. B* **2014**, *2* (18), 2680–2687.

(16) Shchukina, E. M.; Shchukin, D. G. LbL Coated Microcapsules for Delivering Lipid-Based Drugs. *Adv. Drug Deliv. Rev.* **2011**, *63* (9), 837–846.

(17) Delcea, M.; Möhwald, H.; Skirtach, A. G. Stimuli-Responsive LbL Capsules and Nanoshells for Drug Delivery. *Adv. Drug Deliv. Rev.* **2011**, *63* (9), 730–747.

(18) Schlenoff, J. B.; Dubas, S. T.; Farhat, T. Sprayed Polyelectrolyte Multilayers. *Langmuir* **2000**, *16* (26), 9968–9969.

(19) Lee, S. S.; Hong, J. D.; Kim, C. H.; Kim, K.; Koo, J. P.; Lee, K. B. Layer-by-Layer Deposited Multilayer Assemblies of Ionene-Type Polyelectrolytes Based on the Spin-Coating Method. *Macromolecules* **2001**, *34* (16), 5358–5360.

(20) Jiang, C.; Markutsya, S.; Tsukruk, V. V. Collective and Individual Plasmon Resonances in Nanoparticle Films Obtained by Spin-Assisted Layer-by-Layer Assembly. *Langmuir* **2004**, *20* (3), 882–890.

(21) Porcel, C.; Lavalle, P.; Ball, V.; Decher, G.; Senger, B.; Voegel, J. C.; Schaaf, P. From Exponential to Linear Growth in Polyelectrolyte Multilayers. *Langmuir* **2006**, *22* (9), 4376–4383.

(22) Vidyasagar, A.; Sung, C.; Gamble, R.; Lutkenhaus, J. L. Thermal Transitions in Dry and Hydrated Layer-by-Layer Assemblies Exhibiting Linear and Exponential Growth. *ACS Nano* **2012**, *6* (7), 6174–6184.

(23) Schlenoff, J. B.; Dubas, S. T. Mechanism of Polyelectrolyte Multilayer Growth: Charge Overcompensation and Distribution. *Macromolecules* **2001**, *34* (3), 592–598.

(24) Jomaa, H. W.; Schlenoff, J. B. Salt-Induced Polyelectrolyte Interdiffusion in Multilayered Films: A Neutron Reflectivity Study. *Macromolecules* **2005**, *38* (20), 8473–8480.

(25) Picart, C.; Mutterer, J.; Richert, L.; Luo, Y.; Prestwich, G. D.; Schaaf, P.; Voegel, J.-C.; Lavalle, P. Molecular Basis for the Explanation of the Exponential Growth of Polyelectrolyte Multilayers. *Proc. Natl. Acad. Sci.* **2002**, *99* (20), 12531–12535.

(26) Porcel, C.; Lavalle, P.; Decher, G.; Senger, B.; Voegel, J. C.; Schaaf, P. Influence of the Polyelectrolyte Molecular Weight on Exponentially Growing Multilayer Films in the Linear Regime. *Langmuir* **2007**.

(27) Picart, C.; Gergely, C.; Arntz, Y.; Voegel, J. C.; Schaaf, P.; Cuisinier, F. J. G.; Senger, B. Measurement of Film Thickness up to Several Hundreds of Nanometers Using Optical Waveguide Lightmode Spectroscopy. *Biosens. Bioelectron.* **2004**, *20* (3), 553–561.

(28) Glinel, K.; Moussa, A.; Jonas, A. M.; Laschewsky, A. Influence of Polyelectrolyte Charge Density on the Formation of Multilayers of Strong Polyelectrolytes at Low Ionic Strength. *Langmuir* **2002**, *18* (4), 1408–1412.

(29) Schoeler, B.; Kumaraswamy, G.; Caruso, F. Investigation of the Influence of

Polyelectrolyte Charge Density on the Growth of Multilayer Thin Films Prepared by the Layer-by-Layer Technique. *Macromolecules* **2002**, *35* (3), 889–897.

(30) Steitz, R.; Leiner, V.; Siebrecht, R.; V. Klitzing, R. Influence of the Ionic Strength on the Structure of Polyelectrolyte Films at the Solid/Liquid Interface. *Colloids Surfaces A Physicochem. Eng. Asp.* **2000**, *163* (1), 63–70.

(31) Joanny, J. F. Polyelectrolyte Adsorption and Charge Inversion. *Eur. Phys. J. B* **1999**, *9* (6), 117–122.

(32) Joanny, J. F.; Castelnovo, M.; Netz, R. Adsorption of Charged Polymers. *J. Phys. Condens. Matter* **2000**, *12* (8A).

(33) Donath, E.; Walther, D.; Shilov, V. N.; Knippel, E.; Budde, A.; Lowack, K.; Helm, C. A.; Möhwald, H. Nonlinear Hairy Layer Theory of Electrophoretic Fingerprinting Applied to Consecutive Layer by Layer Polyelectrolyte Adsorption onto Charged Polystyrene Latex Particles. *Langmuir* **1997**, *13* (20), 5294–5305.

(34) Lavalle, P.; Picart, C.; Mutterer, J.; Gergely, C.; Reiss, H.; Voegel, J.C.; Senger, B.; Schaaf, P. Modeling the Buildup of Polyelectrolyte Multilayer Films Having Exponential Growth. *J. Phys. Chem. B* **2004**.

(35) Nestler, P.; Pavogel, M.; Helm, C. A. Influence of Polymer Molecular Weight on the Parabolic and Linear Growth Regime of PDADMAC/PSS Multilayers. *Macromolecules* **2013**, *46* (14), 5622–5629.

(36) Bharadwaj, S.; Montazeri, R.; Haynie, D. T. Direct Determination of the Thermodynamics of Polyelectrolyte Complexation and Implications Thereof for Electrostatic Layer-by-Layer Assembly of Multilayer Films. *Langmuir* **2006**.

(37) Voigt, U.; Khrenov, V.; Tauer, K.; Hahn, M.; Jaeger, W.; Von Klitzing, R. The Effect of

Polymer Charge Density and Charge Distribution on the Formation of Multilayers. *J. Phys. Condens. Matter* **2003**.

(38) Decher, G.; Hong, J. D. Buildup of Ultrathin Multilayer Films by a Self-Assembly Process, 1 Consecutive Adsorption of Anionic and Cationic Bipolar Amphiphiles on Charged Surfaces. *Makromol. Chemie. Macromol. Symp.* **1991**, *46* (1), 321–327.

(39) Etienne, O.; Picart, C.; Taddei, C.; Haikel, Y.; Dimarcq, J. L.; Schaaf, P.; Voegel, J. C.; Ogier, J. A.; Egles, C. Multilayer Polyelectrolyte Films Functionalized by Insertion of Defensin: A New Approach to Protection of Implants from Bacterial Colonization. *Antimicrob. Agents Chemother.* **2004**.

(40) Macdonald, M. L.; Samuel, R. E.; Shah, N. J.; Padera, R. F.; Beben, Y. M.; Hammond, P. T. Tissue Integration of Growth Factor-Eluting Layer-by-Layer Polyelectrolyte Multilayer Coated Implants. *Biomaterials* **2011**.

(41) Lee, I. C.; Wu, Y. C. Assembly of Polyelectrolyte Multilayer Films on Supported Lipid Bilayers to Induce Neural Stem/Progenitor Cell Differentiation into Functional Neurons. *ACS Appl. Mater. Interfaces* **2014**.

(42) Arntz, Y.; Ball, V.; Benkirane-Jessel, N.; Boulmedais, F.; Debry, C.; Dimitrova, M.; Elkaim, R.; Haikel, Y.; Hemmerl, J.; Lavalle, P.; et al. Polymers in Biomaterials Science: From Surface Functionalisation to Tissue Engineering. *Actual. Chim.* **2007**.

(43) Zhang, C.; Hirt, D. E. Layer-by-Layer Self-Assembly of Polyelectrolyte Multilayers on Cross-Section Surfaces of Multilayer Polymer Films: A Step toward Nano-Patterning Flexible Substrates. *Polymer.* **2007**.

(44) Huang, X.; Zacharia, N. S. Surfactant Co-Assembly and Ion Exchange to Modulate Polyelectrolyte Multilayer Wettability. *Soft Matter* **2013**.

(45) Fakhrullin, R. F.; Zamaleeva, A. I.; Minullina, R. T.; Konnova, S. A.; Paunov, V. N. Cyborg Cells: Functionalisation of Living Cells with Polymers and Nanomaterials. *Chemical Society Reviews*. 2012.

(46) Thompson, M. T.; Berg, M. C.; Tobias, I. S.; Rubner, M. F.; Van Vliet, K. J. Tuning Compliance of Nanoscale Polyelectrolyte Multilayers to Modulate Cell Adhesion. *Biomaterials* **2005**.

(47) Kocgozlu, L.; Lavalle, P.; Koenig, G.; Senger, B.; Haikel, Y.; Schaaf, P.; Voegel, J.-C.; Tenenbaum, H.; Vautier, D. Selective and Uncoupled Role of Substrate Elasticity in the Regulation of Replication and Transcription in Epithelial Cells. *J. Cell Sci.* **2010**.

(48) Peterson, A. M.; Pilz-Allen, C.; Kolesnikova, T.; Möhwald, H.; Shchukin, D. Growth Factor Release from Polyelectrolyte-Coated Titanium for Implant Applications. *ACS Appl. Mater. Interfaces* **2014**.

(49) Smid, J. Polyelectrolyte Complexes. *American Chemical Society, Polymer Preprints, Division of Polymer Chemistry*; 1991.

(50) Dautzenberg, H. Polyelectrolyte Complex Formation in Highly Aggregating Systems. 1. Effect of Salt: Polyelectrolyte Complex Formation in the Presence of NaCl. *Macromolecules* **1997**.

(51) Bucur, C. B.; Sui, Z.; Schlenoff, J. B. Ideal Mixing in Polyelectrolyte Complexes and Multilayers: Entropy Driven Assembly. *J. Am. Chem. Soc.* **2006**, *128* (42), 13690–13691.

(52) Laugel, N.; Betscha, C.; Winterhalter, M.; Voegel, J. C.; Schaaf, P.; Ball, V. Relationship between the Growth Regime of Polyelectrolyte Multilayers and the Polyanion/Polycation Complexation Enthalpy. *J. Phys. Chem. B* **2006**.

(53) Smith, R. J.; Long, C. T.; Grunlan, J. C. Transparent Polyelectrolyte Complex Thin Films

with Ultralow Oxygen Transmission Rate. *Langmuir* **2018**, *34*, 11086–11091.

(54) Litmanovich, E. A.; Chernikova, E. V.; Stoychev, G. V.; Zakharchenko, S. O. Unusual Phase Behavior of the Mixture of Poly(Acrylic Acid) and Poly(Diallyldimethylammonium Chloride) in Acidic Media. *Macromolecules* **2010**.

(55) Okoye, N. H.; De Silva, U. K.; Wengatz, J. A.; Lapitsky, Y. Photodirected Assembly of Polyelectrolyte Complexes. *Polymer*. **2015**, *60*, 69–76.

(56) de Vasconcelos, C. L.; Bezerril, P. M.; dos Santos, D. E. S.; Dantas, T. N. C.; Pereira, M. R.; Fonseca, J. L. C. Effect of Molecular Weight and Ionic Strength on the Formation of Polyelectrolyte Complexes Based on Poly(Methacrylic Acid) and Chitosan. *Biomacromolecules* **2006**, *7* (4), 1245–1252.

(57) Sui, Z.; Jaber, J. A.; Schlenoff, J. B. Polyelectrolyte Complexes with PH-Tunable Solubility. *Macromolecules* **2006**, *39* (23), 8145–8152.

(58) Michaels, A. S. Polyelectrolyte Complexes. *Ind Eng Chem* **1965**, *57* (10), 32–40.

(59) Shamoun, R. F.; Hariri, H. H.; Ghostine, R. A.; Schlenoff, J. B. Thermal Transformations in Extruded Saloplastic Polyelectrolyte Complexes. *Macromolecules* **2012**, *45* (24), 9759–9767.

(60) Hariri, H. H.; Lehaf, A. M.; Schlenoff, J. B. Mechanical Properties of Osmotically Stressed Polyelectrolyte Complexes and Multilayers: Water as a Plasticizer. *Macromolecules* **2012**, *45* (23), 9364–9372.

(61) Fu, J.; Abbett, R. L.; Fares, H. M.; Schlenoff, J. B. Water and the Glass Transition Temperature in a Polyelectrolyte Complex. *ACS Macro Lett.* **2017**, *80* (3), 1114–1118.

(62) Zhang, Y.; Li, F.; Valenzuela, L. D.; Sammalkorpi, M.; Lutkenhaus, J. L. Effect of Water on the Thermal Transition Observed in Poly(Allylamine Hydrochloride)-Poly(Acrylic Acid)

Complexes. *Macromolecules* **2016**, *49* (19), 7563–7570.

(63) Zhang, Y.; Batys, P.; O'Neal, J. T.; Li, F.; Sammalkorpi, M.; Lutkenhaus, J. L. Molecular Origin of the Glass Transition in Polyelectrolyte Assemblies. *ACS Cent. Sci.* **2018**, *4* (5), 638–644.

(64) Verma, D.; Katti, K. S.; Katti, D. R. Polyelectrolyte-Complex Nanostructured Fibrous Scaffolds for Tissue Engineering. *Mater. Sci. Eng. C* **2009**, *29* (7), 2079–2084.

(65) Rosso, F.; Barbarisi, A.; Barbarisi, M.; Petillo, O.; Margarucci, S.; Calarco, A.; Peluso, G. New Polyelectrolite Hydrogels for Biomedical Applications. *Mater. Sci. Eng. C* **2003**, *23* (3), 371–376.

(66) Lankalapalli, S.; Kolapalli, V. R. M. Polyelectrolyte Complexes: A Review of Their Applicability in Drug Delivery Technology. *Indian J. Pharm. Sci.* **2009**, *71* (5), 481.

(67) Olenych, S. G.; Moussallem, M. D.; Salloum, D. S.; Schlenoff, J. B.; Keller, T. C. S. Fibronectin and Cell Attachment to Cell and Protein Resistant Polyelectrolyte Surfaces. *Biomacromolecules* **2005**, *6* (6), 3252–3258.

(68) Pallab, P.; Jyotsnendu, G.; Gopal, S.; Haladhar, D. S.; Kaushala, P. M.; Jayesh, B.; Rinti, B.; Dhirendra, B. Comparative Evaluation of Heating Ability and Biocompatibility of Different Ferrite Based Magnetic Fluids for Hyperthermia Application. *J. Biomed. Mater. Res. B. Appl. Biomater.* **2007**, *81B* (1), 12–22.

(69) Berger, J.; Reist, M.; Mayer, J. M.; Felt, O.; Gurny, R. Structure and Interactions in Chitosan Hydrogels Formed by Complexation or Aggregation for Biomedical Applications. *European Journal of Pharmaceutics and Biopharmaceutics*. **2004**.

(70) Kawashima, Y.; Handa, T.; Kasai, A.; Takenaka, H.; Lin, S. Y.; Ando, Y. Novel Method for the Preparation of Controlled-release Theophylline Granules Coated with a

Polyelectrolyte Complex of Sodium Polyphosphate–chitosan. *J. Pharm. Sci.* **1985**.

(71) Mi, F. L.; Sung, H. W.; Shyu, S. S. Drug Release from Chitosan-Alginate Complex Beads Reinforced by a Naturally Occurring Cross-Linking Agent. *Carbohydr. Polym.* **2002**.

(72) Shiraishi, S.; Imai, T.; Otagiri, M. Controlled Release of Indomethacin by Chitosan-Polyelectrolyte Complex: Optimization and in Vivo/in Vitro Evaluation. *J. Control. Release* **1993**, *25* (3), 217–225.

(73) Lin, W. C.; Yu, D. G.; Yang, M. C. pH-Sensitive Polyelectrolyte Complex Gel Microspheres Composed of Chitosan/Sodium Tripolyphosphate/Dextran Sulfate: Swelling Kinetics and Drug Delivery Properties. *Colloids Surfaces B Biointerfaces* **2005**, *44* (2–3), 143–151.

Chapter 3: The Princess and the Pea Effect: Influence of the first layer on polyelectrolyte multilayer assembly and properties

Published in *Journal of Colloid and Interface Science*, 2017, 502, 165-171

The Princess and the Pea Effect: Influence of the first layer on polyelectrolyte multilayer assembly and properties

Xuejian Lyu[1], Amy M. Peterson[1,2]

[1]Department of Mechanical Engineering, Worcester Polytechnic Institute, 100 Institute Road, Worcester, MA 01609

[2]Department of Chemical Engineering, Worcester Polytechnic Institute, 100 Institute Road, Worcester, MA 01609

Abstract

In many applications of polyelectrolyte multilayers (PEMs), a base polycation layer is adsorbed to promote adhesion of the PEM to the substrate. In this report, the effect of the first polyelectrolyte adsorbed in a PEM was investigated by assembling PEMs with first layer polycations of different chemistries and molecular weights. In this study, quartz crystal microbalance with dissipation monitoring (QCM-D) was used to monitor the PEM assembly process. First layer choice affects the total mass accumulation of the PEM as well as the stoichiometry of the PEM, although linear growth was observed in all cases. PEM thickness was also affected by first layer choice, although not consistent with changes in mass. Combined with the stoichiometry results, these findings indicate that the structure of a PEM is fundamentally different depending on first layer chemistry and molecular weight. PEM topography is also affected by first layer choice. Selection of appropriate first layer material is therefore an important consideration in the design of a PEM and changing first layer material may be a facile way to tailor the structure and properties of PEMs.

Keywords: Polyelectrolyte multilayer; Polymer coatings; Quartz crystal microbalance; Ellipsometry; Atomic force microscopy, Surface chemistry

1. Introduction

PEMs are polymeric structures that are prepared via layer-by-layer assembly of polycations and polyanions on a substrate. This technique, which was first described in the early 1990's, provides an approach to assemble multi-functional polymer structures.[1–4] PEM coatings have been used for obtaining superhydrophobic [5] and nano-patterned surfaces,[6,7] as well as corrosion inhibition[8] and self-healing.[9] One important application of PEMs is controlled release of biologically relevant molecules from PEM coatings or capsules.[10–15]

Although PEMs have demonstrated uses in a wide range of applications, controlling PEM properties is challenging because of their sensitivity to many material and processing parameters. As is described below, the structure and properties of a PEM are dependent upon many material and assembly parameters including polyelectrolyte molecular weight,[16] pH,[17] and salt concentration.[18–20]

Polyelectrolyte molecular weight has been shown to affect PEM assembly. In work from Sui *et al.*, lower molecular weight poly(sodium 4-styrenesulfonate) (PSS) stripped off polyanions instead of adsorbing to the PEM during the assembly step.[16] Greater stripping was observed with increasing salt concentration, as salt increases polyelectrolyte mobility. Lower molecular weight poly(methacrylic acid) (PMAA) within a PMAA/poly-L-histidine PEM was shown to reduce the amount of burst release and increase sustained release of negatively charged model polypeptides.[21]

Assembly pH is a simple parameter to adjust that changes weak polyelectrolyte solution conformation, leading to differences in the resulting PEMs. Shiratori and Rubner observed that the thickness of weak polyelectrolyte PEMs decrease with increasing assembly pH.[17] We previously reported that assembly pH affects surface energy and the release rate of bone morphogenetic protein 2 (BMP2),[12] with the greatest cumulative BMP2 release occurring from PEMs assembled at pH=4 and lowest cumulative release at pH = 6-7. Total surface energy decreased with increase of assembly pH. However, statistically significant changes in roughness and peak-valley height were not observed in these PEMs, which all used BMP2 as the first layer.

Salt concentration, both as an assembly condition and in a post-assembly annealing, can affect PEM surface morphology as well. Interdiffusion in PEMs assembled from poly (diallyldimethylammonium chloride) (PDADMAC) and PSS was enhanced after annealing in a salt solution.[18] PEMs assembled from PDADMAC and PSS solutions with high salt concentrations exhibited greater surface roughness as compared to PEMs assembled under low salt concentration conditions.[20]

While PEM properties can be modulated by changing assembly conditions and materials, the internal structure of PEMs and how this structure affects bulk material properties are still not fully understood. Within a PEM, electrostatic interactions between oppositely charged polyelectrolytes lead to interpolymer ionic condensation. Hydrogen bonding, van der Waals forces, hydrophobic interactions and dipole interactions are non-Coulombic interactions that are also involved in their assembly.[22,23] Additionally, the relative rigidity and flexibility of polyelectrolytes affects interdiffusion.[24] All of these interactions will affect the assembly process and internal structure of the final PEM film.

Buron *et al*. demonstrated that different functionalization of a substrate can dramatically change PEM structure and properties.[25] The density and distribution of functional groups on a substrate affect initial polyelectrolyte adsorption and thus influence subsequent polyelectrolyte adsorption and the final PEM structure. Precursor layer surface charge has been shown to affect PEM assembly.[26] Peng *et al*. used four bilayers of PEI/PSS as the precursor layer and the surface charge could be tuned with assembly pH. By tuning the surface charge of precursor layer from negative to positive, the following layers will have a slower growth rate at the initial state. The substrate has also been shown to affect polyelectrolyte adsorption.[27] At the initial adsorption stage, polyelectrolytes tend to form islands if there are locations with a high concentration of local charges like scratches, holes, edges, and foreign particles on the substrate surface. Additionally, a PEI anchoring layer has been reported to enhance PEM film amount adsorbed, regardless of substrate material and heterogeneity.[28,29] It was also shown that PEMs deposited from different salt concentration solutions will have different surface wetting ability, and tend to be independent of substrate material after a certain layer number was reached.[30]

The first layer of a PEM functions as a contact layer between the substrate and the rest of the PEM film; thus, the composition of the first layer may have an impact on the properties of the entire film. Peterson *et al*. reported a change of surface roughness when poly-L-histidine hydrochloride (PLH) was used as the first layer material instead of BMP2 in PEMs assembled from poly(methacrylic acid) (PMAA) and PLH.[13] Interestingly, differences in pre-osteoblast proliferation and alkaline phosphatase (ALP) enzyme activity, a marker of osteoblastic differentiation, were also observed that were not consistent with BMP2 release, i.e. cells on some of the BMP2 eluting PEMs exhibited less ALP enzyme activity than non-BMP2 eluting PEMs. These unexpected results highlight the importance of surface topography on cell fate, and also

suggest that changes in the first layer of a PEM could affect surface topography, and potentially other surface properties.

In this study, we explore the role of first layer material selection on PEM assembly, structure and a range of PEM properties. First layer chemistry and molecular weight is shown to affect PEM mass, stoichiometry, thickness, roughness, and water contact angle. These results are discussed within the context of the effect of first layer material selection on PEMs structure and properties and mechanisms are proposed. This is the first time quartz crystal microbalance with dissipation monitoring (QCM-D) has been applied to study the influence of first layer material on PEM assembly. Using QCM-D, mass accumulation was tracked during assembly process, and it was also possible to study the adsorption behavior of PSS and PDADMAC separately.

2. Experimental

2.1 Materials

Polyethylenimine (PEI 600K, branched, M_r 600,000-1,000,000), Poly(allylamine hydrochloride) (PAH, M_w ~17,500), PDADMAC (M_w 100,000-200,000, 20 wt.% in water), PSS (M_w ~200,000, 30 wt.% in water) and PLH (molecular weight ≥ 5000) were purchased from Sigma-Aldrich. Polyethylenimines (PEI 10K, branched, molecular weight 10,000, and PEI 70K, branched, molecular weight 70,000) were purchased from Alfa-Aesar. Polyethylenimines (PEI Linear, molecular weight ~25,000) was purchased from Polysciences. All chemicals were used without additional modification.

2.2 Polyelectrolyte Multilayer Preparation

PEMs were prepared on gold substrates (Q-Sense gold-coated sensors, QSX 301, and gold-coated quartz, purchased from PHASIS). The QSX 301 sensor is comprised of a thin quartz disc

coated with a 100 nm thick gold layer. Quartz substrates were coated with 100 nm of gold to maintain the same structure and properties as the QSX 301 sensor, while providing the necessary thicker quartz substrate for ellipsometry. PEIs with different molecular weights (10K, 70K and 600K), PAH, PLH, and PDADMAC were deposited as the first layers. PSS and PDADMAC were alternatingly deposited after the first layer. When coating PHASIS gold-coated quartz glass, each layer was prepared by immersing the substrate in a 1 mg/mL polyelectrolyte solution for 15 minutes followed by three rinses in 60ml DI water for 1 min each. In total, 11 polyelectrolyte layers (5.5 bilayers) were deposited. When using Q-Sense gold sensors as the substrate, each layer was coated by flowing polyelectrolyte solutions across the sensor as described below.

2.3 QCM-D Analysis

QCM-D was used to characterize the adsorption of each layer during the PEM assembly process. QCM and QCM-D are common analytical techniques used to monitor changes in mass during thin film deposition process.[12,31–33] A quartz crystal with electrodes on two sides is used as the sensor. Applying a voltage over the electrodes causes the quartz to vibrate at its resonance frequency. When the voltage is removed, the oscillation starts to decay. The resonance frequency and energy dissipation factor are extracted from this decay.

QCM-D records shifts in the sensor's resonant frequency and energy dissipation. Changes in the resonant frequency are related to mass changes at the sensor surface. This relationship is described by the Sauerbrey Equation, when the film is considered as rigid, evenly distributed, and sufficiently thin layers:[34]

$$\Delta f = -\frac{2f_0^2}{A\sqrt{\rho_q \mu_q}}\Delta m \tag{1}$$

where f_0 is the resonant frequency, μ_q and ρ_q are the shear modulus and density of the quartz crystal, A is surface area of the crystal, Δf and Δm are frequency change and mass change of the deposited film, respectively. As the film mass increases, the frequency decreases. Energy dissipation (D) represents the energy loss per oscillation period divided by the total energy stored in the oscillator, which is related to the viscoelastic properties of the film. For soft films, the amplitude of oscillation decreases faster than rigid films after the applied voltage on the sensor is removed.

The crystal can be excited to oscillate under different harmonics, or overtones. The number of overtones indicates the number of nodal plans that are parallel to the sensor surface. Only odd overtone numbers, n=1, 3, 5…, are available for the crystal to oscillate. Δf and ΔD are collected under multiple overtones. The frequency and energy dissipation can be described as functions of overtone number, thickness, density, viscosity and elasticity. By fitting the frequency and dissipation data under multiple overtones, variables including film thickness, density, viscosity and elasticity can be extracted.[35,36] In this research, mass accumulations and viscoelastic properties of PEMs were studied based on Δf and ΔD under the 3rd overtone.

By recording the frequency change during the deposition process, the total mass of the PEM film and mass accumulation per layer can be measured. Vogt *et al*. showed that frequency change could be simply related to mass change using the Sauerbrey equation for films that are sufficiently thin (t < 40 nm), which is consistent with the reported PEM films.[37] During the measurement, frequency change of each individual layer (Δf value after rinsing step) was recorded and then converted to mass change using Equation 1.

In this study, QCM-D was performed using a Q-Sense E4 (Biolin Scientific) on QSX 301 gold sensors. 1 mg/mL polyelectrolyte solutions were flowed at a constant flow rate of 50 μl/min through the QCM-D for the same amount of time as the dip coating process (15 min), with a rinsing

step of 10 min in DI water added between each deposition step. Four measurements were taken for each condition.

2.4 Ellipsometry Analysis

Film thickness was characterized using a multi-wavelength Spectroscopic Ellipsometer (SE) system (J. A. Woollam Co.). Ellipsometry measurements were performed on PEMs deposited on gold-coated quartz. The gold layer on quartz has a thickness of 100 nm. The incident beam wavelength is 300 - 800 nm. Within this range, the incident beam penetration depth is approximately 13 nm, so no backside reflection will occur. PEM thickness was measured at incident beam angles of 65°, 70° and 75°. For each condition, three samples were prepared and measurements were collected at three data points per sample (9 data points in total). Thickness values were fitted using dedicated J.A. Woollam software, with fitting parameters Psi and Delta. The fitting model is a gold substrate with one Cauchy layer on top.

2.5 Atomic Force Microscopy

PEM surface topography was characterized using a Nanosurf NaioAFM instrument. Measurements were taken under constant-force contact mode with HQ:CSC17 cantilevers (length: 450 μm, width: 50 μm, thickness: 2 μm). Root mean square (RMS) roughness (Rq) values were calcuated from the AFM results. Samples for AFM were prepared on QCM-D sensors. An area of 12.5 μm×12.5 μm was scanned for each location and three locations were characterized for each sample.

2.6 Water Contact Angle

Water contact angles were measured on PEM surfaces using a contact angle goniometer (Ramé-Hart). Contact angles were recorded at three locations for each sample and three samples were prepared for each condition.

3. Result and Discussion

3.1 QCM-D Analysis

QCM-D was performed to evaluate the effect of first layer selection on the assembly process. Results for mass accumulation during PEM assembly are shown in Figure 1. Each material investigated creates a first layer of a different mass, with all PEIs adsorbing far more than other first layers. PDADMAC, a strong polycation, adsorbs an intermediate amount, which is greater than the common weak polycation (PAH), less than the collection of PEIs, and about the same as the polypeptide weak polycation (PLH).

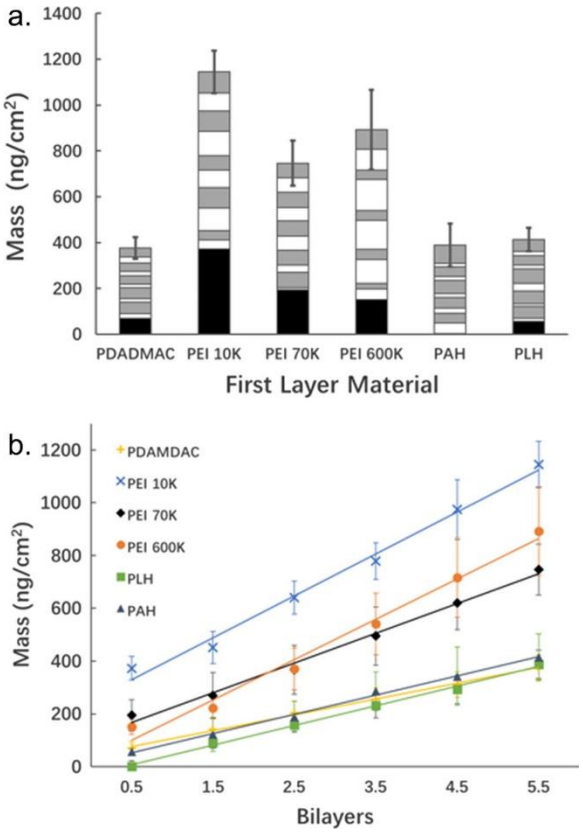

Figure 1. a. Mass accumulation of PEMs with different first layer materials. b. Mass accumulation vs. number of bilayers. All procedure and materials were remained consistent after the deposition of first layer. Error bars indicates standard deviation.

Impact on the total mass of the PEM can also be observed, with PEI first layers resulting in much more massive PEMs. As see in Figure 1b, linear growth is observed for PDADMAC/PSS, regardless of first layer material, which is consistent with previous studies of this PEM.[20,38] Interestingly, the first layer selection changes the rate of PEM growth. PEMs with PEI as first layer material have higher growth rates as compared to other conditions, while PEMs assembled on PDADMAC, PLH and PAH exhibit indistinguishable growth rates (Supporting Information). This difference in growth rate between PEI and other polycations may result from the different molecular structure (branched/linear) or from differences in chemistry. PEI used as a first layer

acts as a uniform anchoring network for the formation of consecutive layers; therefore, higher rate of layer growth can be observed. Meanwhile, strong polyelectrolyte like PDADMAC will be affected by the lateral repulsion between same molecules when adsorbed as first layer, a dense layer is not attained, which could be the reason of lower adsorption amount of PDADMAC when using as first layer material compared to PEI.[28] Certain level of charge density is necessary to achieve homogenous deposition and the continuous growth of the PEM.[39] It should be noted that linear and branched PEI differ in chemistry as well as structure: linear PEI contains only secondary amines, while branched PEI contains a mix of primary, secondary, and tertiary amines. As discussed in previous chapter, difference in molecular structure can affect the inter-layer diffusion ability of first layer, which influence the adsorption of following layers. Therefore, this comparison cannot completely isolate the effects of chemistry from structure. These results suggest that a combination of chemistry and structure are responsible for the difference in PEM assembly on PEIs as compared to other polycations.

As was noted previously, the use of a PEI as the first layer results in more massive PEMs. Adsorption of PEI, regardless of type, is also greater than other first layer materials, which provide a more massive and potentially more homogeneous base layer for the PEM. Similar growth behavior was observed between PSS/PAH PEMs and PSS/PDADMAC PEMs assembled on the same first layer material, indicating that these results may be extended to other PEM systems (Supporting Information). The mass of PEI layers decreases with increasing molecular weight. As molecular weight increases so do chain length and occupied volume of the macromolecule. These larger PEIs will occupy larger volume in solution and thus occupy a larger surface area per macromolecule after adsorption onto the surface. This may lead to a lower layer density, since for the same substrate surface, less material will be adsorbed. $\left|\Delta D/\Delta f\right|$ for a layer of PEI 10K

($0.042 \cdot 10^6$/Hz) is smaller than a layer of PEI 70K ($0.063 \cdot 10^6$/Hz) or PEI 600K ($0.053 \cdot 10^6$/Hz), showing that PEI 10K layer is stiffer than PEI 70K and PEI 600K. These results support the hypothesis that higher molecular weight results in a less densely packed layer. (Note that the $\Delta D/\Delta f$ values mentioned here are for the first layer only). However, the magnitude of $\Delta D/\Delta f$ for a layer of PEI 70K layer is smaller than PEI 600K, indicating that other factors are also important. Interesting, pH value of PEI solution is similar, regardless molecular weight (Table 1), indicating a similar degree of deionization. This indicates that other factors like chain conformation and molecular weight might play a more important role.

Table 1. pH value of different 1mg/ml polycations solution**.**

Polyelectrolyte	pH
PDAMDAC	7.35
PEI 10K	10.45
PEI 70K	10.37
PEI 600K	10.32
PAH	6.73
PLH	3.60

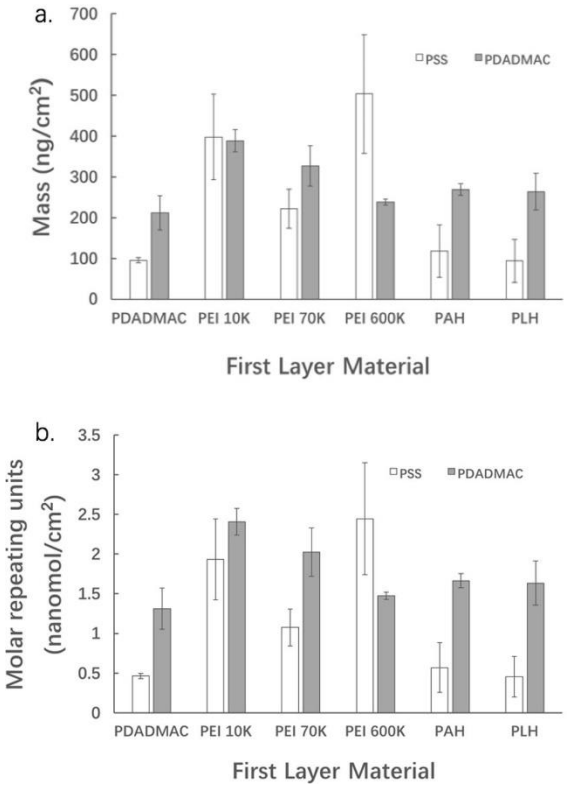

Figure 2. a) Total mass and b) Total molar in repeating unit amount of PSS and PDADMAC in 5.5 bilayers coating excluding the first layer mass. Each total mass and molar amount include 5 layers of the PEM. Error bars indicates standard deviation.

The cumulative adsorptions of PSS and PDADMAC were further calculated, both on weight and molar bases. In all cases, the amount of PDADMAC adsorbed was similar, and no statistically significant differences were observed at a 90% confidence interval. However, stark differences in PSS adsorption were observed. Significantly less PSS was adsorbed with PDADMAC, PAH, or PLH as the first layer, as compared to PEI (10K, 600K) as the first layer ($p < 0.05$). In general, PSS adsorption was greater for systems with PEI as the first layer material. This difference adsorption amount of PSS will lead to a different internal structure of PEMs.

As the molecular weight of PEI layer increases, difference between PSS and PDADMAC mass increase. Twice as much PSS was adsorbed as PDADAMC on PEI 600K first layers, while more PDADMAC is adsorbed than PSS under other first layer conditions. Interestingly, PAH and PLH (pK_a of PAH =8.7, pK_a of PLH =6.0), which are both weak polyelectrolytes, have the same effect as first layer materials in terms of amount of PDADMAC and PSS adsorbed.

The deposition rates (average of 5 layers) of PSS and PDADMAC for the first 5 minutes of adsorption were also calculated based on the QCM-D profile of each single layer. The average deposition rate of each polyelectrolytes was shown in Table 2. Generally, higher deposition rates of PDADMAC and PSS were observed when using PEI as the first layer materials. The deposition rate of PSS when using PEI 10K as the first layer is more than 5 times higher than the deposition rate when using PDADMAC as the first layer.

According to the zone model proposed Ladam *et al.*,[40] the whole PEM can be divided into three zones. The first zone is the initial layer that is adjacent to the substrate; the second zone is the bulk film, which is less affected by the substrate; the third zone is the one that is close to the surrounding environment. It is commonly observed that the initial adsorbed polyelectrolyte in the first zone has a heterogeneous conformation.[40,41] For example, the initial PDADMAC layer adsorbed is not evenly distributed on the substrate surface and may have many voids due to lateral electrostatic repulsion. The subsequent PSS layer is only formed on the locations where PDADMAC is adsorbed, which results in heterogeneous adsorption and low average deposition rate. However, this is not the case when PEI is used as the first layer. Compared to non-PEI first layer polyelectrolytes, PEI can form a uniform anchoring network as the first layer, which facilitates homogeneous adsorption from the very first layers.[29] So, for the same area on the substrate surface, more materials are adsorbed and higher average deposition rates are achieved when using PEI as

the first layer. This also results in a higher total mass accumulation when using PEI as first layer materials, as shown in Figure 1a.

Table 2. Average deposition rates of PSS and PDADMAC for the first 5 minutes of adsorption

First Layer Materials	Deposition Rate of PSS ($ng \cdot cm^{-2} \cdot min^{-1}$)	Deposition Rate of PDADMAC ($ng \cdot cm^{-2} \cdot min^{-1}$)
PDADMAC	3.1 ± 0.3	5.9 ± 1.9
PEI 10K	16.4 ± 4.9	10.5 ± 4.3
PEI 70K	9.2 ± 2.4	11.5 ± 2.3
PEI 600K	12.9 ± 6.2	8.6 ± 3.7
PAH	6.1 ± 4.7	5.4 ± 1.4
PLH	4.9 ± 2.2	7.6 ± 1.2

During the PEMs assembly process, charge overcompensation has been shown to occur with each layer, so the following layers can be adsorbed in sequence due to the excessive charge.[42] The different surface charge densities of the first layer materials may account for differences in adsorption since the degree of charge compensation of the subsequent layers would then also be changed.

Intrinsic charge compensation is defined by electrostatic bonding between polyelectrolyte ion pairs, e.g. bonding between a sulfonate group on a PSS chain and a dimethylammonium group on a PDADMAC chain.[24,42] Complete intrinsic charge compensation requires interdiffusion between polyelectrolyte layers. The alternative to intrinsic charge compensation is extrinsic charge

compensation, which occurs between a polyelectrolyte charged species and a counterion. Energy dissipation, which is shown in Figure 3, is related to the viscoelastic character of the film. Smaller dissipation values indicate a denser and stiffer film. ΔD values during adsorption are consistently lower when a PSS layer is adsorbing than when the previous layer (PDADMAC) is adsorbing. This also happens when using other polyelectrolytes as first layer material (Supporting Information). This indicates that, during the deposition process, as PSS adsorbs onto the previous PDADMAC layer, a stiffer structure was formed, since low ΔD indicates high stiffness. These results are consistent with intrinsic charge compensation between adsorbing PSS and the PDADMAC layer because stoichiometric PSS/PDADMA is glassy at room temperature [43]. PDADMAC tends to adsorb to the surface of the existing PEM and form a less dense layer, indicating that its chargers are compensated mostly by the small counterions. These results are consistent with the findings of Ghostine *et al*.[24] It was shown in their study that PEMs terminated with PDADMAC have excess PDADMAC that is compensated by small counterions on the surface, while PEMs terminated with PSS only have a slightly negative surface charge, with most PSS diffused in to the previous layer. This result is consistent with QCM-D result in this paper, as the low energy dissipation of the PSS layers indicate more interdiffusion to form a more rigid layer.

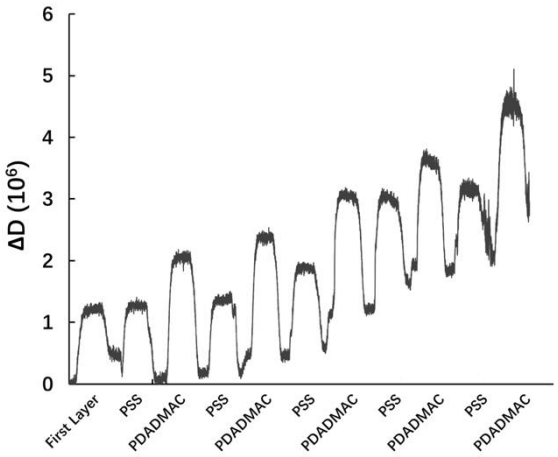

Figure 3. Representative QCM-D energy dissipation vs. layer plot during PEM assembly. PEI 600K was used as the first layer material.

3.2 PEM Thickness

Film thicknesses for PEMs consisting of a designated first layer and five bilayers of PSS/PDADMAC are reported in Figure 4a. There is a statistically significant difference ($p < 0.05$) between thickness of PEMs with PEIs is as the first layer and those using other polycations. The variations in PEM thickness is mainly contributed after the first layer, since no significant thickness differences are observed across the first. While there is a general trend of greater mass accumulation correlating with thicker films, this is not always the case. For example, while PEIs gives both higher thickness and total mass accumulation, the highest mass accumulation condition does not have the highest thickness. These results indicate differences in film density and suggest different internal structures of the PEMs, due to different first layer materials. As discussed previously, lower MW PEI may form a denser first layer and thus have a higher charge density. This could provide the following layer with a more homogeneous substrate and allow for the assembly of a denser PEM. The results in Figure 4b support that assertion, since the PEI 10K PEM has the highest relative density, which is almost twice that of the PEMs assembled on PEI 70K

and PDADMAC. It is important to note that the relative density presented in Figure 4b is not a true density, since QCM-D measurements were performed in an aqueous environment, while ellipsometry was performed on dried films in air.

As discussed previously, the ratio $\Delta D/\Delta f$ can be used to evaluate the stiffness of a film. The results in Table 3 indicate that the PEM with PEI 10K as the first layer material is the stiffest film among PEMs with different PEI as first layer. PEMs assembled on PAH and PLH are somewhat stiffer and exhibit similar relative densities to the PEI 10K PEM. Overall, $\Delta D/\Delta f$ and relative density are highly correlated, suggesting that water plays similar roles in all PEMs prepared. Differences in first layer water content could affect the assembly of subsequent layers. Although water content could be correlated to QCM-D results, further characterization of water content in PEM system, especially for the first layer, was difficult due to the small thickness and mass scales of PEMs.

Table 3. Change in energy dissipation over change in frequency when using different polycations as first layer material**.**

First Layer Material	$\lvert \Delta D/\Delta f \rvert$ of total mass accumulation (10^6/Hz)
PDADMAC	0.056±0.012
PEI 10K	0.041±0.021
PEI 70K	0.075±0.017
PEI 600K	0.062±0.012
PAH	0.027±0.010
PLH	0.035±0.023

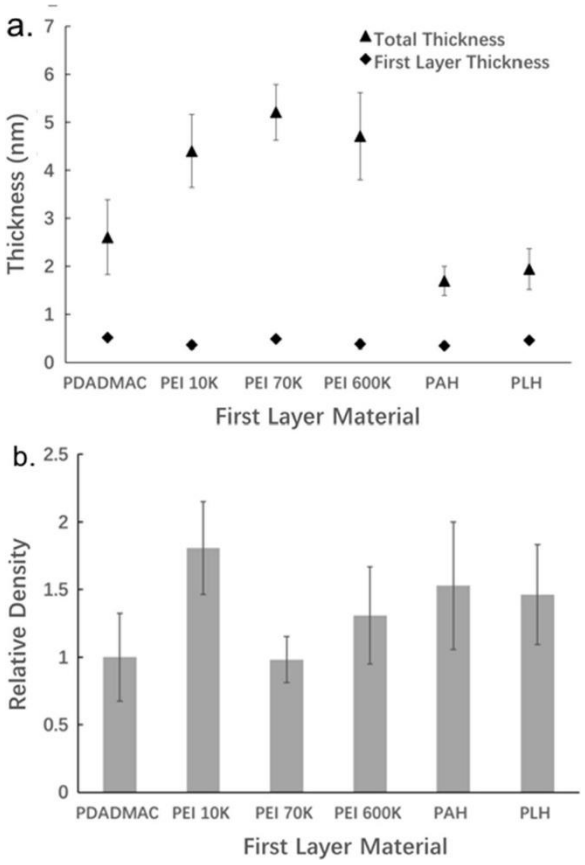

Figure 4. a) Thickness of 5.5 bilayer PEMs for different first layers. Error bars indicates standard deviation. b) Relative density when using different first layer materials calculated from QCM-D mass accumulation and ellipsometry thickness.

3.3 PEM Surfaces

Topography is important to PEM performance for applications including self-cleaning,[44,45] anti-fouling,[46–48] biomedical,[49,50] and adhesive coatings.[51] AFM was performed on PEMs assembled on different first layers, and root mean square roughness was calculated. Results are shown in Figure 6. The roughness of all coatings is very low because the substrate is quite smooth (1.28±0.04 nm). While using PEI as first layer, the coatings have higher roughnesses than with PAH or PLH as the first layer ($p < 0.05$), indicating a more heterogeneous surface. The higher surface roughness can

be explained by the higher mass accumulation rate when using PEI as first layer materials. As shown in Table 2, higher deposition rates of polyelectrolytes were observed when using PEI as first layer material. There is no sufficient time for the deposited materials to diffuse homogeneously across the surface, which result in a surface with higher roughness. No significant differences were measured between the coatings not using PEI as first layer material. Combined, the roughness, thickness and mass accumulation results indicate that, although PEI provides a homogeneous and dense first layer, the growth of following layers become more rapid and less homogeneous.

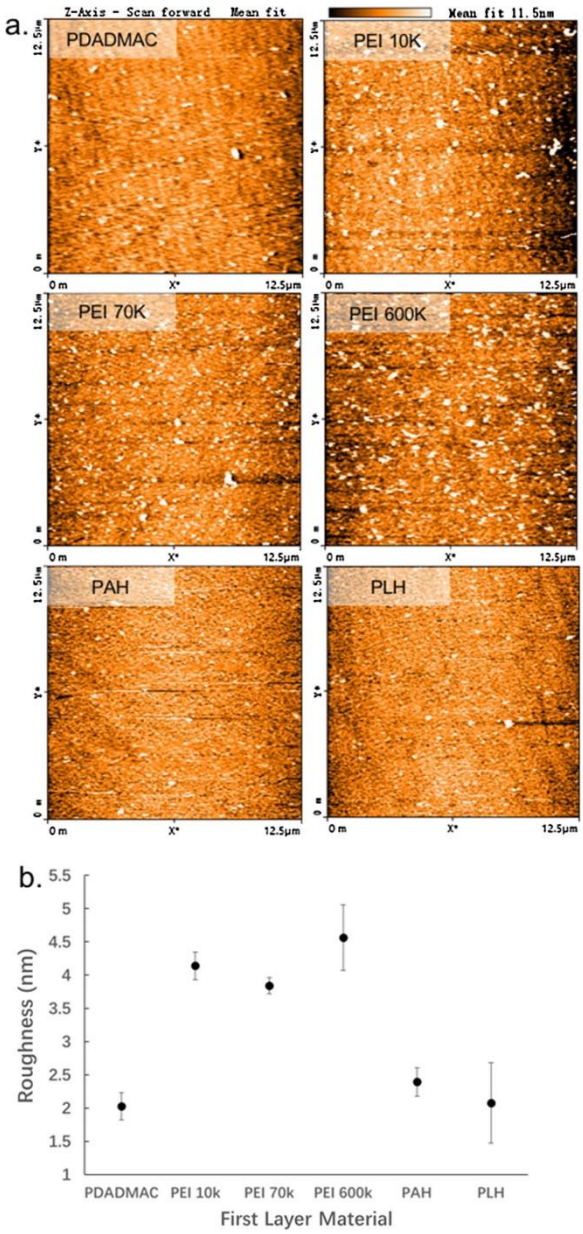

Figure 6. a) Representative AFM images of 5.5 bilayer coating with different first layer material. b) Surface roughness of 5.5 bilayer coating with different first layer material. Error bars indicates standard deviation.

Water contact angle data is shown in Figure 7. All PEMs have a total layer number of 11 and were terminated with PDADAMC, so similar values were anticipated. The small differences are

perhaps due to variations in surface topography. In work from Katarzyna *et al*., the water contact angle of polyelectrolyte-coated silicon wafers terminated with PDADMAC (Si/PEI/PSS/PDADMAC) was measured to be 38±1°,[52] which is in good agreement with Figure 7. These results indicate that the water contact angle is mainly determined by the top layer polyelectrolyte, while the first layer does not have significant effect.

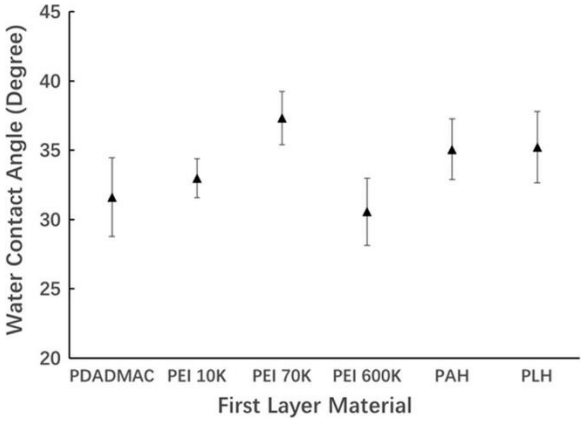

Figure 7. Water contact angle of film surface when using different first layer material.

4. Conclusion

A range of polycations - including strong, weak, branched, and polypeptide – was used to investigate the role of the first layer on assembly and properties of a model PEM. PEIs, which are commonly used to promote adhesion in PEM assembly, were shown to provide a thick base layer as well as thick and massive PEMs. Although all PEI samples showed an increment in total PEM mass, PEI molecular weight could be used to modulate PEM internal structure as well as the ratio of PSS:PDADMAC in the PEM. Non-PEI polyelectrolytes tended to behave similarly, suggesting that the mix of primary, secondary, and tertiary amines that PEIs provide offer a unique opportunity for controlling structure and properties.

During the deposition process, PDADMAC and PSS are not adsorbed in equal amounts, and the difference can be affected dramatically by changing the first layer material. This effect can be observed throughout the entire film. The internal structure also changed, as the density and viscoelastic behavior of PEMs varies when using different first layer material.

These results could have significant implications in the design of PEMs, giving a facile approach to obtain PEMs with tunable properties by changing just the first adsorbed layer. This strategy could be used in nanostructured coatings for medical devices, energy, anti-fouling, and beyond.

5. Acknowledgements

The authors acknowledge Worcester Polytechnic Institute and the Leonard P. Kinnicutt endowment for financial support. The authors are also grateful to Prof. Nancy Burnham for use of the AFM and Prof. Chris Lambert for use of the contact angle goniometer.

References

(1) Gribova, V.; Auzely-Velty, R.; Picart, C. Polyelectrolyte Multilayer Assemblies on Materials Surfaces: From Cell Adhesion to Tissue Engineering. *Chem. Mater.* **2012**, *24* (5), 854–869.

(2) Boudou, T.; Crouzier, T.; Ren, K.; Blin, G.; Picart, C. Multiple Functionalities of Polyelectrolyte Multilayer Films: New Biomedical Applications. *Adv. Mater.* **2010**, *22* (4), 441–467.

(3) Decher, G. Fuzzy Nanoassemblies: Toward Layered Polymeric Multicomposites. *Science*. 1997, pp 1232–1237.

(4) Decher, G.; Hong, J. D.; Schmitt, J. Buildup of Ultrathin Multilayer Films by a Self-Assembly Process: III. Consecutively Alternating Adsorption of Anionic and Cationic Polyelectrolytes on Charged Surfaces. *Thin Solid Films* **1992**, *210–211* (PART 2), 831–835.

(5) Zhai, L.; Cebeci, F. C.; Cohen, R. E.; Rubner, M. F. Stable Superhydrophobic Coatings from Polyelectrolyte Multilayers. *Nano Lett.* **2004**, *4* (7), 1349–1353.

(6) Hiller, J.; Mendelsohn, J. D.; Rubner, M. F. Reversibly Erasable Nanoporous Anti-Reflection Coatings from Polyelectrolyte Multilayers. *Nat. Mater.* **2002**, *1* (1), 59–63.

(7) Kim, Y. S.; Lee, H. H.; Hammond, P. T. High Density Nanostructure Transfer in Soft Molding Using Polyurethane Acrylate Molds and Polyelectrolyte Multilayers. *Nanotechnology* **2003**, *14* (10), 1140–1144.

(8) Andreeva, D. V.; Skorb, E. V.; Shchukin, D. G. Layer-by-Layer Polyelectrolyte/Inhibitor Nanostructures for Metal Corrosion Protection. *ACS Appl. Mater. Interfaces* **2010**, *2* (7), 1954–1962.

(9) Wang, X.; Liu, F.; Zheng, X.; Sun, J. Water-Enabled Self-Healing of Polyelectrolyte Multilayer Coatings. *Angew. Chemie - Int. Ed.* **2011**, *50* (48), 11378–11381.

(10) Zhu, Y.; Shi, J.; Shen, W.; Dong, X.; Feng, J.; Ruan, M.; Li, Y. Stimuli-Responsive Controlled Drug Release from a Hollow Mesoporous Silica Sphere/Polyelectrolyte Multilayer Core-Shell Structure. *Angew. Chemie - Int. Ed.* **2005**, *44* (32), 5083–5087.

(11) Berg, M. C.; Zhai, L.; Cohen, R. E.; Rubner, M. F. Controlled Drug Release from Porous Polyelectrolyte Multilayers. *Biomacromolecules* **2006**, *7* (1), 357–364.

(12) Salvi, C.; Lyu, X.; Peterson, A. M. Effect of Assembly PH on Polyelectrolyte Multilayer

Surface Properties and BMP-2 Release. *Biomacromolecules* **2016**, *17* (6), 1949–1958.

(13) Peterson, A. M.; Pilz-Allen, C.; Möhwald, H.; Shchukin, D. G. Evaluation of the Role of Polyelectrolyte Deposition Conditions in Growth Factor Release. *J. Mater. Chem. B* **2014**, *2* (18), 2680–2687.

(14) Shchukina, E. M.; Shchukin, D. G. LbL Coated Microcapsules for Delivering Lipid-Based Drugs. *Adv. Drug Deliv. Rev.* **2011**, *63* (9), 837–846.

(15) Delcea, M.; Möhwald, H.; Skirtach, A. G. Stimuli-Responsive LbL Capsules and Nanoshells for Drug Delivery. *Adv. Drug Deliv. Rev.* **2011**, *63* (9), 730–747.

(16) Sui, Z.; Salloum, D.; Schlenoff, J. B. Effect of Molecular Weight on the Construction of Polyelectrolyte Multilayers: Stripping versus Sticking. *Langmuir* **2003**, *19* (6), 2491–2495.

(17) Shiratori, S. S.; Rubner, M. F. pH-Dependent Thickness Behavior of Sequentially Adsorbed Layers of Weak Polyelectrolytes. *Macromolecules* **2000**, *33* (11), 4213–4219.

(18) Jomaa, H. W.; Schlenoff, J. B. Salt-Induced Polyelectrolyte Interdiffusion in Multilayered Films: A Neutron Reflectivity Study. *Macromolecules* **2005**, *38* (20), 8473–8480.

(19) Poptoshev, E.; Schoeler, B.; Caruso, F. Influence of Solvent Quality on the Growth of Polyelectrolyte Multilayers. *Langmuir* **2004**, *20* (3), 829–834.

(20) McAloney, R. A.; Sinyor, M.; Dudnik, V.; Cynthia Goh, M. Atomic Force Microscopy Studies of Salt Effects on Polyelectrolyte Multilayer Film Morphology. *Langmuir* **2001**, *17* (21), 6655–6663.

(21) Peterson, A. M.; Möhwald, H.; Shchukin, D. G. pH-Controlled Release of Proteins from Polyelectrolyte-Modified Anodized Titanium Surfaces for Implant Applications. *Biomacromolecules* **2012**, *13* (10), 3120–3126.

(22) V. Klitzing, R.; Wong, J. E.; Jaeger, W.; Steitz, R. Short Range Interactions in

Polyelectrolyte Multilayers. *Curr. Opin. Colloid Interface Sci.* **2004**, *9* (1–2), 158–162.

(23) Kharlampieva, E.; Sukhishvili, S. A. Polyelectrolyte Multilayers of Weak Polyacid and Cationic Copolymer: Competition of Hydrogen-Bonding and Electrostatic Interactions. *Macromolecules* **2003**, *36* (26), 9950–9956.

(24) Ghostine, R. A.; Markarian, M. Z.; Schlenoff, J. B. Asymmetric Growth in Polyelectrolyte Multilayers. *J. Am. Chem. Soc.* **2013**, *135* (20), 7636–7646.

(25) Buron, C. C.; Filiâtre, C.; Membrey, F.; Bainier, C.; Charraut, D.; Foissy, A. Effect of Substrate on the Adsorption of Polyelectrolyte Multilayers: Study by Optical Fixed-Angle Reflectometry and AFM. *Colloids Surfaces A Physicochem. Eng. Asp.* **2007**, *305* (1–3), 105–111.

(26) Peng, C.; Thio, Y. S.; Gerhardt, R. A. Effect of Precursor-Layer Surface Charge on the Layer-by-Layer Assembly of Polyelectrolyte/Nanoparticle Multilayers. *Langmuir* **2012**, *28* (1), 84–91.

(27) Tsukruk, V. V.; Bliznyuk, V. N.; Visser, D.; Campbell, A. L.; Bunning, T. J.; Adams, W. W. Electrostatic Deposition of Polyionic Monolayers on Charged Surfaces. *Macromolecules* **1997**, *30* (21), 6615–6625.

(28) Kolasińska, M.; Krastev, R.; Warszyński, P. Characteristics of Polyelectrolyte Multilayers: Effect of PEI Anchoring Layer and Posttreatment after Deposition. *J. Colloid Interface Sci.* **2007**, *305* (1), 46–56.

(29) Trybała, A.; Szyk-Warszyńska, L.; Warszyński, P. The Effect of Anchoring PEI Layer on the Build-up of Polyelectrolyte Multilayer Films at Homogeneous and Heterogeneous Surfaces. *Colloids Surfaces A Physicochem. Eng. Asp.* **2009**, *343* (1–3), 127–132.

(30) Kolasińska, M.; Warszyński, P. The Effect of Support Material and Conditioning on

Wettability of PAH/PSS Multilayer Films. *Bioelectrochemistry* **2005**, *66* (1–2), 65–70.

(31) Naderi, A.; Claessont, P. M. Adsorption Properties of Polyelectrolyte-Surfactant Complexes on Hydrophobic Surfaces Studied by QCM-D. *Langmuir* **2006**, *22* (18), 7639–7645.

(32) Ishida, N.; Biggs, S. Direct Observation of the Phase Transition for a Poly(N-Isopropylacryamide) Layer Grafted onto a Solid Surface by AFM and QCM-D. *Langmuir* **2007**, *23* (22), 11083–11088.

(33) Liu, G.; Zhao, J.; Sun, Q.; Zhang, G. Role of Chain Interpenetration in Layer-by-Layer Deposition of Polyelectrolytes. *J. Phys. Chem. B* **2008**, *112* (11), 3333–3338.

(34) Sauerbrey, G. Verwendung von Schwingquarzen Zur Wägung Dünner Schichten Und Zur Mikrowägung. *Zeitschrift für Phys.* **1959**, *155* (2), 206–222.

(35) Goka, S.; Okabe, K.; Watanabe, Y.; Sekimoto, H. Multimode Quartz Crystal Microbalance. *Japanese J. Appl. Physics, Part 1 Regul. Pap. Short Notes Rev. Pap.* **2000**.

(36) Benes, E. Improved Quartz Crystal Microbalance Technique. *J. Appl. Phys.* **1984**, *56* (3), 608–626.

(37) Vogt, B. D.; Lin, E. K.; Wu, W. I.; White, C. C. Effect of Film Thickness on the Validity of the Sauerbrey Equation for Hydrated Polyelectrolyte Films. *J. Phys. Chem. B* **2004**, *108* (34), 12685–12690.

(38) Nestler, P.; Paßvogel, M.; Helm, C. A. Influence of Polymer Molecular Weight on the Parabolic and Linear Growth Regime of PDADMAC/PSS Multilayers. *Macromolecules* **2013**, *46* (14), 5622–5629.

(39) Bharadwaj, S.; Montazeri, R.; Haynie, D. T. Direct Determination of the Thermodynamics of Polyelectrolyte Complexation and Implications Thereof for Electrostatic Layer-by-Layer

Assembly of Multilayer Films. *Langmuir* **2006**.

(40) Ladam, G.; Schaad, P.; Voegel, J. C.; Schaaf, P.; Decher, G.; Cuisinier, F. In Situ Determination of the Structural Properties of Initially Deposited Polyelectrolyte Multilayers. *Langmuir* **2000**.

(41) Dejeu, J.; Buisson, L.; Guth, M. C.; Roidor, C.; Membrey, F.; Charraut, D.; Foissy, A. Early Steps of the Film Growth Mechanism in Self-Assembled Multilayers of PAH and PSS on Silica. Polymer Uptake, Charge Balance and AFM Analysis. *Colloids Surfaces A Physicochem. Eng. Asp.* **2006**.

(42) Schlenoff, J. B.; Dubas, S. T. Mechanism of Polyelectrolyte Multilayer Growth: Charge Overcompensation and Distribution. *Macromolecules* **2001**, *34* (3), 592–598.

(43) Shamoun, R. F.; Hariri, H. H.; Ghostine, R. A.; Schlenoff, J. B. Thermal Transformations in Extruded Saloplastic Polyelectrolyte Complexes. *Macromolecules* **2012**, *45* (24), 9759–9767.

(44) Huang, X.; Zacharia, N. S. Surfactant Co-Assembly and Ion Exchange to Modulate Polyelectrolyte Multilayer Wettability. *Soft Matter* **2013**, *9* (32), 7735.

(45) Hannig, M.; Hannig, C. Nanomaterials in Preventive Dentistry. *Nat Nanotechnol* **2010**, *5* (8), 565–569.

(46) Yang, W. J.; Pranantyo, D.; Neoh, K. G.; Kang, E. T.; Teo, S. L. M.; Rittschof, D. Layer-by-Layer Click Deposition of Functional Polymer Coatings for Combating Marine Biofouling. *Biomacromolecules* **2012**, *13* (9), 2769–2780.

(47) Zhu, X.; Jańczewski, D.; Lee, S. S. C.; Teo, S. L. M.; Vancso, G. J. Cross-Linked Polyelectrolyte Multilayers for Marine Antifouling Applications. *ACS Appl. Mater. Interfaces* **2013**, *5* (13), 5961–5968.

(48) Brzozowska, A. M.; Parra-Velandia, F. J.; Quintana, R.; Xiaoying, Z.; Lee, S. S. C.; Chin-Sing, L.; Jańczewski, D.; Teo, S. L. M.; Vancso, J. G. Biomimicking Micropatterned Surfaces and Their Effect on Marine Biofouling. *Langmuir* **2014**, *30* (30), 9165–9175.

(49) Dalby, M. J.; Gadegaard, N.; Herzyk, P.; Agheli, H.; Sutherland, D. S.; Wilkinson, C. D. W. Group Analysis of Regulation of Fibroblast Genome on Low-Adhesion Nanostructures. *Biomaterials* **2007**, *28* (10), 1761–1769.

(50) Zhu, X.; Chen, J.; Scheideler, L.; Reichl, R.; Geis-Gerstorfer, J. Effects of Topography and Composition of Titanium Surface Oxides on Osteoblast Responses. *Biomaterials* **2004**, *25* (18), 4087–4103.

(51) Gao, S. L.; Mäder, E. Characterisation of Interphase Nanoscale Property Variations in Glass Fibre Reinforced Polypropylene and Epoxy Resin Composites. *Compos. - Part A Appl. Sci. Manuf.* **2002**, *33* (4), 559–576.

(52) Hänni-Ciunel, K.; Findenegg, G. H.; von Klitzing, R. Water Contact Angle On Polyelectrolyte-Coated Surfaces: Effects of Film Swelling and Droplet Evaporation. *Soft Mater.* **2007**, *5* (2–3), 61–73.

Chapter 4: Thermal transitions in and structures of dried polyelectrolytes and polyelectrolyte complexes

Published in *Journal of Polymer Science, Part B: Polymer Physics, 2017, 55(8), 684-691*

Thermal transitions in and structures of dried polyelectrolytes and polyelectrolyte complexes

Xuejian Lyu,[1] Brandon Clark,[2] Amy M. Peterson[1,2]

[1]Department of Mechanical Engineering, Worcester Polytechnic Institute, 100 Institute Road, Worcester, MA 01609

[2]Department of Chemical Engineering, Worcester Polytechnic Institute, 100 Institute Road, Worcester, MA 01609

Abstract

Dynamic mechanical analysis (DMA) was used to explore the thermomechanical properties of dried polyelectrolytes and polyelectrolyte complexes (PECs) with different thermal and humidity histories. Although differences in the amount of water remaining in polyelectrolytes and PECs were small for ambient vs. desiccator storage, the properties of polyelectrolyte-based materials were drastically different for different humidity histories. Glass transition temperatures (T_gs) of poly(diallyldimethylammonium chloride) (PDADMAC) were shown to vary by 100°C, depending on humidity and thermal histories. These parameters also change glassy storage modulus values by 100%. Furthermore, we observe that dried PDADMAC is highly lossy. DMA of dried poly(styrene sulfonate) (PSS) was more complex and did not exhibit a glass transition in the tested range. DMA of a PEC of PDADMAC and PSS revealed a humidity history-dependent water melt in the first heating cycle, as well as storage modulus values of dried and annealed PECs that only varied by 17-26% over a 275°C temperature range. Based on these results, we report for the first-time humidity history as controlling structure and properties of polyelectrolyte-based materials

1. Introduction

Polyelectrolyte-based materials, such as polyelectrolyte complexes (PECs) and polyelectrolyte multilayers (PEMs) have found use in medical, anticorrosion, non-flammable, anti-fog, and numerous other applications. PECs are polyelectrolyte structures formed through the mixing of polyanions and polycations and PEMs are formed through layer-by-layer (LbL) adsorption of polyanions and polycations. Coulombic interactions between oppositely charged polyelectrolytes lead to interpolymer ionic condensation in PECs and PEMs, while hydrogen bonding, van der Waals forces, hydrophobic interactions and dipole interactions are also involved in assembly.[1,2]

For many years, PECs were known to be very difficult to process and prepare consistently, which limited their use.[3,4] Recently, there has been renewed interest in PECs due to new fabrication techniques. Porcel and Schlenoff reported on compact PECs formed through ultracentrifugation and demonstrating properties similar to those of tissue.[5] When these PECs are soaked in NaCl solutions, they become extrudable, tough polymers.[6] Alternatively, PEC capsules can be created by ultrasonic spraying.[7] Additionally, PEC films were formed by Ball *et al*. through a single sedimentation of PECs from solution.[8] PECs have found use as hydrogels and tissue engineering scaffolds,[9–11] drug and protein delivery systems,[12–14] conductive membranes,[15] pervaporation membranes,[16] and underwater adhesives.[17]

LbL assembly of polyelectrolytes to form PEMs has found a wide range of applications since Decher first described this technique in the early 1990's.[18,19] PEMs require a substrate, so they have often been used as coatings. PEM coatings have been used for obtaining nano-patterned surfaces,[20] design of superhydrophobic surfaces,[21] and controlled release of biologically relevant molecules[22–24] and corrosion inhibitors.[25] Since PEM growth is on the range of 1-10s of nm per

bilayer, preparing large amounts is difficult. Caruso and Möhwald pioneered the formation of hollow microspheres through PEM assembly on dissolvable microparticles that were subsequently dissolved.[26,27] This advance opened up PEMs to areas including drug delivery,[28,29] nanomaterial microreactors,[30,31] and multicompartment capsules.[32]

Despite the wide range of applications of polyelectrolyte-based materials, measurement of thermal transitions and mechanical properties has been complicated by their affinity for water. Nolte and Rubner observed that poly(allylamine hydrochloride)/poly(acrylic acid) (PAH/PAA) PEMs assembled under certain conditions display "remarkable resistance to swelling and plasticization at low humidity (12-36% RH)." In fact, in one case increasing humidity to 48% RH increased the Young's modulus of a PAH/PAA film from ~8GPa to ~10GPa, followed by decreasing Young's modulus with increasing RH above 48%.[33]

DMA is a popular technique for measuring the thermomechanical properties of polymer composites. DMA is 10-100 times more sensitive to changes occurring at the glass transition than DSC, making this a useful technique with which to explore thermal transitions in polyelectrolyte-based materials. Jaber and Schlenoff demonstrated that PEMs offer enhanced damping vs. other hydrogels.[34] Lutkenhaus *et al.* used DMA on hydrogen bonded LbL films.[35]

In this work, the role of humidity and thermal histories on thermal transitions in polyelectrolytes and PECs were characterized for the first time using DMA. By maintaining an inert, dry atmosphere, thermomechanical behavior was characterized in two polyelectrolytes and their complex.

2. Experimental

2.1 Materials

Poly(diallyldimethylammonium chloride) (PDADMAC, 20 wt.% in water) and poly(sodium 4-styrenesulfonate) (PSS, M_w ~200,000, 30 wt.% in water) were obtained from Sigma-Aldrich and used as received. The as-received stability of both polyelectrolytes was characterized with solid PDADMAC and PS: PDADMAC-s (M_w ~240,000, powder, Polysciences) and PSS-s (M_w ~70,000, powder, Sigma-Aldrich).

2.2 Sample Preparation

Polyelectrolyte samples were prepared by solvent casting of polyelectrolyte water solutions on low surface energy surface. 300 μL PDADMAC or PSS solutions were evaporated under ambient conditions (22.8 ± 1.1°C, 50–60% RH) for at least 3 days on petri dish surfaces. Some samples were subsequently stored in a desiccator (22.8 ± 1.1°C, 10% RH) for an additional 48 hours.

Polyelectrolyte complex (PEC) samples were prepared by mixing equal amounts of 20 mg mL^{-1} PDADMAC and 20 mg mL^{-1} PSS aqueous solutions with a magnetic stir bar. The mixture was centrifuged for 30 seconds at 6000 RPM and the sedimented PEC was then dried under ambient conditions for at least 3 days. Some samples were subsequently stored in a desiccator for an additional 48 h. Images of representative samples are shown in Figure 1.

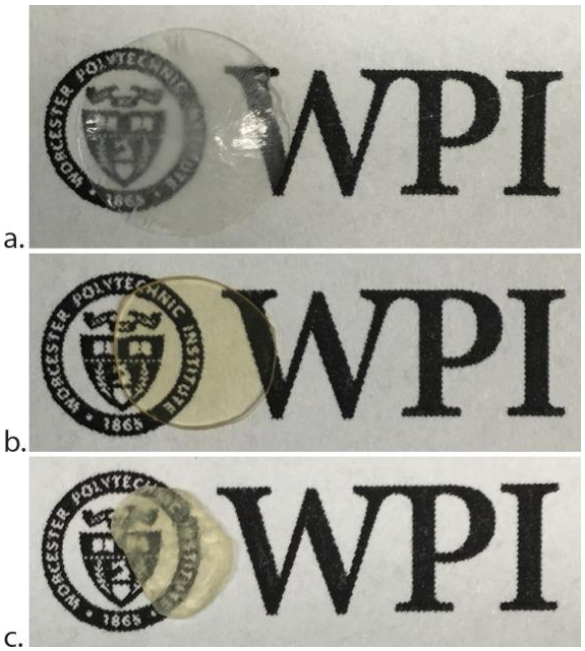

Figure 1. Polyelectrolyte and PEC samples prepared as described in the Experimental section and stored under ambient conditions. a. PDADMAC; b. PSS; c. PEC.

2.3 Dynamic mechanical analysis (DMA)

DMA was performed using a Netzsch DMA 242E (Netzsch, Germany). A compression geometry was used, with a push rod diameter of 1 mm, at a frequency of 1 Hz. Testing was performed in a closed chamber through which N_2 (<5 ppm H_2O) was flowed. The chamber temperature was controlled with liquid nitrogen cooling and electrical heating. Samples were initially cooled to -50°C, then heated to 120°C, followed by annealing at that temperature for different lengths of time (0 min, 30 min, 60 min and 90 min), cooling to -20°C and subsequent heating to 250°C. Temperature heating and cooling occurred at a rate of 2°C min^{-1}. This temperature protocol was determined to be sufficiently low/high in each cycle to capture major thermal transitions regardless of sample preparation/annealing conditions, while simultaneously avoiding degradation and minimizing testing time.

2.4 Thermogravimetric analysis (TGA)

TGA was performed with a Netzsch TG 204 under house N_2. To monitor water content, testing was performed on samples of the same thickness as those for DMA. Samples were put through the same first heating cycle protocol as in the DMA, omitting the cooling step.

2.5 Differential Scanning Calorimetry (DSC)

DSC was performed with a Netzsch DSC 214 Polyma at a heating/cooling rate of 10°C min^{-1}. The first heating cycle increased the temperature to 100°C, followed by 30 min of isothermal annealing, cooling to 25°C, and two heat/cool cycles between 25°C and 225°C.

3. Results and Discussion

3.1 TGA

TGA was used to monitor both water loss and thermal degradation of PDADMAC, PSS, and their complex. As-received PDADMAC powder degrades at 300°C (onset) and as-received PSS powder degrades at 445°C (onset). Results are provided in the Supporting Information and were used to set the upper limit for DMA testing. TGA of polyelectrolyte and PEC samples of the same thickness as DMA samples was performed to measure the amount of water that would be lost during the heating and annealing cycles.

Results for ambient and desiccator PDADMAC are shown in Figure 2 and are compared to the results for PDADMAC-s (PDADMAC that was received and characterized in powdered form) undergoing the same temperature protocol. Prepared samples contained approximately the same amount of water as PDADMAC-s, with ambient samples containing slightly more and desiccator samples containing less. 92% of water in PDADMAC-s is lost in the initial healing, while most of the water (68% for ambient, 65% for desiccator) is lost in the initial heating to 120°C. This result

indicates that both types of prepared sample have the same proportion of bound vs. unbound water. The percentages are based on the assumption that all possible water that could be lost has evaporated after 90 min at 120°C, which is discussed in greater detail below.

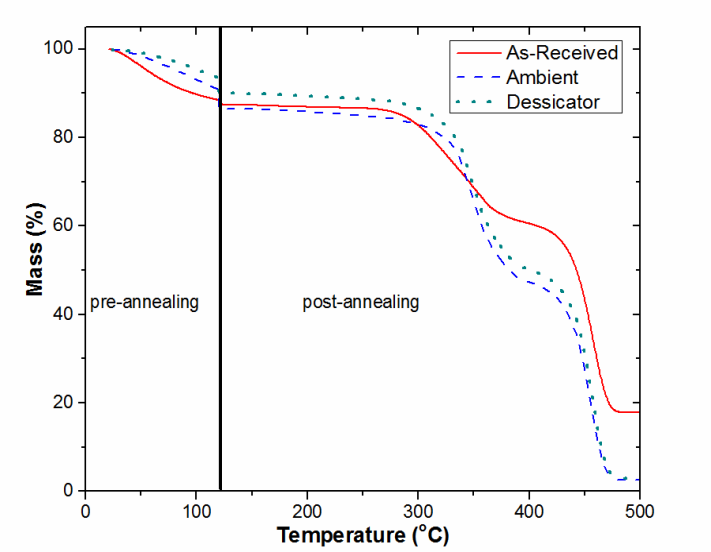

Figure 2. TGA of PDADMAC undergoing the annealing temperature protocol under a N_2 atmosphere.

Results for ambient PSS are compared to PSS-s in Figure 3. Prepared samples stored under ambient conditions contained more water than the as-received powder (PSS-s) and lost more water during the annealing step than as-received powder, suggesting the presence of more bound water. Approximately 58% of the water is lost in the initial heating to 120°C for ambient PSS.

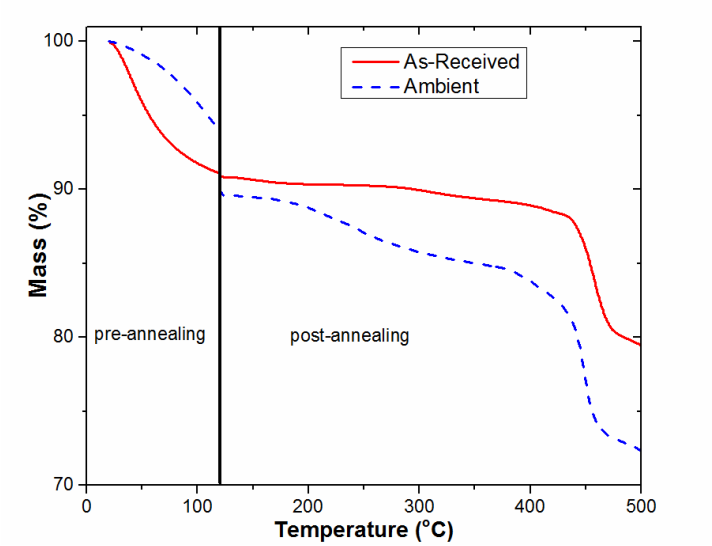

Figure 3. TGA of PSS undergoing the annealing temperature protocol under a N_2 atmosphere.

In the case of PEC samples, very little water is lost during annealing, either as compared to total PEC mass (2.3 ± 0.2 wt.% for ambient samples, 1.9 ± 0.4 wt.% for desiccator samples) or as compared to total water loss (17.7 ± 4.5% for ambient samples, 26.3 ± 6.3% for desiccator samples). More of the water is unbound in the PECs than in the individual polyelectrolytes, most likely because the charged species within a PEC can electrostatically bind with one another. The thermal stability of the PEC is greater than either individual polyelectrolyte, also a result of electrostatic bonding.

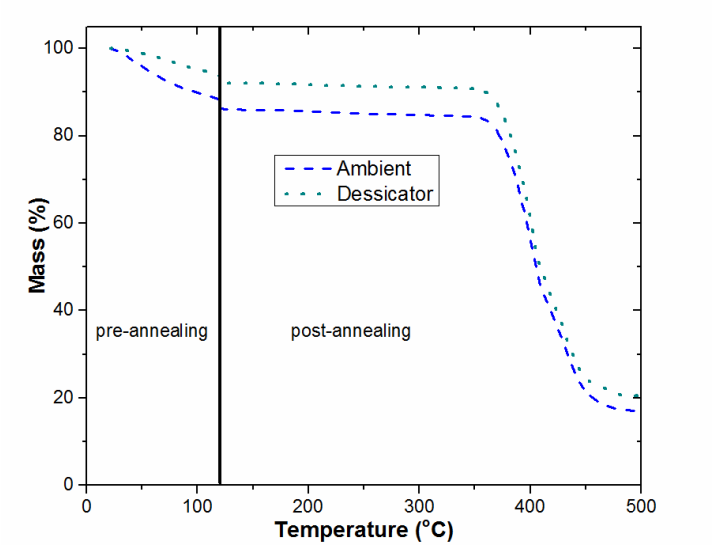

Figure 4. TGA of PEC undergoing the annealing temperature protocol under a N_2 atmosphere.

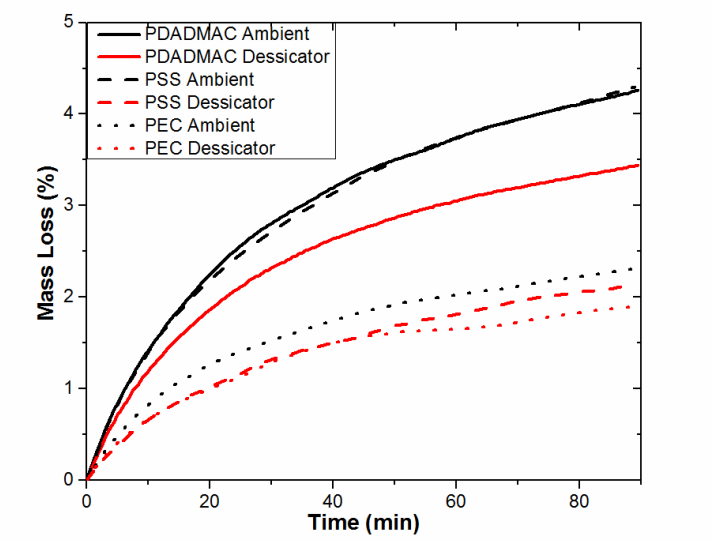

Figure 5. Isothermal mass loss at 120°C.

The amount of water lost during annealing is, in general, limited, as shown in Figure 5. In all cases, less than 5 wt.% is lost during annealing. In all cases, ambient-stored samples lose more water during annealing than desiccator-stored samples of the same material. The fraction of water remaining is based on the assumption that all possible water that could be lost has evaporated after

90 min at 120°C. After 30 min, all samples are losing water at a rate of less than 20 μg min^{1} mg^{-1} sample, which is on the same order as the noise in the DTGA signal is (± 0.05 %/min). Therefore, the initial assumption is reasonable.

TGA results are summarized in Table 1. Samples stored in a desiccator consistently contain less water, although the ratio of bound to unbound water is maintained between ambient and desiccator samples of the same polyelectrolyte. As discussed above, this behavior is not observed in the PEC. Results for low RH PSS are summarized in Table 1, but were not discussed above, since PSS stored in a desiccator was not characterized via DMA. TGA of PSS stored in a desiccator is provided in the Supporting Information.

Table 1. Summary of TGA results, including amount of unbound and bound water for polyelectrolytes and their PEC for ambient (50-60% RH) and desiccator (10% RH) storage at 22.8 ± 1.1°C.

Material	Storage RH (%)	Unbound water (wt.%)	Bound water (wt.%)
PDADMAC	50-60	9.1	4.3
	10	6.5	3.4
PDADMAC-s	50-60	12	1.0
PSS	50-60	7.1	4.3
	10	3.1	2.3
PSS-s	50-60	8.9	0.25
PEC	50-60	12	2.3
	10	6.1	1.9

3.2 DMA

3.2.1 PDADMAC behavior

Storage environment can significantly affect thermomechanical properties of polyelectrolytes. PDADMAC was characterized with DMA after storage under ambient conditions and after storage in a desiccator. Representative first heating cycle results are shown in Figure 6. Storage modulus decreases gradually with increasing temperature up to the onset of the glass transition, at which point there is a sharp drop off in storage modulus concurrent with a peak in tan δ – this behavior is consistent with a glass transition and will be referred to as such. Samples stored in a desiccator exhibit a much higher glass transition temperature (T_g = 59.5°C vs. 23.6°C based on inflection in

storage modulus, 70.4°C vs. 42.9°C based on tan δ peak); however, they are less stiff at both the same pre-T_g temperatures and the same temperature below T_g (Table 2). These results indicate that PDADMAC has a different structure when stored under ambient and desiccator conditions, even though the water content is similar.

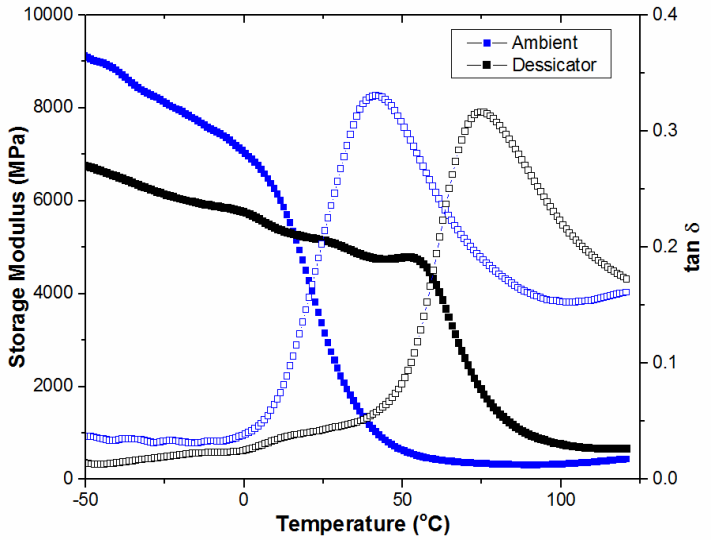

Figure 6. DMA of PDADMAC stored under ambient conditions and in a desiccator. Storage modulus values are solid points and tan δ values are hollow.

Table 2. Comparison of T_g and glassy storage modulus values for PDADMAC. Given values are averages, standard deviations are provided in parentheses.

Storage Conditions	T_g (ºC)	Storage modulus at 0ºC (MPa)	Storage modulus at T_g - 50ºC (MPa)
Ambient	23.6	6700	7760
Desiccator	59.5	5630	5380

Instead of a post-T_g rubbery plateau, an increase in storage modulus is observed above 90°C for ambient PDADMAC and 115°C for desiccator PDADMAC as temperature increases in Figure 6, related to the evaporation of water. To determine dry thermomechanical behavior, after a first heating cycle (Figure 6), samples were annealed at 120°C for different amounts of time to remove any remaining water, then cooled and re-heated while DMA measurements were recorded. Isothermal DMA results show storage modulus increasing and plateauing with time during annealing (Supporting Information).

Figure 7 shows the post-annealing, second heating cycle DMA results for PDADMAC, which highlight the effect of annealing time for both ambient and desiccator storage conditions. T_g increases with increasing annealing time, up to 153°C for ambient samples and 125°C for desiccator samples. For comparison, DSC shows a thermal transition in PDADMAC of 113°C (Supporting Information).

PDADMAC T_g values vary greatly in the literature, ranging from 24°C to 170°C, depending on water content.[36–38] It has been observed that increasing water decreases the T_g due to water acting as a plasticizer. The values reported in Figures 6 and 7 span the majority of this range (24–153°C) and demonstrate the importance of both thermal and humidity history.

Several interesting characteristics are observed in dried and annealed PDADMAC, which confirm that PDADMAC exhibits humidity history-dependent structure. Samples stored under ambient conditions are capable of higher T_gs upon annealing than desiccator-stored samples for all but the 0 min annealing condition. Glassy storage modulus values decrease with increasing annealing time for samples stored under ambient conditions, while glassy storage modulus values increase with increasing annealing time for samples stored in a desiccator.

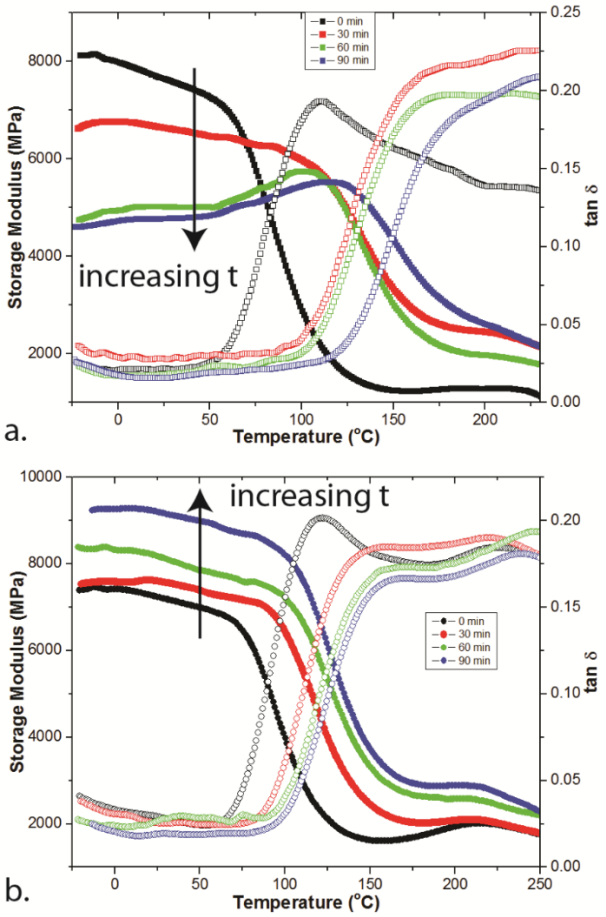

Figure 7. Second heating cycle DMA of PDADMAC after heating to 120°C and annealing for 0–90 minutes. PDADMAC stored a. under ambient conditions; b. in a desiccator. Storage modulus = solid points, tan δ = unfilled points.

Ambient samples show a residual stress peak in storage modulus on the second heating cycle for the 60- and 90-min annealing conditions, while desiccator samples do not. We attribute this to the stresses frozen in during annealing of the ambient sample. Since desiccator samples have less water, there is less mobility at the start of annealing.

For all non-zero annealing times of ambient samples, tan δ does not decrease after the glass transition. This is very different from the pre-annealing behavior of PDADMAC, indicating that

the loss of water results in higher T_g materials with lossy rubbery phases that are not able to rearrange to reduce their viscous response to an applied force. This is particularly intriguing because 9.1 wt.% of water is lost prior to annealing, as compared to 4.3 wt.% water during annealing, suggesting that this small amount of bound water is essential for structural rearrangement.

Based on these results, it is clear that water content plays a significant role in the thermomechanical properties of PDADMAC. However, it should not be overlooked that the protocol for removing water *in situ* requires heating above the initial measured glass transitions of PDADMAC for both storage conditions. The annealing process removes water and also provides an opportunity for polymer rearrangement. Imré *et al.* observed that thermal history affected PEC conductivity, and Köhler *et al.* found that thermal history affects thermally induced shrinkage/expansion of PEM capsules.[38–40] Therefore the effect of annealing temperature may be significant in the final thermomechanical properties, independent of water content, and is an area for further research.

3.2.2 PSS Behavior

PSS samples stored under ambient conditions were also characterized with DMA in a dry, inert atmosphere. A significant drop in storage modulus consistent with a glass transition (T_g = -41.0 ± 2.2°C based on storage modulus inflection point) was observed for the first heating cycle (Figure 8a). After the transition, there is a rise in storage modulus, consistent with a drying process. TGA of PSS prepared under ambient conditions shows that heating PSS to 120°C removes 7.1 wt.% water.

PSS exhibited no glass transitions in the second heating cycle, regardless of annealing time

(Figure 8b). Instead, there is a trough in storage modulus in the range 125–150°C, where storage modulus values drop to 62–78% of the initial value, followed by full (98-103%) recovery of storage modulus at 250°C. The gradual decline in storage modulus corresponds with an increase in tan δ, with tan δ values tending to plateau around 150°C and converging to a value of 0.075. As compared to PDADMAC, dried and annealed PSS is less lossy. There does not appear to be a relationship between storage modulus and annealing time. Far less water is lost during annealing that in the initial process, so there is less water-related change in stiffness in PSS than PDADMAC.

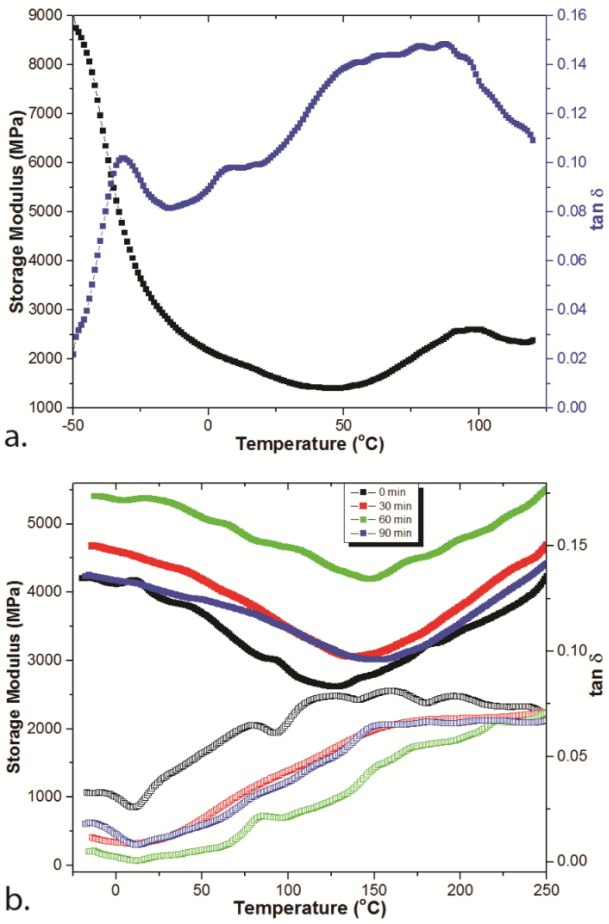

Figure 8. a. DMA of PSS stored under ambient conditions; b. Second heating cycle DMA of ambient-stored PSS after heating to 120°C and annealing for 0 – 90 minutes. Storage modulus = solid points, tan δ = unfilled points.

The lack of measured glass transition in the second heating cycle is consistent with the PSS-water interaction reported by Yildirim *et al*. that results in a lower critical solution temperature-like transition thermal transition in the range of 70-75°C.[41] This thermal transition is related to water's transition from a hydrogen bonder to a plasticizer, resulting in more mobile water above 70-75°C. Without water, the thermal transition does not occur. However, we do not observe a thermal transition at 70-75°C in the first heating cycle, where there is still 9 wt.% water presents. Since DMA in the current work was performed under high dry nitrogen flow rates, water is purged from the testing environment instead of staying within the sample and acting as a plasticizer.

3.2.3 Polyelectrolyte Complex Behavior

Representative first heating cycle results for ambient and desiccator PEC samples are shown in Figure 9. Unlike the DMA scans of the individual polyelectrolytes, both ambient and desiccator samples show a clear drop in storage modulus around 0°C, consistent with water melting. The size of this peak decreases with increased storage time, indicating that water content has yet to reach equilibrium. Pre-melt storage modulus values decrease with decreasing water content under ambient conditions, highlighting the different roles that water can play in polyelectrolyte structures. However, even though ambient-stored PEC has greater water content and a larger percentage of unbound water according to TGA (Table 1), the observed effect of water melting is greater in desiccator-stored PEC. This, combined with the lack of correlation between water content and pre-melt storage modulus, suggests that the desiccator-stored PEC has a different structure than PEC stored under ambient conditions, and that water interacts with this material in a different way. Probing these interactions is an area of future investigation.

Water melting in PSS and PDADMAC may be obscured by other transitions. Additionally, more water is unbound in the PEC than in the individual polyelectrolytes, as is discussed above. The dip in storage modulus assigned to water melting is recovered by 30°C, which would not be the case if 1) it were not a solvent melting and 2) the solvent did not evaporate rapidly. These results lend support to the previous assertion that a lower critical solution temperature-like transition is not observed in PSS because the water is rapidly purged from the system.

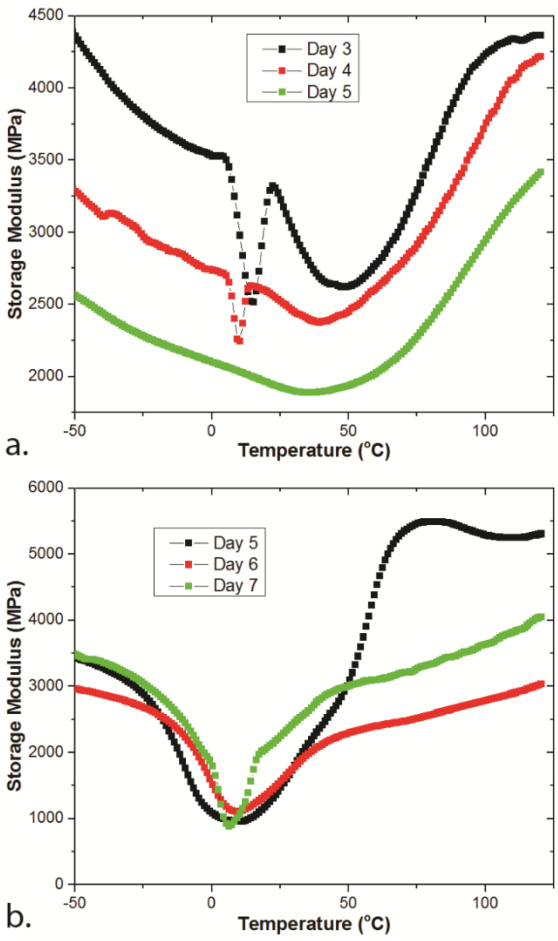

Figure 9. First heating cycle storage moduli of PEC stored under a. ambient conditions or b. in a desiccator for different amounts of time.

Post-annealing DMA results for PEC are shown in Figure 10. The results are very similar to PSS (Figure 8), although the drop in storage modulus is far less pronounced. PEC samples stored under ambient conditions exhibit minima in storage modulus in the range 133-147°C, where storage modulus values drop to 77–87% of the initial value, followed by more than full (98-115%) recovery of initial values at 250°C. In comparison, PEC samples stored in a desiccator exhibit minima in storage modulus in a broader range (123-150°C), where storage modulus values drop to 75–85% of the initial value, followed by full (93-110%) recovery of initial values at 250°C.

The tan δ curves are relatively indistinguishable from one another, regardless of humidity history, increasing with increasing temperature and plateauing at 0.04. No trends are observed in storage modulus values as a function of annealing time, perhaps because approximately 2 wt.% water is lost during 90 min annealing (Figure 5). However, samples stored under ambient conditions exhibited much less variation in storage modulus than desiccator samples. One explanation for the difference in variation could be that humidity history affects the pre-annealing structure and how water interacts with the PEC, which can affect the final structures.

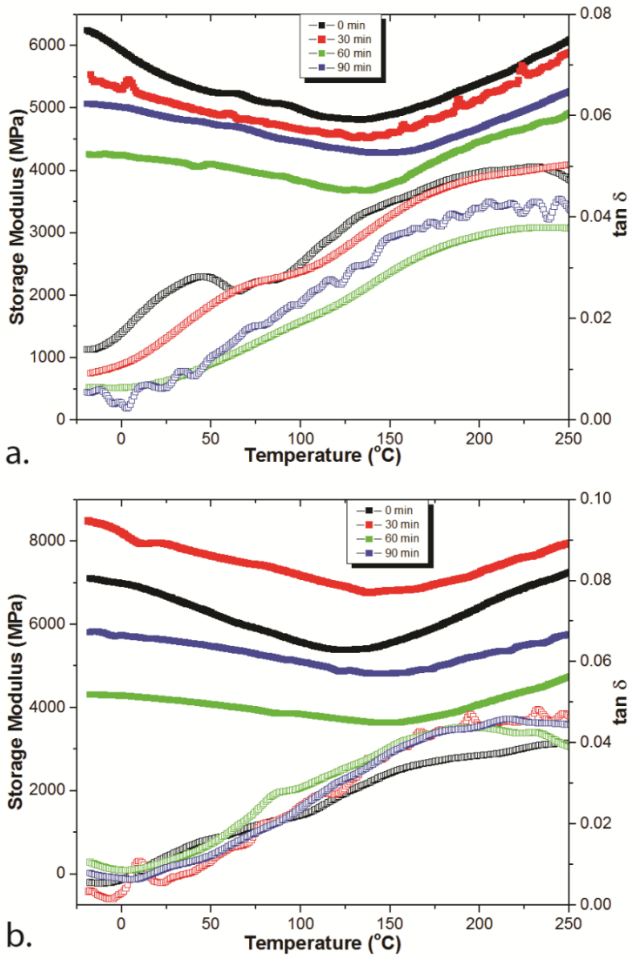

Figure 10. Second heating cycle DMA of PEC after heating to 120°C and annealing for 0–90 minutes. PEC stored a. under ambient conditions; b. in a desiccator. Storage modulus = solid points, tan δ = unfilled points.

Under both storage conditions, storage modulus does not change more than 26% over 275°C, which is highly atypical and offers the potential to use PECs as high stiffness materials with consistent properties over a large operating temperature range.

4. Conclusions

DMA was used to explore the thermomechanical properties and structures of polyelectrolytes and PECs, and TGA was used to correlate changes in properties with water content. Substantial differences in thermomechanical behavior were seen between the polyelectrolytes and were observed as a function of storage conditions and, in some cases, annealing/drying time.

T_gs of PDADMAC were observed to vary by 100°C, depending on storage environment and drying/annealing time. These parameters also change glassy storage modulus values by 100%. Dried PDADMAC is highly lossy.

While the initial samples of PSS, which contained 11.4 wt.% water, exhibited a transition consistent with a glass transition at -41°C, dried PSS did not exhibit a clear glass transition in the tested range. Instead, storage modulus gradually decreased, reaching a minimum around 125-150°C, then increased to recover its initial value.

DMA of the PEC revealed a humidity history-dependent water melt in the first heating cycle, as well as storage modulus values of dried and annealed PECs that only varied by 17-26% over a 275°C temperature range. Based on these results, we report for the first time humidity history as controlling structure and properties of polyelectrolyte-based materials. Ongoing work is focused on understanding humidity hysteresis and continuing to explore the role of water in physical and mechanical properties of polyelectrolyte-based structures.

References

(1) R. von Klitzing, H. Möhwald, *Macromolecules* **1996**, *29*, 6901-6906.

(2) J. Koetz, S. Kosmella, *Polyelectrolytes and Nanoparticles*, Springer-Verlag Berlin,

Heidelberg, **2007**.

(3) N. Karibyants, H. Dautzenberg, *Macromolecules* **1997**, *9297*, 7803-7809.

(4) A. S. Michaels, R. G. Miekka, *J. Phys. Chem.* **1961**, *65*, 1765-1773.

(5) C. H. Porcel, J. B. Schlenoff, *Biomacromolecules* **2009**, *10*, 2968-2975.

(6) R. F. Shamoun, A. Reisch, J. B. Schlenoff, *Adv. Funct. Mater.* **2012**, *22*, 1923-1931.

(7) Q. Wang, J. B. Schlenoff, *Adv. Mater.* **2015**, *27*, 2077-2082.

(8) V. Ball, M. Michel, V. Toniazzo, D. Ruch, *Ind. Eng. Chem. Res.* **2013**, *52*, 5691-5699.

(9) D.-Y. Ji, T.-F. Kuo, H.-D. Wu, J.-C. Yang, S.-Y. Lee, *Carbohydr. Polym.* **2012**, *89*, 1123-1130.

(10) S. D. Nath, C. Abueva, B. Kim, B. T. Lee, *Carbohydr. Polym.* **2015**, *115*, 160-169.

(11) T. C. Lim, M. F. Leong, H. Lu, C. Du, S. Gao, A. C. A. Wan, J. Y. Ying, *Biomaterials* **2013**, *34*, 7064-7072.

(12) M.-R. Park, B.-B. Seo, S.-C. Song, *Biomaterials* **2013**, *34*, 1327-1336.

(13) X. Shi, Y. Du, L. Sun, B. Zhang, A. Dou, *J. Appl. Polym. Sci.* **2006**, *100*, 4614-4622.

(14) H.-J. Cho, S. Chong, S.-J. Chung, C.-K. Shim, D.-D. Kim, *Pharm. Res.* **2012**, *29*, 1007-1019.

(15) D. S. Salloum, J. B. Schlenoff, *Electrochem. Solid-State Lett.* **2004**, *7*, E45-E47.

(16) S. Y. Nam, Y. M. Lee, *J. Memb. Sci.* **1997**, *135*, 161-171.

(17) Q. Zhao, D. W. Lee, B. K. Ahn, S. Seo, Y. Kaufman, J. N. Israelachvili, J. H. Waite, *Nat. Mater.* **2016**, *15*, 407-412.

(18) G. Decher, J. D. Hong, J. Schmitt, *Thin Solid Films* **1992**, *210–211*, 831-835.

(19) G. Decher, *Science* **1997**, *277*, 1232-1237.

(20) C. Zhang, D. E. Hirt, *Polymer* **2007**, *48*, 6748-6754.

(21) X. Huang, N. S. Zacharia, *Soft Matter* **2013**, *9*, 7735-7742.

(22) J. Zhang, L. S. Chua, D. M. Lynn, *Langmuir* **2004**, *20*, 8015-8021.

(23) J. A. Lichter, K. J. Van Vliet, M. F. Rubner, *Macromolecules* **2009**, *42*, 8573-8586.

(24) R. Magboo, A. M. Peterson, *Encycl. Surf. Colloid Sci.* **2016**, 1519-1533.

(25) E. V. Skorb, D. V. Andreeva, *Polym. Chem.* **2013**, *4*, 4834.

(26) F. Caruso, R. A. Caruso, H. Möhwald, *Science* **1998**, *282*, 1111-1114.

(27) F. Caruso, R. A. Caruso, H. Möhwald, *Chem. Mater.* **1999**, *11*, 3309-3314.

(28) E. M. Shchukina, D. G. Shchukin, *Adv. Drug Deliv. Rev.* **2011**, *63*, 837-846.

(29) M. Delcea, H. Möhwald, A. G. Skirtach, *Adv. Drug Deliv. Rev.* **2011**, *63*, 730-747.

(30) D. G. Shchukin, I. L. Radtchenko, G. B. Sukhorukov, *J. Phys. Chem. B* **2003**, *107*, 86-90.

(31) D. G. Shchukin, G. B. Sukhorukov, *Adv. Mater.* **2004**, *16*, 671-682.

(32) M. Delcea, A. Yashchenok, K. Videnova, O. Kreft, H. Möhwald, A. G. Skirtach, *Macromol. Biosci.* **2010**, *10*, 465-474.

(33) A. J. Nolte, N. D. Treat, R. E. Cohen, M. F. Rubner, *Macromolecules* **200**8, *41*, 5793-5798.

(34) J. A. Jaber, J. B. Schlenoff, *Chem. Mater.* **2006**, *18*, 5768-5773.

(35) J. L. Lutkenhaus, K. D. Hrabak, K. McEnnis, P. T. Hammond, *J. Am. Chem. Soc.* **2005**, *127*, 17228-17234.

(36) A. Vidyasagar, C. Sung, R. Gamble, J. L. Lutkenhaus, *ACS Nano* **2012**, *6*, 6174–6184.

(37) S. C. Yeo, A. Eisenberg, *J. Macromol. Sci. Part B* **1977**, *13*, 441–484.

(38) A. W. Imre, M. Schönhoff, C. Cramer, *J. Chem. Phys.* **2008**, *128*, 134905.

(39) K. Köhler, D. G. Shchukin, H. Möhwald, G. B. Sukhorukov, *J. Phys. Chem. B* **2005**, *109*, 18250-18259.

(40) K. Köhler, H. Möhwald, G. B. Sukhorukov, *J. Phys. Chem. B* **2006**, *110*, 24002-24010.

(41) E. Yildirim, Y. Zhang, J. L. Lutkenhaus, M. Sammalkorpi, *ACS Macro Lett.* **2015**, *4*, 1017-10

Chapter 5: Humidity tempering of polyelectrolyte complexes

Published in *Macromolecules,* 2018, 51, 10003-10010

Humidity tempering of polyelectrolyte complexes

Xuejian Lyu,[1] Amy M. Peterson[1,2]

[1]Department of Mechanical Engineering, Worcester Polytechnic Institute, 100 Institute Road, Worcester, MA 01609

[2]Department of Chemical Engineering, Worcester Polytechnic Institute, 100 Institute Road, Worcester, MA 01609

Keywords: Polyelectrolyte complex, relative humidity, humidity tempering, chain rearrangement

Abstract

Water plays an important role in the structure and properties of polyelectrolyte-based materials. In this study, the effect of humidity history on the structure and properties of dried polyelectrolyte complexes (PECs) was studied. PECs were assembled from poly(diallyldimethylammonium chloride) and poly(sodium 4-styrenesulfonate) solutions, then dried under controlled humidity conditions. After exposure to higher humidities (humidity tempering), both room temperature storage modulus and flexural modulus of the resulting PEC increased. Water from the humid air plasticized the PEC, increasing mobility and facilitating chain reorganization during humidity tempering, which resulted in a structure with more intrinsic electrostatic bonds (cross-links) and higher moduli. Humidity tempering can achieve a 35% increase in PEC stiffness during room temperature processing with water as the only solvent. Based on these results, humidity tempering is presented as a novel approach to tailoring the structure and mechanical properties of

polyelectrolyte-based materials under mild conditions, which makes this approach very appealing to biomaterials and controlled release.

1. Introduction

Polyelectrolyte complexes (PECs), which are formed through electrostatic interactions between oppositely charged polyelectrolytes, have garnered sustained interest for their interesting properties and range of potential applications. For example, PECs have been found to have self-healing, anti-corrosion, and biocompatible abilities, among other capabilities.[1–3] Applications of PECs include ion exchange membranes,[4] flocculants,[5] drug delivery materials,[6,7] injectable hydrogels, and tissue engineering scaffolds.[8,9]

Polyelectrolyte-based materials can take many forms. The simplest organization of a PEC is achieved through mixing of oppositely charged polyelectrolyte solutions, which results in random ionic condensation. Under high ionic strength conditions, PECs can form a polyelectrolyte-rich liquid phase known as a complex coacervate.[10] Polyelectrolyte multilayers (PEMs), another category of PECs, are formed through alternating layer-by-layer (LbL) deposition of oppositely charged polyelectrolytes on a substrate.

Given the wide range of structures and properties that can be achieved by PECs, PEC assembly and processing are important areas of investigation. The formation of PECs is affected by many material and assembly parameters, including ionic strength, polyelectrolyte molecular weight, pH, and polyelectrolyte choice.[11–19] In order to achieve homogeneous materials and more desirable properties, PEC processing techniques have also been studied. Homogeneous PEC films can be formed through single-step sedimentation.[20] The sedimentation rate can be varied by changing ionic strength and salt type in polyelectrolyte solutions. Alternatively, PECs plasticized with a salt

solution can be extruded to form a denser, tough material.[21] PECs assembled from poly(allylamine hydrochloride) (PAH) and poly(acrylic acid) (PAA) exhibited self-healing abilities after treatment with a salt solution.[22,23] While NaCl solutions can introduce self-healing ability by increase chain mobility, salt solutions containing multivalent metal ions like $CuCl_2$ can increase the rigidity of those PECs by forming additional cross-links.

Since polyelectrolytes have strong affinities for water, water plays an important role in the structure and properties of polyelectrolyte-based materials. Hariri *et al*. showed that water functions as a plasticizer in PECs and PEMs, since the elastic moduli of both increase after dehydration under defined osmotic stress.[24] Post-assembly treatment also affects the structure and properties of PEMs. PEMs assembled from PAH and PAA exhibit thickness hysteresis during swelling and deswelling using humidified air, which indicates a change in the internal structures of PEMs.[25] Viscoelastic properties of PEMs assembled from PAH and PAA were affected by swelling in an organic solvent/water solution.[26] While PEM exhibited a large swelling ratio in pure water, exposure to organic solvent can lead to a densification increases in rigidity. Thermal behavior of hydrated PECs, including transition temperatures, is also affected by the presence of water.[27–31]

Although properties of polyelectrolyte-based materials depend on assembly conditions and post-assembly treatment, the relationship between internal structure and bulk material properties is still not fully understood. Within a PEC, many types of interactions affect bulk material properties, including hydrogen bonding, van der Waals forces, hydrophobic interactions, and dipole interactions.[32,33] For examples, hydrogen bonds in poly(ethylenimine) (PEI)/ PAA complexes are weakened when heated above 60 °C, which allows for increased water uptake.[34] Previously, we reported that storage conditions and thermal annealing strongly affect the thermal

and mechanical properties of polyelectrolytes and their complexes.[27] By changing the storage conditions and thermally annealing, glass transition temperature (T_g) values of poly(diallyldimethylammonium chloride) (PDADMAC) were shown to vary by 100°C and storage modulus varied by 100%. PECs of PDADMAC and poly(sodium 4-styrenesulfonate) (PSS) showed a storage condition-dependent water melt in the first heating before thermal annealing for both storage conditions (ambient and desiccator). However, PECs stored in a desiccator exhibited a larger drop in storage modulus than PECs stored in ambient during the water melt, which indicates that humidity history can dictate structure and properties of polyelectrolyte-based materials.

In this paper, the role of water in PECs and its influence on mechanical properties and internal structure are explored using dynamic mechanical analysis (DMA) and mechanical testing. DMA in a humidity-controlled environment allowed for *in situ* monitoring of changes in viscoelastic behavior during drying and humidification cycles. Humidity history is shown to have a significant impact on PEC structure and properties. Based on these results, we propose humidity tempering as a gentle, room temperature processing method for tailoring of PECs.

2. Experimental

2.1 Materials.

PDADMAC (M_w 100,000-200,000, 20 wt.% in water) and PSS (M_w ~200,000, 30 wt.% in water) were obtained from Sigma-Aldrich and used as received.

2.2 Sample preparation.

PECs were prepared by mixing 25 mL each of 20 mg/mL PDADMAC and 20 mg/mL PSS in a 100 mL borosilicate glass beaker with magnetic stirring. After the PEC precipitated from solution,

the mixture was transferred into a 50 mL Falcon tube and settled for 24 hours. The supernatant was then poured out and the sedimented PEC was transferred from the tube to a polystyrene petri dish for further drying. PECs were dried under ambient conditions [24±1℃ (room temperature), ~50% relative humidity (RH)] for at least 3 days, then stored in a desiccator (room temperature, RH < 10%) for an additional 48 hours prior to any characterization or tempering.

Unless otherwise specified, humidity tempering of PECs refers to the following humidity protocol: 6 h at 10% RH, 6 h at 30% RH, 6 h at 50% RH, 6 h at 30% RH, and 6 h at 10%.

2.3 Water uptake measurements

To determine equilibrium water uptake at different RHs and to investigate the kinetics of water uptake in PECs, samples were stored under different RHs in a chamber with a humidity controller (MHG32, ProUmid, Deutschland) that operated by flowing humidified air under constant flow rate (120 mL/min). Masses were recorded regularly using a scale until equilibrium water uptake was observed. Water uptake was calculated according to Equation 1:

$$Mass\ change\ (\%) = \frac{M_t - M_0}{M_t} \times 100\% \quad (1)$$

where M_t is the mass of the PEC after storage under a specified RH for time t and M_0 is the initial PEC mass. Thickness of flat PEC pieces during storage under different humidity conditions was also tracked using a micrometer. All measurements were performed at room temperature.

2.4 Dynamic mechanical analysis

DMA was performed using a Netzsch DMA 242E (Netzsch, Germany) with a MHG32 modular humidity generator (ProUmid, Deutschland), using the same humidity-controlled environment as water uptake measurement. A compression geometry push rod of 1 mm diameter was used for mechanical analysis. PEC samples were placed on a rigid platform, while the compression was applied at a frequency of 1 Hz and a target amplitude of 5 μm. The small diameter geometry and

low target amplitude were selected to avoid any potential confinement issues related to PEC swelling as well as to limit the effect of DMA testing on water uptake. DMA was performed at 25°C and RH was varied between 10% and 70%, with RH deviation from the set value of ± 0.5%.

2.5 Thermogravimetric Analysis

Thermogravimetric analysis (TGA) was performed with a Netzsch TG 204 under N_2. To determine water content, testing was performed on PEC samples before and after 50% RH humidity tempering. Samples were put through a heating cycle from 25 ℃ to 400 ℃ with a heating rate of 10 K/min.

2.6 Modulated Differential Scanning Calorimetry

Modulated Differential Scanning Calorimetry (MDSC) was performed on PECs after humidity tempering with a heat-cool-heat cycle. PEC was heated from 80°C to 300°C at a heating rate of 2 K/min with an amplitude of 1.272 K and a period of 60 s. Samples were then cooled to 80°C at 5 K/min, followed by a second heating with the same conditions as the first heating. Inflection points of the reversing heat flow curves from the second heating cycle were taken as the T_g.

2.7 Flexural testing

Flexural testing was conducted on an Instron 5567A using a 3-point bend geometry in accordance with ASTM D790-17. PEC samples prepared using the method described above were fabricated into bars with rectangular cross section (thickness: 3.2±0.1 mm, width: 10.0±0.1 mm). A 0.01 mm/mm/min strain rate was used for flexural testing. Flexural modulus (E_{bend}) was calculated based on the initial linear region of the stress-strain curve. Other mechanical properties including ultimate flexural stress (σ_{max}) and ultimate flexural strain (ε_{max}) were also calculated in accordance with ASTM D790-17.

3. Result and Discussion

3.1 Water uptake

Water uptake kinetics at constant RH is shown in Figure 1. After humidity tempering at 70% RH, PECs exhibited the highest mass change of 19.2%, while PECs under 30%, 50% and 60% RH increased in mass by 2.3%, 4.7% and 9.7%, respectively. Water uptake rate under all RH conditions decreased significantly after 10 hours. The absolute humidities that correspond with 70%, 60%, 50% and 30% RH at 25°C are 0.016 kg/m^3, 0.014 kg/m^3, 0.012 kg/m^3 and 0.007 kg/m^3, respectively. Although the relationship between relative and absolute humidities at this temperature is approximately linear, the initial rate of water uptake at 70% RH (3.74%/hour) was substantially greater than at 50% (0.61%/hour) and 30% RH (0.59%/hour). Since water has been shown to act as a plasticizer for PECs, the absorption of a larger amount of water may enable extra free volume within a PEC network, facilitating even greater water uptake in the high RH condition.[35] The water absorption behavior under different RH conditions was fit to an empirical equation: $M_t/M_\infty = kt^n$, to further explain the diffusion mechanism.[36,37] M_t and M_∞ are water absorbed at time t and at saturation, respectively. k is constant, and n is the exponent to describe the diffusion mechanism. When $n = 0.5$, diffusion follows the Fickian diffusion mechanism, which occurs when the chain relaxation time is much shorter than the water diffusion. When $0.5 < n < 1$, anomalous transportation happens, in which the chain relaxation time is similar to the water diffusion. The fitting results showed that $n = 0.5$ under 70% RH, while $0.5 < n < 1$ under RH condition of 60% and 50% (Appendix 3, Table 1S). This further demonstrates that PECs are more plasticized under 70% RH condition than lower RH conditions, which affect the diffusion mechanism by enabling extra free volume within a PEC network. Interestingly, $n = 0.52$ under 30% RH, which is close to Fickian diffusion. Similar results were previously observed by Kügler *et al*.

A possible explanation is that Fickian-like behavior is observed at lower humidities due to a relative increase in diffusion time as compared to chain relaxation time due to the low concentration gradient.[38] As a result, the chain relaxation time remains shorter than the diffusion time, giving an *n* value close to 0.5.

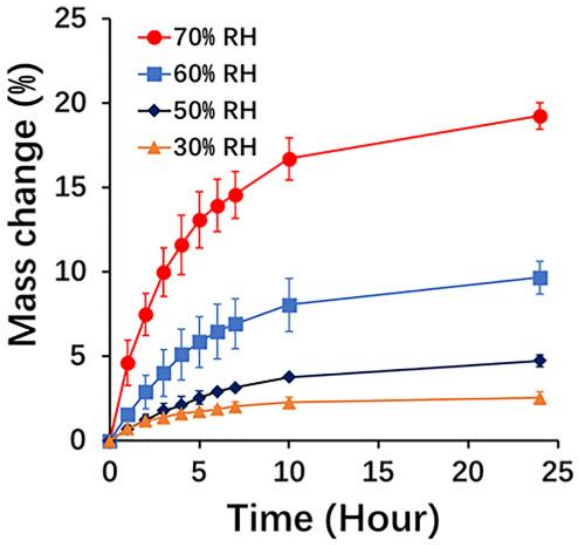

Figure 1. PEC water uptake (wt.%) under 30%, 50% and 70% relative humidity at 25°C calculated based on Equation 1. Error bar represents standard deviation.

To study the effect of RH on PEC structure and properties, water uptake and loss during stepwise RH changes was also measured and is shown in Figure 2a. Each RH condition was held for six hours. After the first six hours at 10% RH, less than 0.5 wt.% water was taken up, which is consistent with the testing conditions being very close to the initial storage conditions (<10% RH). As RH increased stepwise, the amount of absorbed water also increased. However, there was no obvious difference between water loss when RH decreased from 50% to 30% and from 30% to 10%. When compared to the PEC after hydrating steps at a given RH, the PEC after dehydrating steps had a higher water content. The relative thickness, shown in Figure 2b, exhibited a trend

similar to the mass change in Figure 2a, but at a much smaller scale. The maximum thickness change (between the initial 10% RH and 50% RH) was less than 2%. Combined, these mass uptake and thickness results demonstrate hysteresis in the response of PECs to humidifying/dehumidifying conditions, similar to the hysteresis in PEMs observed by Secrist and Nolte.[25]

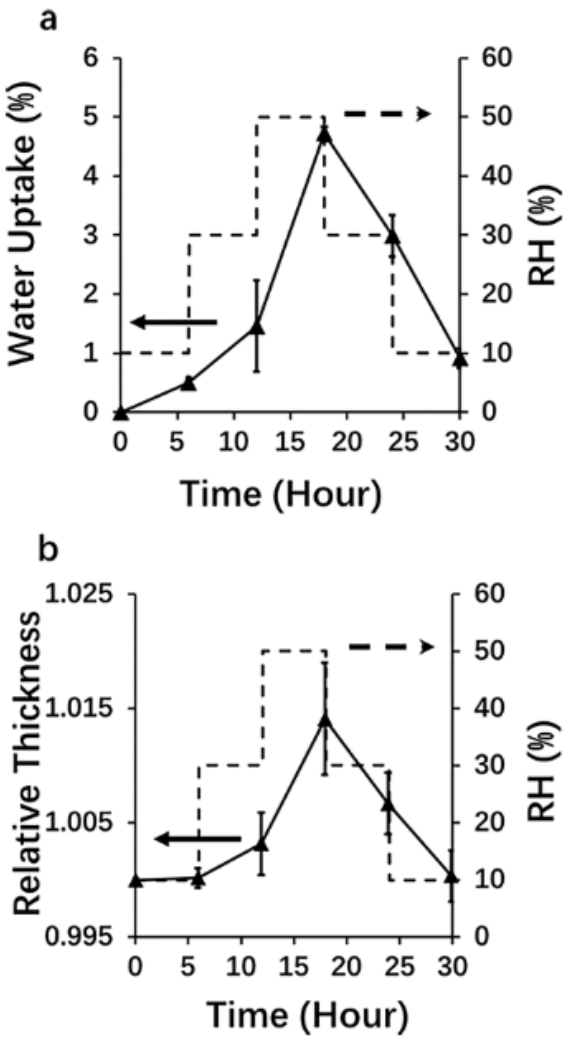

Figure 2. a) PEC water uptake (wt.%) calculated based on Equation 1 b) PEC thickness change vs. relative humidity during stepwise changes in relative humidity. The left y-axis corresponds to water uptake or relative thickness, while the right y-axis corresponds to RH. Error bars represent standard deviation.

3.2 DMA characterization

To further investigate the effect of RH on PEC structure and properties, PECs were characterized using DMA. Figure 3 shows PEC room temperature storage modulus as the RH was increased and decreased in a stepwise manner. The stepwise RH conditions for DMA were the

same as for water uptake and thickness measurements. During the first 6 hours (RH = 10%), storage modulus increased slightly, then reached equilibrium. Since the PEC was previously stored in a desiccator (RH < 10%), the small changes observed are likely due to re-equilibration at 10% RH after loading into the DMA under ambient (RH = 50-60%) conditions. When RH was increased to 30%, storage modulus decreased immediately, presumably due to the plasticizing effect of water that diffused into the system. After the initial modulus drop, storage modulus began to increase. This behavior was repeated in a more drastic way when RH was increased from 30% to 50%. This behavior may be explained by the formation of additional electrostatic bonds between PDADMAC and PSS due to increased chain mobility facilitated by higher water content. These bonds, which will be discussed in greater detail below, act as noncovalent cross-links and increase the stiffness of the PEC. When RH decreased from 50% to 30%, PEC storage modulus increased because of the removal of water, a plasticizer, from the system. When RH decreased from 30% to 10%, storage modulus decreased first, then increased slightly. The final storage modulus of the PEC under 10% RH was 52±20% higher than storage modulus at the beginning of the test, which demonstrates hysteresis in the response of PECs to humidity and further indicates that humidity tempering can be used to tailor the structure and properties of PECs.

Storage modulus increased at a higher rate at 50% RH than at 30% RH. As shown in Figure 2, the PEC had a higher water uptake amount under 50% RH than the water uptake under 30% RH. The rate of storage modulus increase under 50% RH was higher than the rate of change under 30% RH. This correlation suggests that the increases in storage modulus during humidification are tied to PEC water content and the increased mobility that water provides.

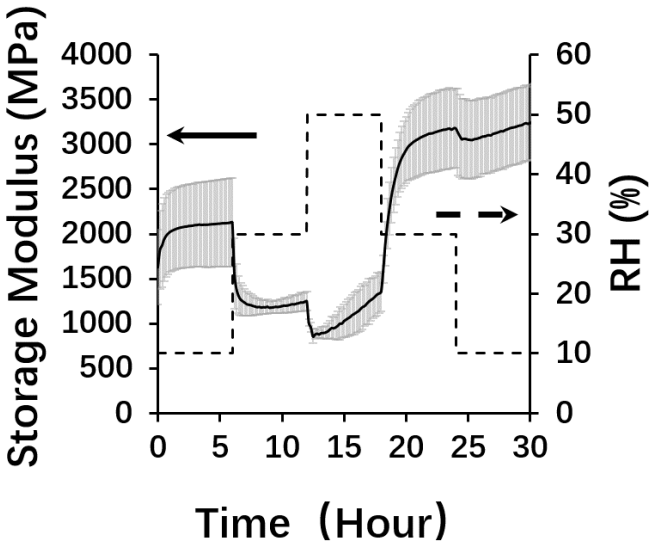

Figure 3. PEC storage modulus during stepwise humidification and dehumidification. Each step had a duration of six hours. Error bars represents standard deviation.

DMA calculates moduli based on the sample's initial thickness, so substantial changes in thickness during humidification and dehumidification could lead to inaccurate modulus values. However, as seen in Figure 2b, the highest thickness change was 1.4%, which occurred upon humidification from 10% to 50% RH. This is substantially smaller in magnitude than the changes in storage modulus, which increased as much as 50%. Combined, these results indicate that the effect of thickness on measured storage modulus was negligible.

PECs were also tempered for longer periods of time at a single RH (30%, 50%, or 70%). Figure 4 shows the PEC's response to tempering at 30% and 50% RH. PECs tempered at 70% RH tended to crack during testing due to the drastic change in humidity, which made it difficult to obtain reliable results (Appendix 3, Figure S1).

PECs were equilibrated at 10% RH (the initial storage condition) for 6 hours, followed by tempering at a higher RH for 25 hours, and dehumidification at 10% RH for 24 hours. Results for tempering at 30% and 50% RH are shown in Figure 4. The initial equilibration resulted in an increase in storage modulus, which plateaued after approximately 5 hours, presumably due to re-equilibration and loss of water after the PEC was exposed to ambient RH during loading in the DMA (Appendix 3, Figure S2). When RH increased from 10% to 50%, storage modulus initially decreased sharply due to plasticization with water, then started to increase, similar to the behavior seen in Figure 3. After 18 hours at 50% RH, storage modulus began to reach equilibrium (storage modulus rate of change < 50 MPa/h). Based on the results shown in Figure 1, the rate of water uptake at 50% RH was quite low after 10 hours (0.068 wt.%/h), while the storage modulus still had a relatively high rate of change at this point (341.8 MPa/h). These results indicate that storage modulus increases were primarily driven by changes in the internal structure that facilitated more intrinsic electrostatic bonding within the PEC.

Storage modulus values at 30% and 50% RH followed similar paths for the first 9 hours of tempering. However, after that point, PEC storage modulus under 50% RH continued to increase, while PEC storage modulus under 30% RH leveled off. The final storage modulus at 50% RH was on average 53% higher than the final storage modulus at 30% RH and was 70±14% higher than the untampered storage modulus. These results provide additional evidence that the primary role of water in humidity tempering is to facilitate greater bonding with the PECs. Additionally, the similar initial behavior indicates that electrostatic bonding is kinetically limited for the first 9 hours of tempering but becomes thermodynamically limited at longer tempering times.

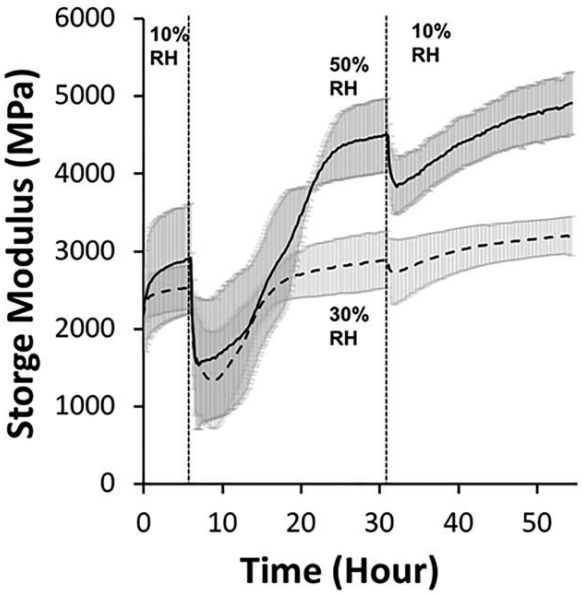

Figure 4. PEC storage modulus under extended humidity tempering at 50% RH (solid line) and 30% RH (dotted line). Error bars represents standard deviation.

Storage modulus changes after humidity tempering are proposed to be caused by changes in the internal structure of the PEC. When RH increases from 10% to 50% at 25°C, the absolute humidity increases from 0.002 kg/m^3 to 0.012 kg/m^3. As humidity increases, more water is available to diffuse into the PEC. Water can disrupt the intrinsic electrostatic bonds between polyelectrolytes and decrease the cross-link density of the PEC.[24] This may explain the initial drop in storage modulus upon increasing RH from 10% to 50%, which lasted for 1.2 hours. However, water uptake results did not equilibrate until ~10 hours of humidification had passed, indicating that water diffusion and storage modulus increase occurred simultaneously after the initial modulus drop. We propose the following explanation for the longer tempering time storage modulus increase: As mobility increases, chains can rearrange with greater ease. Within the PEC, some charges along the polyelectrolytes were initially compensated by small counterions. During the rearrangement process, counterion-compensated repeat units start to form ion pairs, which act as electrostatic

cross-links. This increase in PEC cross-link density leads to the observed increase in storage modulus.

The number of electrostatic bonds between oppositely charged polyelectrolytes directly contributes to the stiffness of the PEC, while the plasticizing effect of water will decrease the stiffness. As discussed above, after plasticization by water, polyelectrolyte mobility increases, facilitating more electrostatic bonding between polyelectrolyte chains. However, the rate of water uptake is initially faster than that of electrostatic bonding between polymer chains, so plasticization dominates at the start of each humidification step. During humidity tempering, the number of intrinsically compensated electrostatic bonds (cross-links) increases over time, and their contribution to stiffness eventually surpasses the plasticizing effect. According to Figure 4, this transition occurs after approximately 4 hours at 50% RH, at which point storage modulus started to increase in a non-linear behavior consistent with more traditional cross-linking mechanisms.[39,40]

A description of the relationship between modulus and cross-link density was developed by Smith and applied in previous research by Hariri *et al.* and Jaber and Schlenoff:[24,41,42]

$$\frac{\nu RT}{G} = \frac{1}{\Phi} - \frac{6\bar{C}_n}{5q^2\bar{n}} \quad (2)$$

G can be estimated from the number of moles of sub chains per unit volume (ν), which is proportional to the cross-link density c (ν = 3c). $\bar{n}$ is the geometric mean number of bonds in the network chain, $\bar{C}_n$ is a characteristic ratio given by $\bar{C}_n = n^{0.57}$, and q, a dimensional factor which for backbone with carbon−carbon single bonds, is equal to 0.83. E=3G when assuming Poisson's ratio is 0.5, so G in the equation can be substitute with E/3, while values of Φ, $\bar{C}_n$, q, and n were determined in previous research.[41]

In considering the effect of water plasticization on PEC mechanical properties, the relationship between plasticizer and elastic modulus can be expressed using an empirical equation:[43]

$$E = E_o e^{-kr_p} \quad (3)$$

E_0 is the modulus without plasticizer and E is the actual modulus. k is a constant represents plasticizer efficiency. r_p is the molar ratio of the plasticizer, so in this case it is the molar ratio of water to PEC. E_0 is affected by cross-link density, while E is affected by both cross-link density and plasticizer ratio. E_0 of PEC can be determined from previous research, in which the same PEC was annealed at 120 ºC for an extended period of time in an N_2 environment to full remove water.[27] For the PEC before humidity tempering, r_p and E can be determined from Table 1 and Figure 4, respectively. With known r_p, E_0, and E, the plasticizer efficiency k can be calculated and assumed to remain constant.

Combining Equation 2 and 3, the relationship between cross-link density c, modulus E and plasticizer ratio r_p can be expressed as:

$$\frac{9cRT}{E/e^{-kr_p}} = \frac{1}{\Phi} - \frac{6\bar{C}_n}{5q^2\bar{n}} \quad (4)$$

During humidity tempering, r_p can be determined based on Figure 1 and Table 1, so cross-link density c can be calculated using experimentally determined values of E and r_p. Cross-link density as a function of time during tempering at 30% RH and 50% RH are shown in Figure 5. While the PEC has a higher cross-link density at the end of humidity tempering under 50% RH than 30% RH, cross-link density of PEC increased at a similar rate under 50% and 30% RH at the beginning of humidity tempering. This finding is consistent with the similar storage moduli shown in Figure 4 for the first ~10 hours of humidity tempering. While cross-link density levels out for 30% RH tempering, it appears to continue to increase approximately linearly for 50% RH tempering. These results suggest that the kinetics of cross-link formation are diffusion limited for the 8-10 hours of tempering. At later time points, cross-link kinetics appears to be modulated by water content; however, since water act as a plasticizer and a cross-linking agent (through hydrogen bonding), a

more precise analysis cannot be provided based on the current data. The decrease in cross-link density upon humidification provides strong support for hydrogen bonding between water and polyelectrolytes. Therefore, the increase in cross-link density during humidity tempering was not only caused by increases in intrinsic ion pairs, but also by the formation of hydrogen bonds.

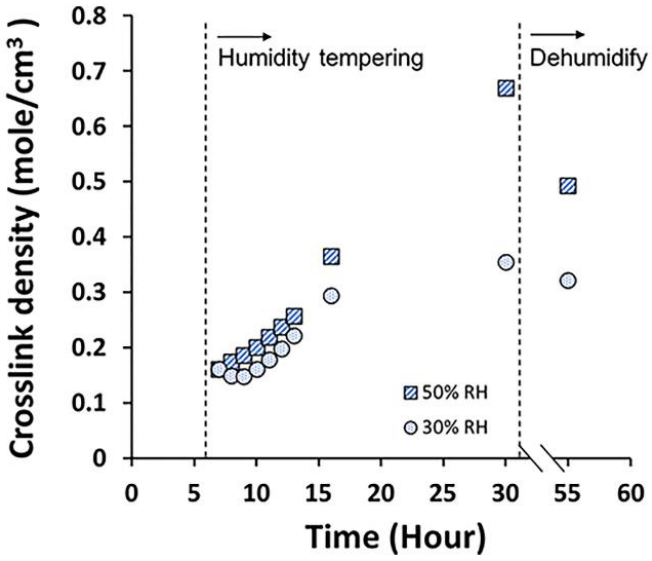

Figure 5. Calculated cross-link density in PECs during humidity tempering at 30% RH and 10% RH, and after dehumidification at 10% RH.

When plasticized by water, polyelectrolytes within the PEC gain extra mobility to reorganize into structures with higher electrostatic cross-link density and higher modulus. This requires movements between neighboring intrinsic sites and the combining of extrinsic sites, as shown in Figure 6. As discussed previously, while water uptake under 30% and 50% RH are different, increase rate of cross-link density at the beginning of 30% and 50% RH are similar. These results indicate that the reorganization process is limited by the exchange rate of polyelectrolyte sites, rather than the diffusion of water. Recent work from Fares *et al.* proposed a self-exchange behavior

between neighboring polyelectrolyte ion pairs under limited chain mobility conditions, which is consistent with humidity tempering results.[44]

Multiple exposures to higher humidity were also investigated, to determine if equilibrium swelling and reorganization can be achieved in a single humidification/dehumidification cycle. Specimens were exposed to two cycles of 50% RH for 24 hours and 10% RH for 24 hours. Upon re-exposure to 50% RH, the PEC recovered to the same E' level 2 hours faster than the initial exposure. PECs also exhibited faster water uptake up re-exposure to 50% RH. However, the maximum water uptake is the same with first time exposure (Appendix 3, Figure S3). This indicates that PEC structural rearrangements reached an equilibrium during the first exposure to 50% RH, as re-exposure did not change the final E' or the maximum water uptake.

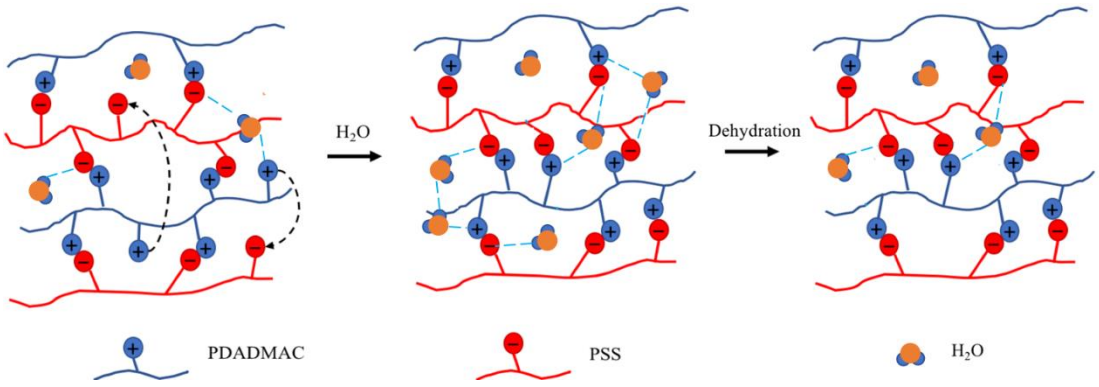

Figure 6. Proposed mechanism: Increases in environmental water content during humidity tempering facilitate polyelectrolyte chain mobility and the formation of additional electrostatic bonds between polyanions and polycations in the PEC. Extrinsically bound counterions omitted for clarity.

3.3 PEC Thermal Transitions

Zhang *et al.* recently demonstrated that the T_g of polyelectrolyte-based structures is controlled by the number of water molecules surrounding an intrinsically bonded ion pair.[30] Specifically, $1/T_g$ was found to be proportional to the natural log of the ratio of water molecules to intrinsic ion pairs. As the ratio of water molecules to intrinsic ion pairs increase in the PEC, T_g decreases. Based on this approach, T_g values were calculated based on the water content from TGA. Humidity tempering was performed under 25°C, which means PECs were glassy under all humidity tempering conditions.

Table 1. Water content and calculated T_g of PEC before, during and after humidity tempering under 50% RH

	Before humidity tempering	**25 hours at 50% RH humidity tempering**	**After 50% RH humidity tempering**
PEC water content (wt.%)	8.0 ± 2.9	15.1 ± 0.9	8.3 ± 0.5
Calculated T_g (ºC)	248	133	242

Interestingly, humidity tempered PECs exhibited a T_g of 225±8°C (Figure 7), which is substantially lower than the calculated T_g based on water content (242°C). Thermal transitions in PECs relate to the lifetime of hydrogen bonds between water and PSS.[31] The lifetime of hydrogen bonds can be defined as the time period between bond formation and breakage.[45] The lifetime of hydrogen bonds between water and extrinsically bonded PSS has been shown to be temperature

insensitive, while hydrogen bond lifetime between water and intrinsically bonded PSS decreases with increases temperature, indicating that water bonding with intrinsically bonded PSS dominates the thermal transition.[30] Based on this framework, we propose that humidity tempering shifts T_g values away from the relationship reported by Zhang *et al.* because tempering facilitates the formation of additional intrinsic ion pairs. Given the same water content, PECs with higher intrinsic ion pair density will be more sensitive to increases in temperature, which results in a lower T_g.

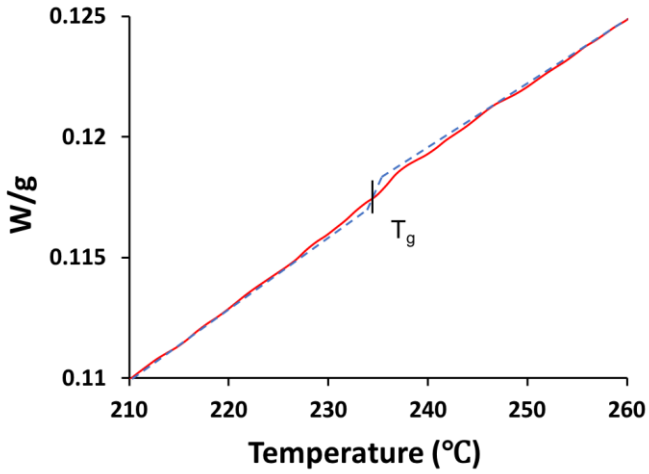

Figure 7. Representative reversing heat flow curve of PEC after humidity tempering under 50% RH. Dotted line represents trend of the curve before and after the inflection point. Replicas of data included in Appendix 3.

3.4 Flexural testing

Static mechanical properties of PEC were also characterized by flexural testing to further demonstrate the effect of humidity tempering. Flexural test results for the as-prepared PEC and humidity tempered PEC are shown in Figure 8. Table 2 compares the mechanical properties of

humidity tempered and untempered PEC. After humidity tempering under 50% RH as shown in Figure 4, E_{bend} of the PEC increased by 35.4%. Humidity tempered PECs also exhibit higher σ_{max}. These increases E_{bend} and σ_{max} result from the increase in cross-link density facilitated by the humidity tempering process. Both humidity tempered and untempered PECs had brittle fracture behavior, with <4% ultimate flexural strain before and after humidity tempering.

Table 2. Mechanical properties of tempered and untempered PEC

	Untempered PEC	**Tempered PEC**
E (MPa)	2318 ± 205	3138 ± 146
σ_{max} (MPa)	71.6 ± 22.9	105 ± 10.6
ε_{max} (%)	3.65 ± 1.37	3.54 ± 0.57

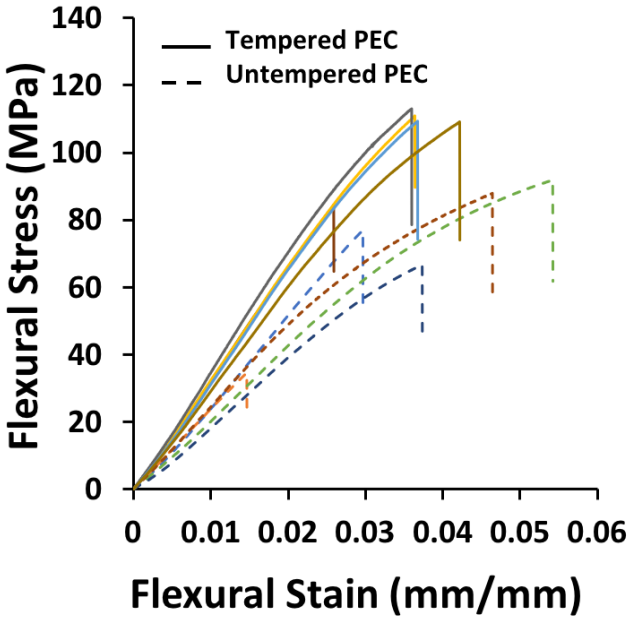

Figure 8. Results of flexural testing of humidity tempered and untempered PEC.

Conclusions

PECs were assembled through mixing aqueous solutions of PDADMAC and PSS. DMA and flexural testing were used to measure the effect of humidity history on mechanical properties of PEC. After humidity annealing, the PEC showed improvements in storage modulus, flexural modulus, and flexural strength. During humidity tempering, polyelectrolyte chains within a PEC gain extra mobility due to the plasticization by water, which allows them to rearrange and form a structure with more intrinsically compensated electrostatic bonds. Humidity tempering results in a more highly cross-linked structure that has mechanical properties consistent with the increase in cross-link density yet has a lower T_g. This anomaly is explained by the existing theory regarding the source of the glass transition in polyelectrolyte-based structures.

Based on these results, we report for the first time that humidity tempering can be used to control the mechanical properties of PEC. These results highlight the potential of polyelectrolyte-

based materials for new applications where tailoring of mechanical properties is desired, yet mild processing conditions are necessary. Humidity tempering offers room temperature processing with water as the only necessary solvent, which makes it a low energy, green approach to polymer processing. Potential applications such as drug-/biologic-eluting structures will be further studied. While this material can potentially be used in implanted devices, further research is needed to study the mechanical response of this material to exposure to salt buffered environments. Future works will include humidity tempering of PEMs, which are more kinetically trapped structures than PECs due to their layer-by-layer assembly. Investigation of PEMs will help to discover the driving forces for chain rearrangement during humidity tempering and could provide further insight into the structural differences between PEMs and PECs. Effect of salt will be studied in future work as well. Including salt in the initial PEC formation will not only change the ratio between intrinsic and extrinsic ion pairs in the PEC's initial state, but also could improve the ability of PECs to uptake water. PEC assembled under different salt concentration will be tested under different RH conditions to study the effect of salt on humidity tempering.

References

(1) Lyu, X.; Peterson, A. M. The Princess and the Pea Effect: Influence of the First Layer on Polyelectrolyte Multilayer Assembly and Properties. *J. Colloid Interface Sci.* **2017**, *502*, 165–171.

(2) Tsukruk, V. V.; Bliznyuk, V. N.; Visser, D.; Campbell, A. L.; Bunning, T. J.; Adams, W. W. Electrostatic Deposition of Polyionic Monolayers on Charged Surfaces.

Macromolecules **1997**, *30* (21), 6615–6625.

(3) Andreeva, D. V.; Fix, D.; Möhwald, H.; Shchukin, D. G. Self-Healing Anticorrosion Coatings Based on pH-Sensitive Polyelectrolyte/Inhibitor Sandwichlike Nanostructures. *Adv. Mater.* **2008**, *20* (14), 2789–2794.

(4) B. Smitha; S. Sridhar; Khan, A. A. Polyelectrolyte Complexes of Chitosan and Poly(Acrylic Acid) As Proton Exchange Membranes for Fuel Cells. **2004**, 2233–2239.

(5) Petzold, G.; Nebel, A.; Buchhammer, H.-M.; Lunkwitz, K. Preparation and Characterization of Different Polyelectrolyte Complexes and Their Application as Flocculants. *Colloid Polym. Sci.* **1998**, *276* (2), 125–130.

(6) Shu, X. Z.; Zhu, K. J. A Novel Approach to Prepare Tripolyphosphate/Chitosan Complex Beads for Controlled Release Drug Delivery. *Int. J. Pharm.* **2000**, *201* (1), 51–58.

(7) Nujoma, Y. N. Erodible Drug Release From an Drug-Polyelectrolyte Complex. **1995**, *31* (10), 937–940.

(8) Ji, D. Y.; Kuo, T. F.; Wu, H. Da; Yang, J. C.; Lee, S. Y. A Novel Injectable Chitosan/Polyglutamate Polyelectrolyte Complex Hydrogel with Hydroxyapatite for Soft-Tissue Augmentation. *Carbohydr. Polym.* **2012**, *89* (4), 1123–1130.

(9) Nath, S. D.; Abueva, C.; Kim, B.; Lee, B. T. Chitosan-Hyaluronic Acid Polyelectrolyte Complex Scaffold Crosslinked with Genipin for Immobilization and Controlled Release of BMP-2. *Carbohydr. Polym.* **2015**, *115*, 160–169.

(10) Wang, Q. F.; Schlenoff, J. B. The Polyelectrolyte Complex/Coacervate Continuum. *Macromolecules* **2014**, *47* (9), 3108–3116.

(11) Dautzenberg, H. Polyelectrolyte Complex Formation in Highly Aggregating Systems. 1. Effect of Salt: Polyelectrolyte Complex Formation in the Presence of NaCl.

Macromolecules **1997**, *30* (25), 7810–7815.

(12) Fredheim, G. E. Polyelectrolyte Complexes: Interactions Between Lignosulfonate and Chitosan. *Biomacromolecules* **2003**, *4*, 232–239.

(13) Biesheuvel, P. M.; Stuart, M. A. C. Cylindrical Cell Model for the Electrostatic Free Energy of Polyelectrolyte Complexes. *Langmuir* **2004**, *20* (11), 4764–4770.

(14) Gamzazade, A. I.; Nasibov, S. M. Hydrodynamic and Molecular Characteristics of Polyelectrolyte Complexes between Sodium Dextransulfate and Chitosan Hydrochloride. *Carbohydr. Polym.* **2002**, *50* (4), 345–348.

(15) Jomaa, H. W.; Schlenoff, J. B. Salt-Induced Polyelectrolyte Interdiffusion in Multilayered Films: A Neutron Reflectivity Study. *Macromolecules* **2005**, *38* (20), 8473–8480.

(16) Poptoshev, E.; Schoeler, B.; Caruso, F. Influence of Solvent Quality on the Growth of Polyelectrolyte Multilayers. *Langmuir* **2004**, *20* (3), 829–834.

(17) McAloney, R. A.; Sinyor, M.; Dudnik, V.; Cynthia Goh, M. Atomic Force Microscopy Studies of Salt Effects on Polyelectrolyte Multilayer Film Morphology. *Langmuir* **2001**, *17* (21), 6655–6663.

(18) Sui, Z.; Salloum, D.; Schlenoff, J. B. Effect of Molecular Weight on the Construction of Polyelectrolyte Multilayers: Stripping versus Sticking. *Langmuir* **2003**, *19* (6), 2491–2495.

(19) Shiratori, S. S.; Rubner, M. F. PH-Dependent Thickness Behavior of Sequentially Adsorbed Layers of Weak Polyelectrolytes. *Macromolecules* **2000**, *33* (11), 4213–4219.

(20) Ball, V.; Michel, M.; Toniazzo, V.; Ruch, D. The Possibility of Obtaining Films by Single Sedimentation of Polyelectrolyte Complexes. *Ind. Eng. Chem. Res.* **2013**, *52* (16), 5691–5699.

(21) Shamoun, R. F.; Reisch, A.; Schlenoff, J. B. Extruded Saloplastic Polyelectrolyte

Complexes. *Adv. Funct. Mater.* **2012**, *22* (9), 1923–1931.

(22) Zhang, H.; Wang, C.; Zhu, G.; Zacharia, N. S. Self-Healing of Bulk Polyelectrolyte Complex Material as a Function of PH and Salt. *ACS Appl. Mater. Interfaces* **2016**, *8* (39), 26258–26265.

(23) Reisch, A.; Roger, E.; Phoeung, T.; Antheaume, C.; Orthlieb, C.; Boulmedais, F.; Lavalle, P.; Schlenoff, J. B.; Frisch, B.; Schaaf, P. On the Benefits of Rubbing Salt in the Cut: Self-Healing of Saloplastic PAA/PAH Compact Polyelectrolyte Complexes. *Adv. Mater.* **2014**, *26* (16), 2547–2551.

(24) Hariri, H. H.; Lehaf, A. M.; Schlenoff, J. B. Mechanical Properties of Osmotically Stressed Polyelectrolyte Complexes and Multilayers: Water as a Plasticizer. *Macromolecules* **2012**, *45* (23), 9364–9372.

(25) Secrist, K. E.; Nolte, A. J. Humidity Swelling / Deswelling Hysteresis in a Polyelectrolyte Multilayer Film. *Macromolecules* **2011**, 2859–2865.

(26) Gu, Y.; Huang, X.; Wiener, C. G.; Vogt, B. D.; Zacharia, N. S. Large-Scale Solvent Driven Actuation of Polyelectrolyte Multilayers Based on Modulation of Dynamic Secondary Interactions. *ACS Appl. Mater. Interfaces* **2015**, *7* (3), 1848–1858.

(27) Lyu, X.; Clark, B.; Peterson, A. M. Thermal Transitions in and Structures of Dried Polyelectrolytes and Polyelectrolyte Complexes. *J. Polym. Sci. Part B Polym. Phys.* **2017**, *55* (8), 684–691.

(28) Fu, J.; Abbett, R. L.; Fares, H. M.; Schlenoff, J. B. Water and the Glass Transition Temperature in a Polyelectrolyte Complex. *ACS Macro Lett.* **2017**, *80* (3), 1114–1118.

(29) Zhang, Y.; Li, F.; Valenzuela, L. D.; Sammalkorpi, M.; Lutkenhaus, J. L. Effect of Water on the Thermal Transition Observed in Poly(Allylamine Hydrochloride)-Poly(Acrylic Acid)

Complexes. *Macromolecules* **2016**, *49* (19), 7563–7570.

(30) Zhang, Y.; Batys, P.; O'Neal, J. T.; Li, F.; Sammalkorpi, M.; Lutkenhaus, J. L. Molecular Origin of the Glass Transition in Polyelectrolyte Assemblies. *ACS Cent. Sci.* **2018**, *4* (5), 638–644.

(31) Yildirim, E.; Zhang, Y.; Lutkenhaus, J. L.; Sammalkorpi, M. Thermal Transitions in Polyelectrolyte Assemblies Occur via a Dehydration Mechanism. *ACS Macro Lett.* **2015**, *4* (9), 1017–1021.

(32) V. Klitzing, R.; Wong, J. E.; Jaeger, W.; Steitz, R. Short Range Interactions in Polyelectrolyte Multilayers. *Curr. Opin. Colloid Interface Sci.* **2004**, *9* (1–2), 158–162.

(33) Kharlampieva, E.; Sukhishvili, S. A. Polyelectrolyte Multilayers of Weak Polyacid and Cationic Copolymer: Competition of Hydrogen-Bonding and Electrostatic Interactions. *Macromolecules* **2003**, *36* (26), 9950–9956.

(34) Gu, Y.; Weinheimer, E. K.; Ji, X.; Wiener, C. G.; Zacharia, N. S. Response of Swelling Behavior of Weak Branched Poly(Ethylene Imine)/Poly(Acrylic Acid) Polyelectrolyte Multilayers to Thermal Treatment. *Langmuir* **2016**, *32* (24), 6020–6027.

(35) Hirai, Y.; Nakajima, T. Sorption of Water Vapor into Polyelectrolyte Complex of Poly(Styrenesulfonic Acid)/Poly(4-Vinyl-N-Ethylpyridinium Bromide). *J. Macromol. Sci. Part B* **1991**, *30* (1), 141–153.

(36) Tanchak, O. M.; Barrett, C. J. Swelling Dynamics of Multilayer Films of Weak Polyelectrolytes. *Chem. Mater.* **2004**, *16* (14), 2734–2739.

(37) Lee, S. W.; Lee, D. Integrated Study of Water Sorption/Desorption Behavior of Weak Polyelectrolyte Layer-by-Layer Films. *Macromolecules* **2013**, *46* (7), 2793–2799.

(38) Kügler, R.; Schmitt, J.; Knoll, W. The Swelling Behavior of Polyelectrolyte Multilayers in

Air of Different Relative Humidity and in Water. *Macromol. Chem. Phys.* **2002**, *203* (2), 413–419.

(39) Gillham, J. K. Review: Torsional Braid Analysis of Polymers. *J. Macromol. Sci. Part B* **1974**, *9* (2), 209–237.

(40) Gillham, J. K. Characterization of Thermosetting Materials by Torsional Braid Analysis. *Polym. Eng. Sci.* **1976**, *16* (5), 353–356.

(41) Jaber, J. A.; Schlenoff, J. B. Mechanical Properties of Reversibly Cross-Linked Ultrathin Polyelectrolyte Complexes. *J. Am. Chem. Soc.* **2006**, *128* (9), 2940–2947.

(42) Smith, T. L. Modulus of Tightly Crosslinked Polymers Related to Concentration and Length of Chains. *J. Polym. Sci. Polym. Symp.* **1974**, *46* (1), 97–114.

(43) Sothornvit, R.; Krochta, J. M. Plasticizer Effect on Mechanical Properties of β-Lactoglobulin Films. *J. Food Eng.* **2001**, *50* (3), 149–155.

(44) Fares, H. M.; Schlenoff, J. B. Diffusion of Sites versus Polymers in Polyelectrolyte Complexes and Multilayers. *J. Am. Chem. Soc.* **2017**, *139* (41), jacs.7b07905.

(45) Astley, T.; Birch, G. G.; Drew, M. G. B.; Mark Rodger, P. Lifetime of a Hydrogen Bond in Aqueous Solutions of Carbohydrates. *J. Phys. Chem. A* **1999**, *103* (26), 5080–5090.

Chapter 6: Polyelectrolyte-based materials for drug delivery

Abstract

Two charged biopolymers, starch and gelatin, were investigated for drug delivery applications. Starch (amylose and amylopectin) was used to fabricate thin films for drug delivery through the buccal mucosa. Starch was gelatinized with plasticizer added to form flexible thin films. Swelling and degradation behavior of starch films under simulated saliva environment was studied. Starch film can swell up to 295% in 60 min under simulated saliva environment. During degradation studies, starch films started to fell apart after 20 min and almost complete degraded in 60 min. A two-step functionalization method was also studied by using Carbonyldiimidazole (CDI) and L-lysine to introduce charged functional group to starch films. By introducing positively charged function group to starch molecules, adhesion property with negatively charged buccal mucosal mucin could potentially be improved, as shown in the following diagram. Results showed that starch films were successfully activated by CDI, and L-lysine functionalization introduced positively charge functional group. Gelatins for capsules were fabricated into thin films and characterized under humidity controlled DMA. Gelatins from different resources showed large modulus variation under humidity change. Short time aging under 40℃ did not show substantially affected mechanical properties of gelatin films.

6.1 Starch Film for Oral Adhesive Drug Delivery Patches

6.1.1 Motivation

Oral drug delivery methods have the potential to provide relief to large group of patients with higher efficiency. With the rapid drug absorption through the buccal mucosa, sleep aids could be delivered by oral adhesive patches. However, for drug delivery through buccal mucosa, unidirectional delivery is preferred. This is due to the common bitterness of many common active ingredients. Therefore, the patches need to adhere to the buccal mucosa effectively during drug release, as shown in Figure 1. Also, to avoid a choking hazard, the patch needs to degrade in soon after the drug release.

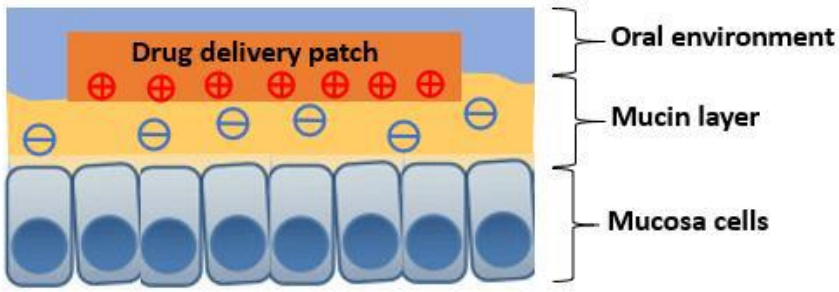

Figure 1. Functionalized drug delivery patch in oral environment

6.1.2 Methodology

Starch film fabrication

5 wt% of starch [mixture of amylose and amylopectin (Ratios: 100% amylose, 50% amylose + 50% amylopectin, 100% amylopectin)] and 2 wt% of glycerol were dispersed in water. Glycerol was added as plasticizer. The mixture was heated up to 90 ℃ in water bath under magnetic stirring for 30 min to get complete gelatinization. After gelatinization, the solution was cooled down to

room temperature and defoamed using Thinky mixer. The solution was then poured into a petri dish and dry under 60 ℃ for 24 hours to get starch films.

Swelling and degradation study

Swelling and degradation behavior of as-prepared starch films was studied using simulated saliva fluid (SSF) and simulated saliva fluid with α-amylase (SSF-A), respectively. SSF was prepared using the following formulations, while SSF-A was prepared by adding 125 U/ml of α-amylase (1500 U/mg) into SSF. [1,2]

Table 1. Components in simulated saliva fluid without α-amylase

Components	Concentrations
Sodium carboxymethyl cellulose	10.0 g/L
KCl	8.3 mM
$MgCl_2•6H_2O$	0.29 mM
$CaCl_2•2H_2O$	1.13 mM
K_2HPO4	4.62 mM
KH_2PO4	2.40 mM

In swelling study, as-prepared starch films were immersed in SSF under 37 ℃ for 1 hour, mass change of starch films were tracked every 10 min. In degradation study, as-prepared starch films were immersed in SSF-A under 37℃ for 1 hour, degradation behavior of starch films were recorded every 10 min.

Starch film functionalization

As buccal mucin is negatively charged, introducing positively charged function group to starch molecules could potentially improve adhesion.[3] L-lysine was selected to functionalize starch films and carbonyldiimidazole (CDI) was used to activate imidazole carbamate intermediate for L-lysine functionalization.[4] The reaction mechanism of L-lysine functionalization is shown in Scheme 1.

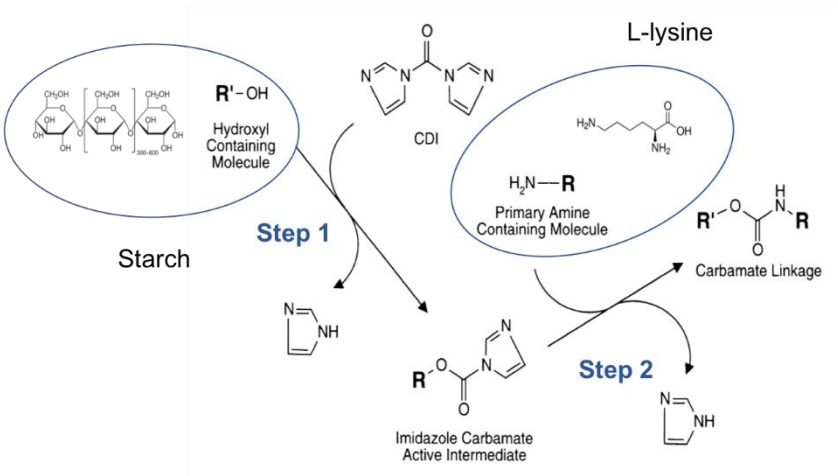

Scheme 1. L-lysine functionalization reaction mechanism (adjusted form Ref. 4)

As-prepared starch film was washed in 25 wt%, 50 wt%, 75 wt% and 100 wt% of DMF in water. Then starch films were added to a 50 mg/mL CDI in DMF solution, reacted under room temperature for 2 hours. Starch film were then removed from solution and washed 3 times in pure DMF (Half of starch film was cut off and kept for further FTIR characterization). 10 mg of L-lysine was dissolved in water and starch films were added into L-lysine solution, reacted under room temperature for 2 hours. Starch film were removed from solution and washed 3 times in water, then dried under ambient condition and kept for further FTIR characterization.

6.1.3 Result and Discussion

Starch film fabrication

After drying for 24 hours, starch films were removed from substrates. Images of starch films with and without glycerol as a plasticizer are shown in Figure 1. Starch films without plasticizer are easy to break and hard to peel off substrate while starch films with glycerol is flexible and easy to peel off substrate. Starch film with glycerol added are also less transparent than starch film without glycerol.

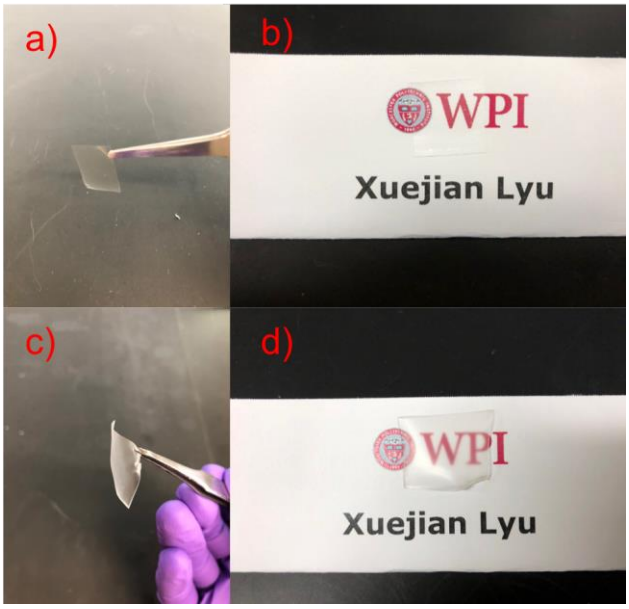

Figure 1. As prepared starch film (100% amylose) a) and b) without glycerol, c) and d) without glycerol.

Swelling and degradation study

As shown in Figure 2, mass of starch film gradually increased and reached 266 % in the first 20 min. Figure 2 also indicates that the swelling behavior will reach equilibrium when mass change reached 295% in 1 hour. Figure 3 showed the degradation behavior of starch films in SSF-A under

37 ℃. α-amylase has a drastic impact on starch films. All starch films were not able to remain original shape after 20 min and almost fully degraded in 60 min. Although starch films were assembled with different ratio of amylose and amylopectin, based on the results of degradation study, there is no obvious change in degradation rate between different starch films under current α-amylase concentration.

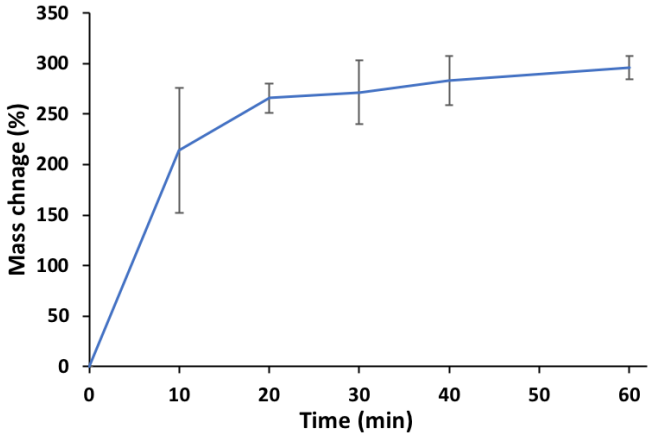

Figure 2. Swelling behavior of starch films (100% amylose) in SSF under 37 ℃.

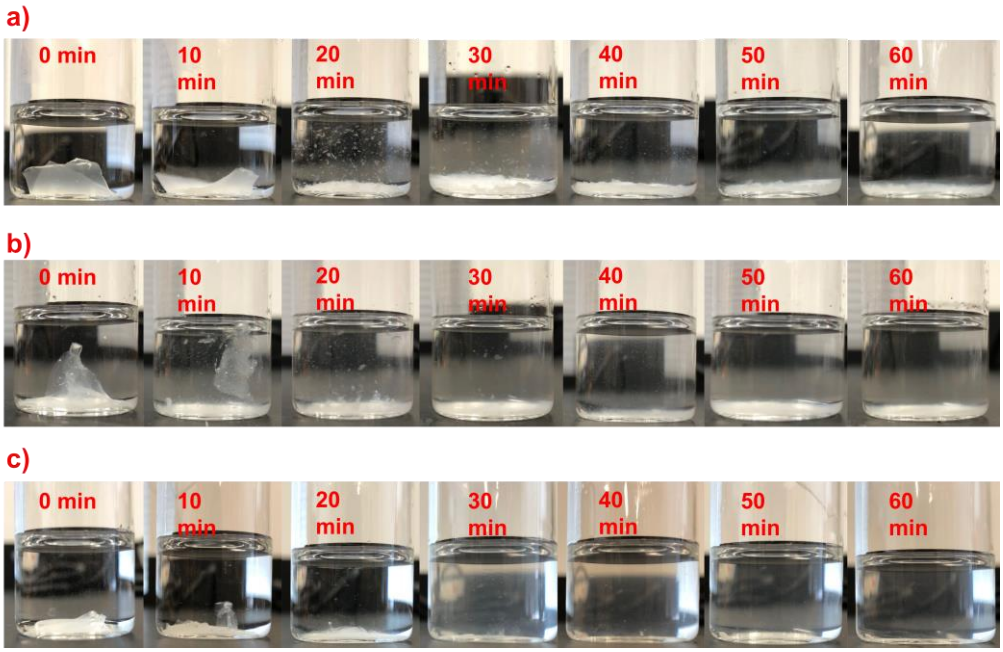

Figure 3. Degradation behavior of starch films in SSF-A under 37 ℃. a) 100 % amylose, b) 50% amylose + 50% amylopectin, c) 100% amylopectin.

Starch film functionalization

Figure 4 shows the FTIR spectra of starch and CDI activated starch films. After CDI activation, an obvious ester C=O stretch peak appears, which indicates that -OH on starch was successfully activated by CDI and formed an imidazole carbamate intermediate. As illustrated in Scheme 1, the primary amide group on L-lysine will then react with the intermediate and form a carbamate linkage. Figure 5 shows the FTIR spectra of L-lysine functionalized starch films after CDI activation. An amide I C=O stretch peak was observed when the L-lysine concentration is 10mg/ml. This indicated that the formation of carbamate linkage, which means that L-lysine successfully reacted with CDI activated starch. However, no carbamate linkage peak was observed when the L-lysine concentration of 1mg/ml. This means that, in order for the reaction to occur, a higher L-lysine concentration is necessary.

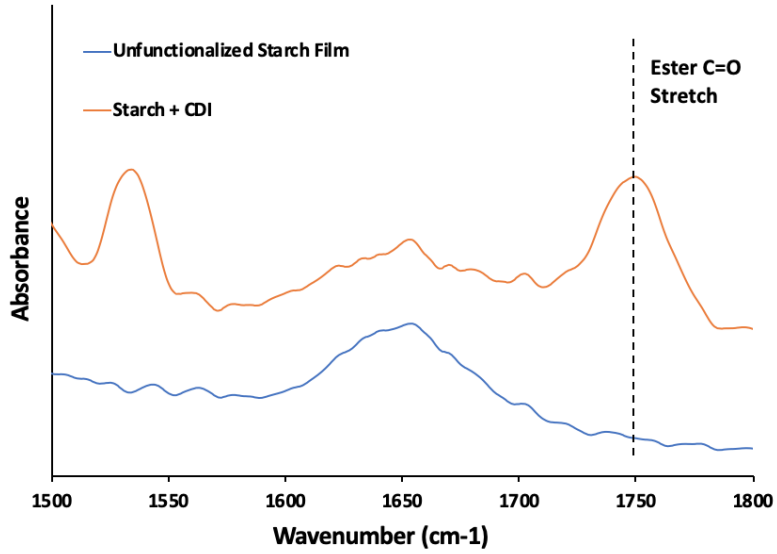

Figure 4. FTIR result of unfunctionalized starch film, CDI activated starch film and L-lysine functionalized starch film.

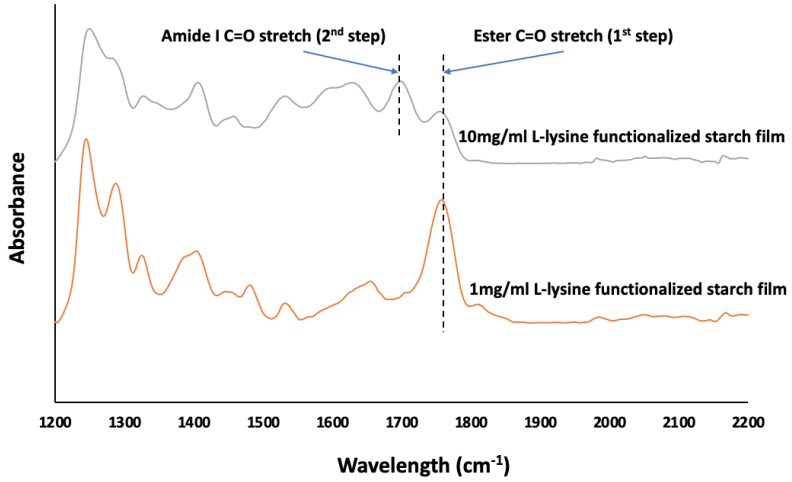

Figure 5. FTIR result of L-lysine functionalized starch film after CDI activation.

6.1.4 Conclusion

Starch film was assembled with glycerol as plasticizer. Degradation study showed that the films will degrade in 60min in simulated saliva environment, which means starch film can be applied as choking-hazard-free drug delivery patches. In order to improve the adhesive ability to negatively

charged buccal mucin, starch films were functionalized by l-lysine to introduce positively charged group on starch molecules. Future study will be focused on quantitively characterize mucoadhesive ability of functionalized starch film. The surface of starch film also needs to be modified to achieve unidirectional drug release.

6.2 Dynamic Mechanical Property Analysis of Gelatin for Capsules

6.2.1 Motivation

Gelatin, which is a mixture of peptides and proteins produced by partial hydrolysis of collagen extracted from various animal resources, represents a desirable form for oral delivery when made into capsules. However, current gelatin formulations demonstrate poor mechanical property and shelf stability in regions with warm climates. Thus, exploration of gelatin formulations with better mechanics and stability is necessary. Humidity controlled DMA has been demonstrated to be effective on studying the mechanical response of materials under humidity variation. Gelatin films with glycerol as plasticizer were fabricated using a solvent casting method, and characterized with humidity controlled DMA. By studying the mechanical properties of gelatins from different resources, gelatin capsule formulations with better performance under humidity variation can be developed.

6.2.2 Methodology

Gelatin film fabrication

Gelatins from different sources (pork skin, fish, animal bone) were used to fabricate thin films. 4 wt% of gelatin and 2 wt% of glycerol were dissolved in DI water under 40℃ water bath. The solution was cooled down to room temperature poured into a petri dish. The solution was dried for 48 hours in ambient condition to get gelatin films.

Dynamic mechanical analysis

DMA was performed using a Netzsch DMA 242E (Netzsch, Germany) with a MHG32 modular humidity generator (ProUmid, Deutschland) at room temperature with a tensile geometry. RH was varied in a sequence of 30%-50%-70%-90%-30%, with each humidity condition lasting for 1 hour.

6.2.3 Result and Discussion

Humidity controlled DMA result of gelatin films from different sources was shown in Figure 6. Different gelatin films showed similar response to humidity change. Gelatin films from pork skin have the highest modulus while gelatin films from animal bones have the lowest modulus under same humidity condition. Storage modulus of gelatin films decreased with humidity increase. When relative humidity decreased from 90% back to 30%, modulus of gelatin films starts to recover. However, the modulus is not fully recovered in 1 hour. The modulus drop with humidity increase is due to the plasticizing effect of water, as water is a good solvent for gelatins.

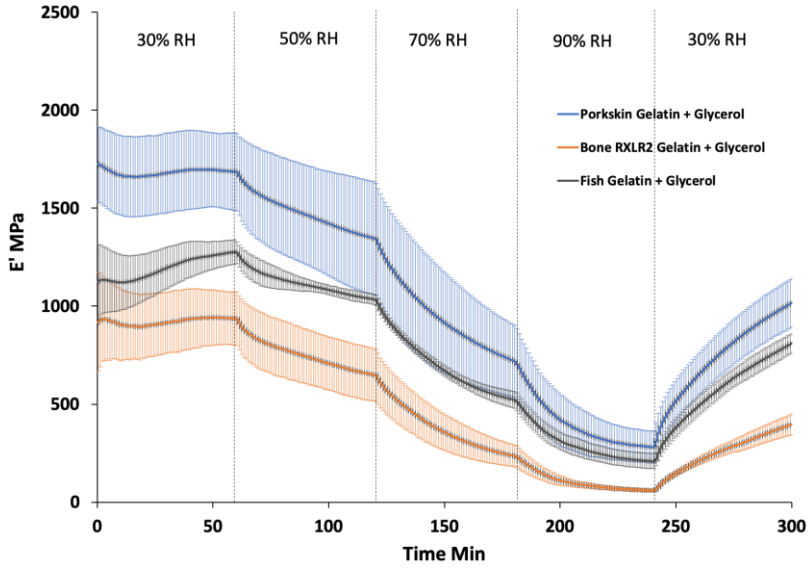

Figure 6. Humidity controlled DMA of gelatin films fabricated from pork skin, bone and fish.

Gelatin films fabricated from pork gelatins were stored at 40℃ for 1 week to study the effect of aging. DMA result of gelatin films before and after aging are shown in Figure 7. Based on the

results, 1 week of aging at 40°C showed no obvious effect on modulus and humidity response of gelatin films. Longer aging time or higher aging temperature will be explored in future research.

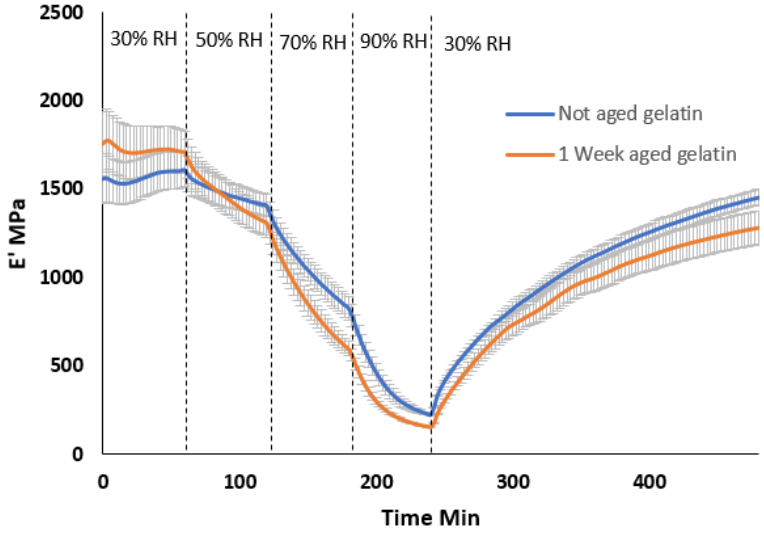

Figure 7. Humidity controlled DMA of gelatin films before and after aging.

7.2.4 Conclusion

Gelatin films were assembled using gelatins from different sources. Although the humidity response of different gelatin films is similar, the storage modulus is different under same relative humidity. Humidity change has drastic influence on modulus of gelatin films, due to the plasticization effect of water in humid air. Short time aging (1 week) did not show an obvious effect on mechanical property of gelatin films. Future study will include fabrication and characterization of gelatin films with different formulations, and exploration of film formulation with optimized performance and stability.

References

(1) Takai, N.; Yamaguchi, M.; Aragaki, T.; Eto, K.; Uchihashi, K.; Nishikawa, Y. Effect of

Psychological Stress on the Salivary Cortisol and Amylase Levels in Healthy Young Adults. *Arch. Oral Biol.* **2004**, *49* (12), 963–968.

(2) Shi, R.; Zhu, A.; Chen, D.; Jiang, X.; Xu, X.; Zhang, L.; Tian, W. In Vitro Degradation of Starch/PVA Films and Biocompatibility Evaluation. *J. Appl. Polym. Sci.* **2010**, *115* (1), 346–357.

(3) Khutoryanskiy, V. V. Advances in Mucoadhesion and Mucoadhesive Polymers. *Macromol. Biosci.* **2011**, *11* (6), 748–764.

(4) Hermanson, G. T. *Bioconjugate Techniques*; 2008.

Chapter 7: Conclusions and Future Directions

In this dissertation, polyelectrolytes including PDADMAC and PSS were used to assemble PEMs and PECs. In chapter 3, PEMs from PDADMAC and PSS were assembled using LbL dip-coating method with different polyelectrolytes as first layer materials. Strong or weak polycations with different molecular weight and structure were selected as the base layer of PEMs. The deposition process was tracked using QCM-D. It was shown that PEMs with different first layer materials have different total mass accumulation and single layer mass. The total mass accumulation even showed a first-layer molecular weight dependent behavior when using different PEIs as the first layer material. Surface morphology of PEMs also showed first layer material selection dependent behavior, with higher surface roughness observed when using PEI as first layer material. However, the water contact angle of PEMs is not influenced by different first layer materials. This indicates that changing first layer material affects internal structure and surface morphology of PEMs, while maintaining other surface properties like surface chemistry constant. This PEM system with different first layer materials could be applied to model the surface property of substrate for cell culturing to better understand the role of surface properties on cell adhesion and proliferation.

In Chapter 4, thermal mechanical behavior of PDADMAC and PSS was studied using DMA after storage under ambient condition and in a desiccator. PECs assembled from PDADMAC and PSS were also characterized by DMA. Tg of PDADMAC showed ~100℃ increase after annealing under 120℃ for different time. The water content of PDADMAC decreased with increase annealing time, which indicated that Tg increased with decreasing of water content. Tg of PSS was also observed during first heating cycle. However, after thermal annealing, no detectable glass transition behavior was observed for PSS. PEC from PDADMAC and PSS showed storage-condition-dependent/humidity-history-dependent thermo mechanical behavior under DMA

characterization as well. These results reveled the importance of water in physical and mechanical properties of polyelectrolyte-based structures.

In Chapter 5, PECs were assembled from PDADMAC and PSS using the same method described in Chapter 4. Humidity controlled DMA was used to characterize the influence of relative humidity on mechanical behavior of PECs under room temperature. Water content of PECs was characterized using TGA and thermal transition temperatures of PECs was characterized by M-DSC. Modulus of PECs decreased at the beginning of humidity tempering, which is due to the plasticization effect of water. After the initial decrease, modulus of PEC started to increase. This is due to the reorganization of PEC network and the formation of additional crosslinks under water plasticization. After humidity tempering, PEC achieved a stiffness increase of 35%, which is confirmed by flexural test. These results highlighted the potential of polyelectrolyte-based materials for new applications where tailoring of mechanical properties is desired, yet mild processing conditions are necessary.

In Chapter 6, humidity tempering approach was further applied to other bioderived polyelectrolytes, and their application as drug delivery materials was studied. Oral drug delivery patches were assembled based on starch films. Degradation study on starch films showed that the materials will fully degrade in an oral environment, which can prevent choking hazards. Starch films were further functionalized using L-lysine to obtain positively charged surfaces, which can possibly improve adhesion between the film and buccal mucosa. Gelatin from different resources were fabricated into thin films and characterized by humidity controlled DMA as well. Humidity variation showed a huge impact on mechanical property of gelatin films.

In summary, we designed a PEM model system that can be applied to tune the surface morphology while maintaining the surface chemistry by only changing the first layer materials.

This allowed us to achieve tailorable surface properties in PEM assembly. By studying the fundamental relationship between water and the PEC system, we demonstrated that water can enable the chain rearrangement of polyelectrolytes by providing extra mobility. Water not only works as a plasticizer, but also forms hydrogen bonding in the PEC system. This revealed the importance of humidity history, which has typically been neglected in the PEC processing. It also allowed us to apply humidity tempering as a novel processing technique to increase the storage modulus of the PEC.

The QCM-D work in this research demonstrated that the mass accumulation behavior of PEMs is first layer material dependent. However, polyelectrolytes selected as the first layer materials in this study have different structures and chemistry at the same time, which makes it difficult to completely isolate the effects of different factors. New materials selection strategy could be applied for future work, such as including linear polyelectrolytes with only different chain lengths or molecular weights. It is possible that there is more information buried in the QCM-D profile. Developing more QCM-D raw data interpretation strategies is also necessary to improve our understanding of the internal structure change during polyelectrolyte adsorption.

Cell proliferation and differentiation are shown to be impacted by the surface properties of culturing substrates.[1–3] PEMs can be applied for modifying surface properties of the substrates for cell culture. Tailoring topography of PEMs while maintaining the surface chemistry was achieved in this research. This provided an opportunity to study the effect of surface roughness on cell proliferation and differentiation independently.[4] Continuous work can focus on tailoring properties of PEMs assembled from weak polyelectrolytes. Applying current strategy to weak polyelectrolyte combinations can potentially tailor the properties of PEMs more substantially, as the weakened bonding between polyelectrolyte layers assists the interlayer diffusion of polyelectrolytes.

Prior to the work presented in this thesis, there had been little exploration of low water content PECs, and reported properties varied significantly. The inconsistency of properties is largely due to the kinetic limitations and history-dependent variables during their formation. Our study revealed the influence of storage conditions and humidity history on the structure and properties of PECs, which is crucial for understanding the path-dependent behavior of PECs. Humidity tempering was demonstrated to increase the storage modulus of the PEC up to 70%. The storage modulus increase is explained by the formation of extra crosslinks under water plasticization. Water not only provides extra mobility for polyelectrolyte chains, but also forms hydrogen bonds within the PEC system. This understanding of the influence of water in PEC systems is valuable for developing room temperature, solvent-free processing techniques for PECs. During humidity tempering, storage modulus of the PEC changes with time. The modulus increased more substantially when the PEC was tempered under higher humidity condition. This is the first time that humidity was applied to tailor the mechanical properties of PECs. In future work, modulus of the PEC can possibly be tuned more precisely by controlling the tempering time and humidity. Although humidity tempering of PECs has proved that PECs have humidity history dependent structure and mechanical properties, the interaction between water molecules and the PEC network is still not fully understood. Further exploration on water-polyelectrolytes interaction could represent future research.

Similar to humidity tempering of unmodified PEC, humidity tempering of PEC assembled under different salt concentrations could be studied. While salt ions can improve the processability of PECs by reducing the amount of intrinsic ion pairs, there will be space for extra water in PEC after salt doping. PECs can be extruded under salt annealing, which an effective approach to improve the processability of PECs.[5] However, ion-pairs of PECs are broken under salt doping,

which decreases the mechanical property of PECs. Applying humidity tempering to extruded PECs provides a potential approach to achieve high processability PEC without sacrificing the mechanical properties. Including effect of salt in PEC humidity study could help to develop potential application of PECs in implanted devices, as exposure to salt buffered environments is necessary for those applications.

Different approaches to tailor the mechanical properties of other bioderived polyelectrolyte systems should be studied as well. Humidity tempering was applied to gelatin films in this research. Gelatin films showed a substantial modulus change under humidity variation. However, the mechanical properties of gelatin films were not improved after humidity tempering. This indicates a different mechanism of interaction between water and gelatin, compared with the interaction between water and the PEC system. Future work could focus on assembling novel materials by combining gelatin and polyelectrolyte complexes to achieve improved performance under humidity variation.

The results in this thesis not only demonstrate that the structure and properties of polyelectrolyte-based materials can be tailored by different approaches, but also expanded the potential applications of those materials. More fundamental mechanism research is necessary to achieve fully tailorable structure and properties of those materials. Based on the information and techniques gained in this study, we can achieve a better understanding of relationship between structure and functionality of those materials, and continue to develop novel structures for use in biomedical applications.

References

(1) Curran, J. M.; Chen, R.; Hunt, J. A. Controlling the Phenotype and Function of Mesenchymal Stem Cells in Vitro by Adhesion to Silane-Modified Clean Glass Surfaces. *Biomaterials* **2005**.

(2) Mafi, P. Adult Mesenchymal Stem Cells and Cell Surface Characterization - A Systematic Review of the Literature. *Open Orthop. J.* **2011**.

(3) Gupta, M.; Sarangi, B. R.; Deschamps, J.; Nematbakhsh, Y.; Callan-Jones, A.; Margadant, F.; Mège, R. M.; Lim, C. T.; Voituriez, R.; Ladoux, B. Adaptive Rheology and Ordering of Cell Cytoskeleton Govern Matrix Rigidity Sensing. *Nat. Commun.* **2015**.

(4) Ding, I.; Walz, J. A.; Mace, C. R.; Peterson, A. M. Early HMSC Morphology and Proliferation on Model Polyelectrolyte Multilayers. *Colloids Surfaces B Biointerfaces* **2019**.

(5) Shamoun, R. F.; Reisch, A.; Schlenoff, J. B. Extruded Saloplastic Polyelectrolyte Complexes. *Adv. Funct. Mater.* **2012**, *22* (9), 1923–1931.

Appendix 1: Chapter 3 Supplementary Material

Table 1s. Growth rate of PEMs (ng/cm^2 per bilayer) when using different first layer materials.

First Layer Material	Growth Rate (ng/cm^2 per bilayer)
PDAMDAC	61.36
PEI 10K	154.39
PEI 70K	110.45
PEI 600K	148.08
PAH	71.51
PLH	77.24

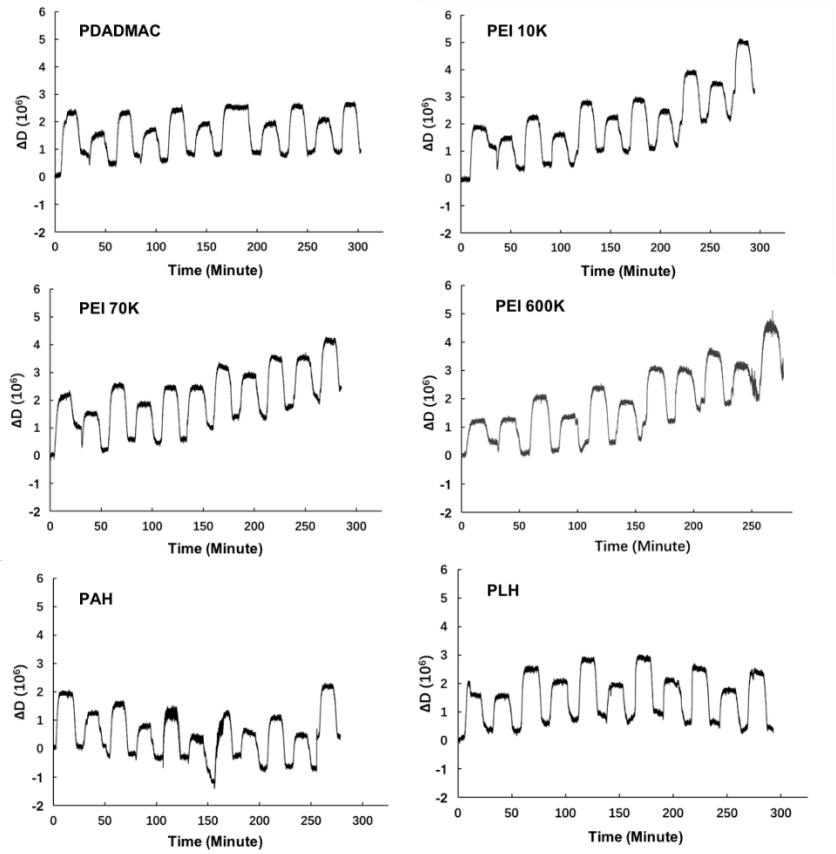

Figure 1s. Energy dissipation curves of PEMs with different first layer material

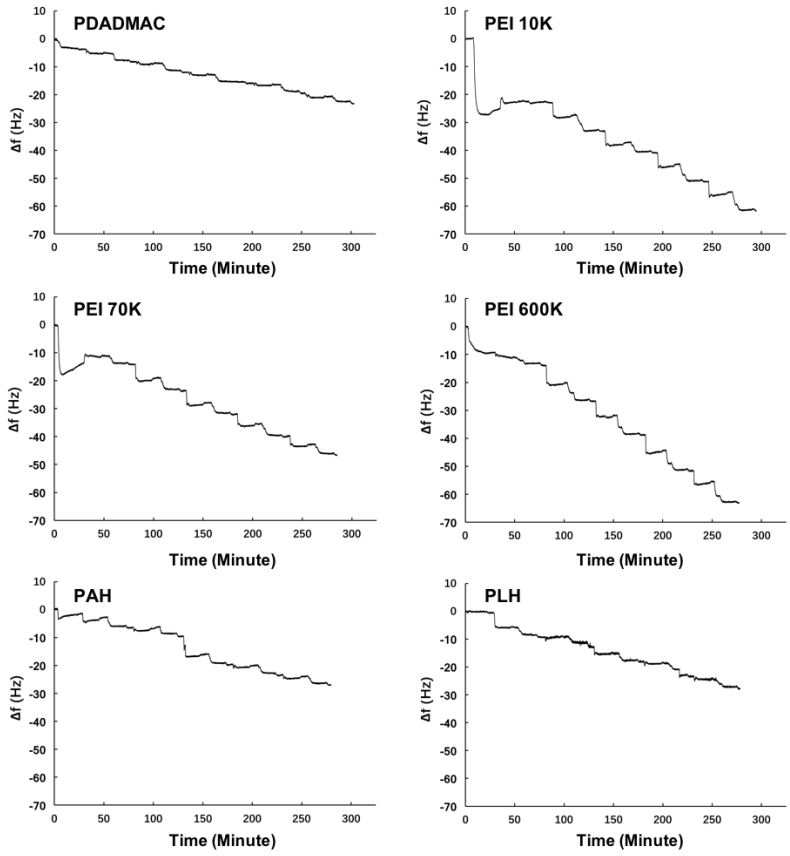

Figure 2s. Frequency change of PEMs with different first layer material

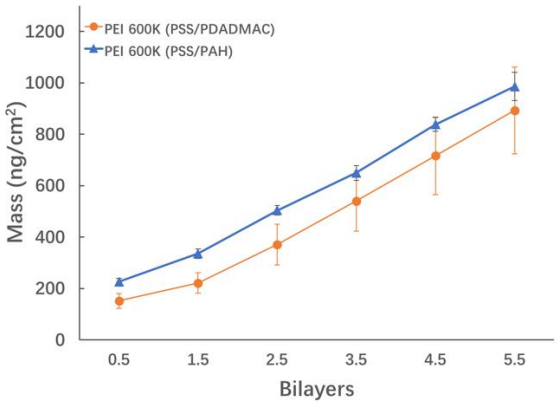

Figure 3s. Comparison between (PSS/PAH) system and (PSS/PDADMAC) system on same first layer material (PEI 600K).

Appendix 2: Chapter 4 Supplementary Material

Thermogravimetric analysis (TGA)

Results show that PDADMAC-s retains 2.5 wt.% water under ambient conditions and degrades at 300°C (onset) and PSS-s retains 8.5 wt.% water under ambient conditions and degrades at 445°C (onset).

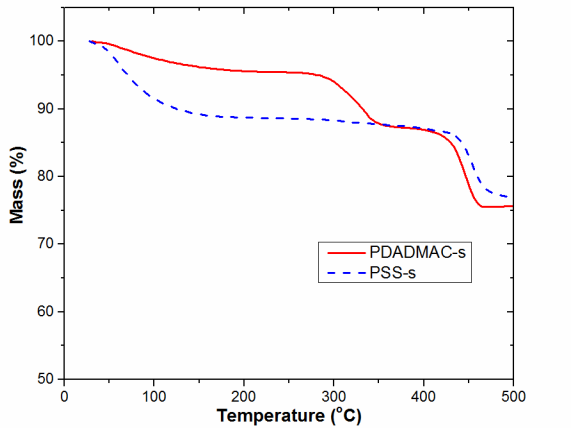

Figure S1. TGA of as-received powdered PDADMAC and PSS.

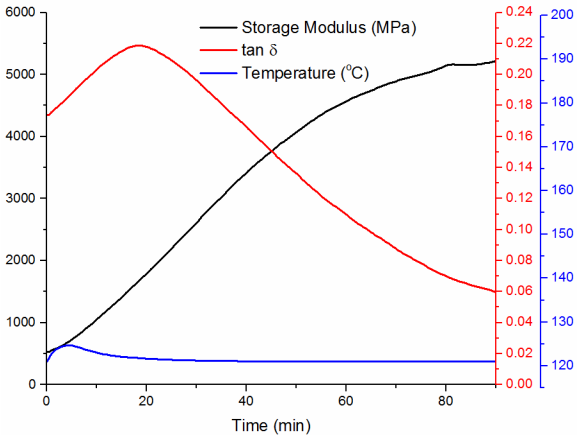

Figure S2. Isothermal DMA of PDADMAC at 120 °C. PDADMAC sample was prepared under ambient conditions.

Differential Scanning Calorimetry (DSC)

Results for the second and third heating cycles showed a PDADMAC thermal transition of 113°C and 109°C, respectively (Figure S4). Cooling cycles did not show any thermal transitions. For PSS, a thermal transition is observed at 117°C for both the second and third heating cycles. The endothermic peak following the thermal transition is larger in the second heating cycle than the third. An additional thermal transition is observed at 278°C in the second heating cycle, but not in the third.

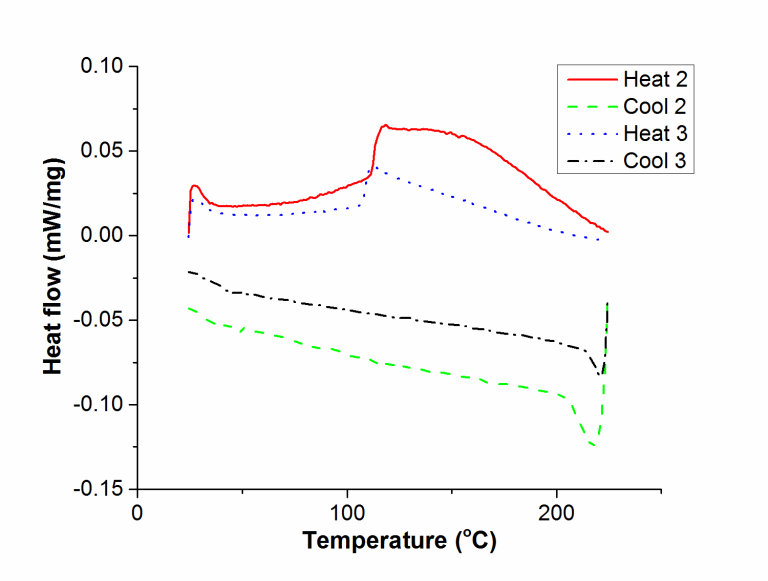

Figure S3. DSC of PDADMAC. Exo down.

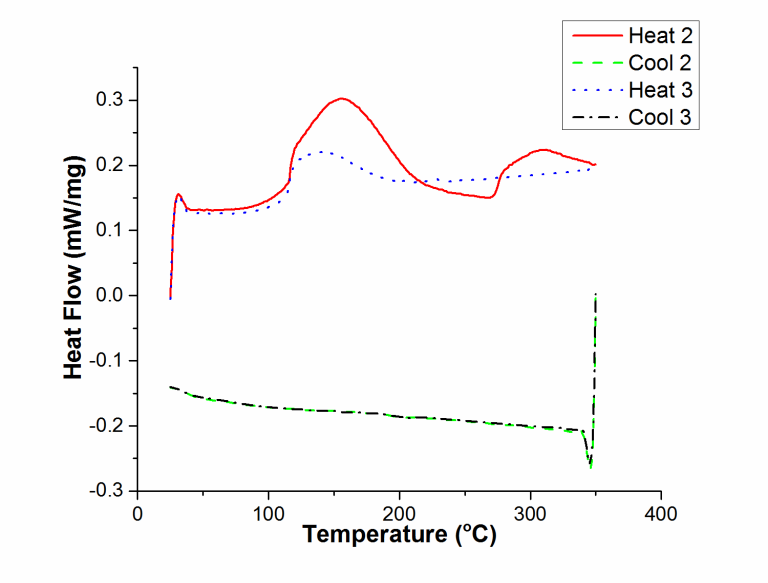

Figure S4. DSC of PSS. Exo down.

It is important to note that the DSC results are from samples in which the polyelectrolyte solution was pipetted directly into the DSC pan (i.e., no solid sample was prepared). The first heat and hold at 100°C is designed to remove water, but the majority of the initial sample is water. When solid polyelectrolyte and PEC samples were prepared as described above under ambient conditions and tested, no thermal transitions were observed, even in temperature modulated DSC. Therefore, we hypothesize that water plays an important role in the thermal transitions observed in Figures S3 and S4.

Appendix 3: Chapter 5 Supplementary Material

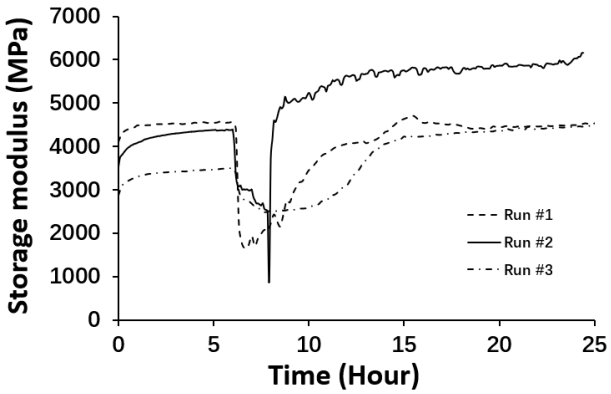

Figure S1. PEC storage modulus under 70% RH highlighting the inconsistent results caused by PEC cracking.

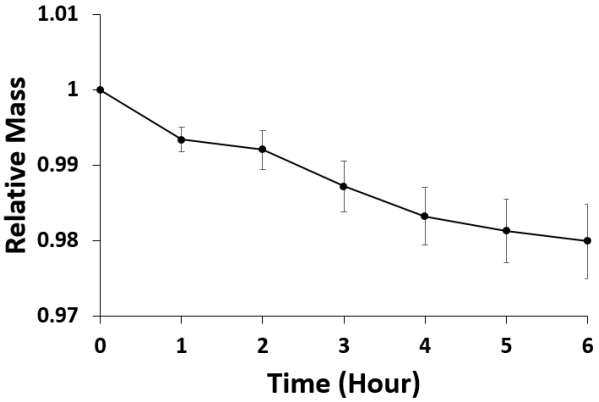

Figure S2. Mass loss of PEC under 10% RH after exposure to ambient conditions for 5 min.

Table 1S. Exponent fitting of water diffusion mechanism ($M_t/M_\infty = kt^n$) under different RH conditions.

RH	30%	50%	60%	70%
n	0.52	0.68	0.62	0.50

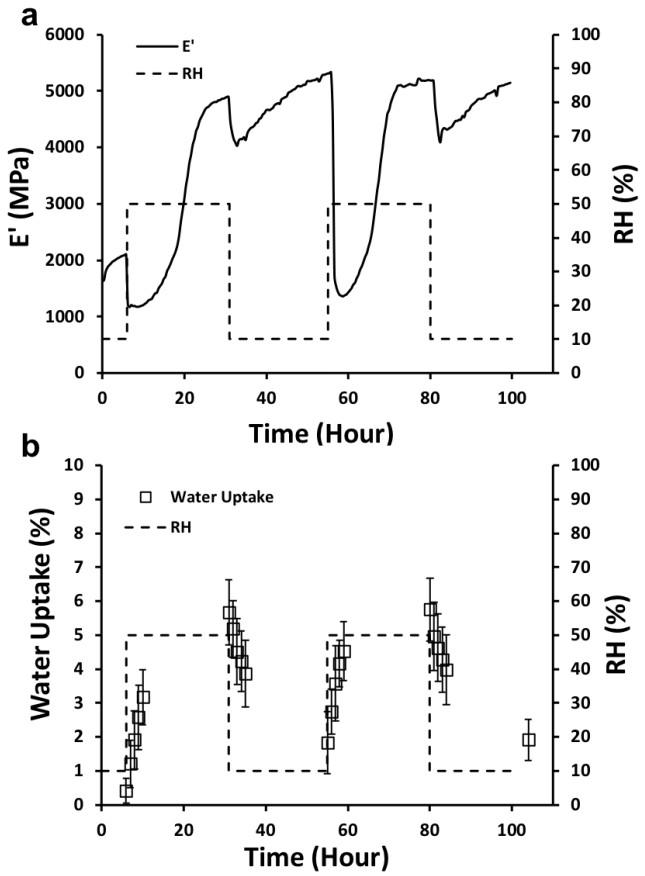

Figure S3. a) Storage modulus and b) water uptake of PEC during re-exposure under 50% RH

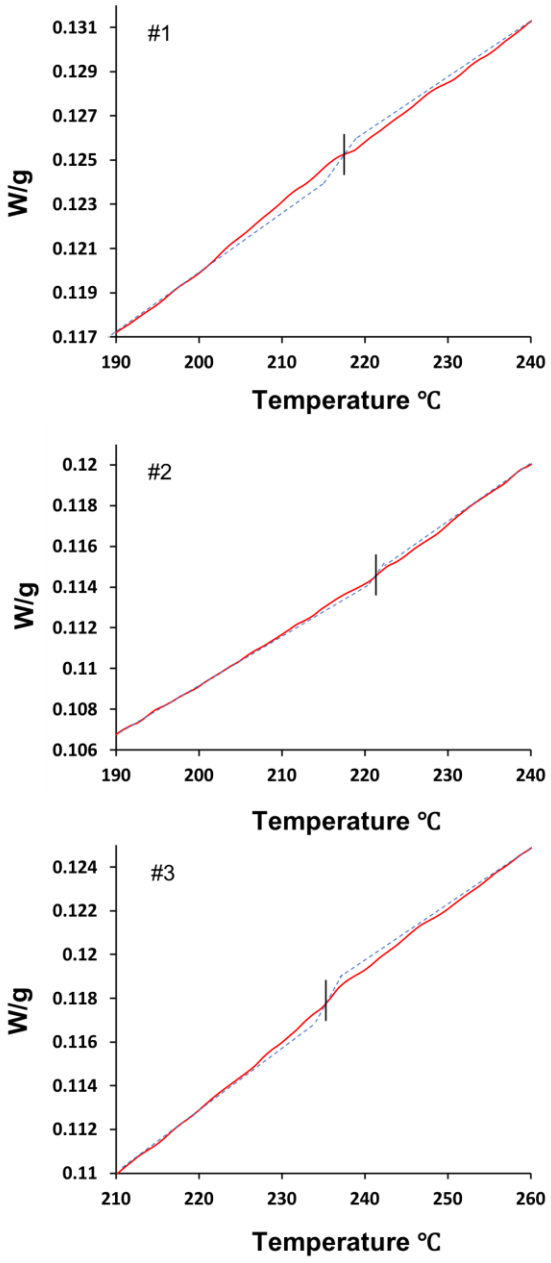

Figure S4. Reversing heat flow curves of PEC after humidity tempering under 50% RH